Viral regulation of nutrient assimilation by algae and prokaryotes

Dissertation zur Erlangung des
Doktorgrades der Naturwissenschaften
- Dr. rer. nat. -
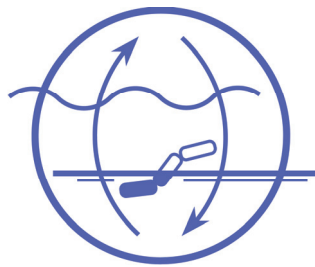
dem Fachbereich Geowissenschaften
der Universität Bremen

vorgelegt von

Abdul Rahiman Sheik

Bremen, Oktober 2012

Die vorliegende Arbeit wurde in der Zeit von April 2009 bis September 2012 am Max Planck Institut für Marine Mikrobiologie angefertigt.

1. Gutachter: Prof. Dr. Marcel Kuypers

2. Gutachterin: Dr. Corina Brussaard

Tag des Promotionskolloquiums: 10. Dezember 2012

Summary

Viruses are the most abundant entities in the ocean and represent a large portion of 'lifes' genetic diversity. As mortality agents, viruses catalyze transformations of particulate matter to dissolved forms. This viral catalytic activity may influence the microbial community structure and affect the flow of critical elements in the sea. However, the extent to which viruses mediate bacterial diversity and biogeochemical processes is poorly studied. The current thesis, using a single cell approach, provides rare and novel insights in to how viral infections of algae influence host carbon assimilation. Furthermore this thesis details how cell lysis by viruses regulates the temporal bacterial community structure and their subsequent uptake of algal viral lysates.

Chapter 2 shows how viruses impair the release of the star-like structures of virally infected *Phaeocystis globosa* cells. The independent application of high resolution single cells techniques using atomic force microscopy (AFM) visualized the unique host morphological feature due to viral infection and nanoSIMS imaging quantified the impact of viral infection on the host carbon assimilation. Prior to cell lysis, substantial amounts of newly produced viruses (~ 68%) were attached to *P. globosa* cells. The hypothesis that impediment of star-like structures in infected *P. globosa* cells leads to enhanced grazing was proposed. The scenario of enhanced grazing is in sharp contrast to the current view that viral infections divert the organic carbon transfer from higher trophic levels (e.g., grazers).

In chapter 3, during early hours of viral infection, the application of secondary-ion mass spectrometry (nanoSIMS) showed a high transfer of infected *P. globosa* biomass towards *Alteromonas* cells well before the latent period, which stimulated its initial doubling in abundance, attachment to algal cell surroundings. Following algal viral lysis, the succession of bacterial populations consisted of *Alteromonas* and *Roseobacter* cells and an efficient transfer of *P. globosa* viral lysates by these specific bacterial members (Day 2). The sharp increase of these two genera, which occurred in aggregate-association, declined in abundance due to plausible phage mediated lysis. The potential phage mediated lysis appeared to result in aggregate dissolution and was responsible for regeneration of dissolved inorganic carbon (55% of the particulate ^{13}C-organic carbon) and generation of plentiful recalcitrant organic

carbon. The findings such as algal leakage during infection substantiate a previously undocumented role of viruses, which appears to be responsible for alterations in the marine ecosystem process such as bacterial community structure and carbon availability.

In chapter 4, it appears that viral infection of *Micromonas pusilla* cells led to the hindrance of pyrenoid synthesis (starch and proteins) and much of the newly assimilated material was diverted towards viral production. Viral lysis of *M. pusilla* led to dominance of *Alteromonas* cells and *Bacteroidetes*, where as *Alteromonas* cells dominated the bacterial communities in non-infected cultures through out the experiment. The ecological implication of viral mediated starch impediment in *M. pusilla* cells may lead to the release of labile proteins and increased levels of polysaccharides, which potentially directs the marine pelagic system to more regenerative processes.

Zusammenfassung

Viren sind die zahlreichsten „Lebensformen" in den Ozeanen und bilden das größte Reservoir genetischer Diversität im marinen Ökosystem. Indem sie ihren Wirt töten wandeln Viren partikuläres in gelöstes Material um. Diese kalatytische Aktivität kann die Struktur der mikrobiellen Population ebenso wie den Fluss entscheidender Elemente im Meer beeinflussen. Wie genau und zu welchem Ausmaß Viren die Struktur der bakteriellen Gemeinschaften sowie biogeochemische Prozesse beeinflussen ist bisher kaum erforscht. Die vorliegende Arbeit präsentiert, basierend auf hochauflösenden „single cell" Methoden, neue Erkenntnisse über die Auswirkungen viraler Infektionen auf die Kohlenstoff Assimilation des Wirtes. Des weiteren wurden die Auswirkungen der viralen Lyse von Algen auf die temporäre bakterielle Gemeinschaftsstruktur, sowie über die Aufnahme der Zelllysate durch Bakterien untersucht.

In Kapitel zwei wird beschrieben wie die Freisetzung sternähnlicher Strukturen durch *Phaeocystis globosa* Zellen während viraler Infektionen vermindert wird. Die Anwendung hochauflösender Rasterkraftmikroskopie ermöglichte die Visualisierung der veränderten Zellstrukturen infizierter Algen. Mit Hilfe eines nano Sekundärionenmassenspektrometers (nanoSIMS) konnten die Auswirkungen der viralen Infektion auf die Kohlenstoff Assimilation des Wirtes quantifiziert werden.
Noch vor der Zelllyse waren erhebliche Mengen ($\sim$ 68%) neu produzierter Viren mit *P.globosa* Zellen verbunden. Es wird hypothetisiert, dass die Verminderung der sternähnlichen Strukturen in infizierten *P.globosa* Zellen zu vermehrtem Fraß führt. Diese Hypothese steht im starken Kontrast zur momentanen Auffassung, nach der virale Infektionen den Transfer organischen Kohlenstoffs in höhere trophische Ebenen vermindern.

Im 3. Kapitel wird mit Hilfe des nanoSIMS gezeigt das ein hoher Transfer von Biomasse der infizierten *P.globosa* Zellen zu *Altermomonas* Zellen bereits in den frühen Stunden der Infektion stattfand, weit bevor die latente Phase eintrat. Die initiale Verdoppelung der Alteromonas Zellzahlen sowie deren Anheftung an Algenzellen wurde so stimuliert. Die bakterielle Population nach der viralen Lyse bestand aus einer Abfolge von *Alteromonas* und *Roseobacter* und einem effizienten Transfer viraler *P. globosa* Lysate an diese spezifischen Bakterien. Die sprunghaft

angestiegenen Zellzahlen beider Gattungen gingen anschließend zurück, vermutlich durch Bakteriophagen vermittelte Zelllyse. Die Zellaggregate der Bakterien lösten sich auf und die Lyse der Zellen resultierte in der Regenerierung von gelöstem inorganischen Kohlenstoff (55% des partikulären 13C organischen Kohlenstoffs) sowie der Erzeugung schwer abbaubaren organischen Kohlenstoffs. Diese Erkenntnisse untermauern eine bisher undokumentierte Rolle von Viren im marinen Ökosystem bei Prozessen wie Änderungen der bakteriellen Biodiversität sowie Verfügbarkeit von Kohlenstoff.

In Kapitel 4 wird beschrieben wie die virale Infektion von *Micromonas pusilla* Zellen die Synthese von Isoprenoiden (Stärke und Proteine) verhinderte, während neu assimilierte Bausteine zur Virensynthese verwandt wurden. Nach der Lyse der *M. pusilla* Zellen dominierten Alteromonas sowie Bacteriodetes Zellen die bakterielle Gemeinschaft, wobei Alteromonas auch in den nicht infizierten Kulturen die vorherrschende Bakteriengattung war. Die Verhinderung der Stärke Synthese in *M. pusilla* Zellen könnte zur Freigabe labiler Proteine und Polysacharide führen, wodurch regenerative Prozesse im marinen pelagischen System verstärkt würden.

Table of Contents

Chapter 1. Viruses in the sea

The discovery: *In 1915, Frederick William Twort reported bacterial lytic phenomena and believed that responsible agent to be a lytic enzyme. Later in an independent study, Felix d'Herelle discovered a bacterial virus and coined the term 'Bacteriophage' (Duckworth, 1987).*

Since virology emerged as one of the major fields in science, the question has been repeatedly asked 'What is a virus?' The word virus commonly refers to a biological agent that causes disease when introduced into a healthy host and can be isolated from the diseased host ambience. Thus, it satisfies the scientific standard as per Koch's postulates to be described as an infectious biological agent (Rivers, 1937). Viruses are small particles (10-200 nm in size), composed of a proteinaceous coat commonly called capsid. Within this capsid, genetic material, DNA or RNA, is packed, either double-stranded or single-stranded. Viruses fall outside of the current definition of 'living' as they lack vital cell organelles that are essential to reproduce. Thereby, viruses inevitably depend on host metabolism, soon after infection, they control the host cellular machinery and can be vaguely referred to 'host hijack'. On our green planet, viruses are known to infect most of the living forms and hence their occurrence is known wherever life is documented.

1.1 Global abundance of marine viruses

The existence of viruses in the marine environment has been documented for many decades as noticed by the isolation of a bacteriophage (Spencer, 1955; Torrella and Morita, 1979) or by the presence of virus-like particles within phytoplankton hosts (Pienaar, 1976). This early documentation of marine viruses were considered insignificant due to their numerically low abundances and presumed low ecological impact. It was not until late in the 1980's, when a Norwegian group revealed that the abundance of viruses in marine environments was in fact high (Bergh et al., 1989). This recognition has renewed scientific interest and revolutionized our perception of viruses in oceanic environments.

Furthermore, in the last decades, the advent of new methodologies to study and enumerate single cells, have provided more accurate and efficient means for enumerating viruses. The application of direct counting methods such as electron microscopy (Borsheim et al., 1990; Proctor and Fuhrman, 1990), epifluorescence

microscopy (Hennes and Suttle, 1995; Noble and Fuhrman, 1998; Wen et al., 2004) and flow cytometry (Marie et al., 1999; Marie et al., 2001; Brussaard, 2004b, 2009) have provided unprecedented evidence for an enormous abundance of viruses in the sea (Suttle and Fuhrman, 2010). At present, it is estimated that on average there are $\sim 10^7$ viruses per milliliter of surface seawater (Suttle, 2007), ranging from $\sim 10^8$ viruses mL^{-1} in the productive coastal environments (Wommack and Colwell, 2000; Brussaard and Martínez, 2008) to $\sim 3 \times 10^6$ viruses mL^{-1} in the deep sea (Danovaro et al., 2001; Danovaro et al., 2008). The estimated global abundance of viruses in the sea is $\sim 10^{30}$ and a viral concentration of ~ 17 femtomolar (Breitbart, 2012). Viruses are the most abundant biological entities in the oceans, comprising approximately 94% of the nucleic-acid-containing particles, $\sim 5\%$ of the biomass, and the second largest component of biomass after prokaryotes (Suttle, 2005, 2007).

Marine viruses besides being the abundant entities, are also the most diverse and dynamic components of the microbial communities. Viral abundance is seasonally, temporally and spatially variable. Typically, viral abundance decreases from the nutrient rich coastal habitats to oligotrophic offshore waters (Boehme et al., 1993; Cochlan et al., 1993; Evans et al., 2009b; De Corte et al., 2010) and is higher in summer and autumn than in winter (e.g., (Weinbauer et al., 1995)). Viral abundance is highest in the euphotic zone and decreases exponentially with depth (Wommack and Colwell, 2000; De Corte et al., 2010; Parsons et al., 2011). Viral distribution differs significantly among varied oceanic habitats in response to changes in the biotic (e.g., host abundances) and abiotic factors (e.g., nutrients) (Rowe et al., 2008; Evans et al., 2009b; De Corte et al., 2010; Evans and Brussaard, 2012). For example, viral abundance differs and is influenced by the environmental conditions in transition zones of two water masses e.g., thermocline and pycocline layers (detailed in a review by (Danovaro et al., 2011)). Another example, in the chemocline layer of the Baltic Sea, it was shown that viral abundance decreased within the oxic layer with a subsequent increase in the anoxic layer (Weinbauer et al., 2003).

The most striking temporal variations in viral abundances are observed during phytoplankton blooms (Bratbak et al., 1990; Tarutani et al., 2000; Brussaard et al., 2005a; Baudoux et al., 2006). For example, in coastal North Sea, viruses infecting the microalgae *Phaeocystis* are generally between 0 and 5% of the total viral population and their abundance is independent of whether or not *Phaeocystis* is the dominant phytoplankton (Brussaard et al., 2007). However, during bloom maxima,

Phaeocystis viruses can represent up to ~ 30% of the total viral abundance (Brussaard et al., 2004a; Brussaard et al., 2005a). Recently, a high-resolution multi-year time series study in the Sargasso Sea ascribed the temporal and vertical patterns of viral abundance was related to the changes in water-column stability and the distribution of specific host lineages (Parsons et al., 2011).

Others have documented the volatile nature of viral abundance occurring over shorter time periods (Jiang and Paul, 1994; Weinbauer et al., 1995). Remarkably, drastic changes in the virus abundances (by factor of 2-4) has been reported between 20-40 min intervals (Bratbak et al., 1996). Temporal variations of viruses have also been observed on a diel scale (Weinbauer et al., 1995). For example, in the North Sea, it appears that viruses time their infection to the night, subsequent lysis occurs the following afternoon (Winter et al., 2004).

Beyond simply enumerating viruses, studies conducted in the last years have demonstrated that viruses encompass enormous genetic diversity and can act as a reservoir of genes for microbial communities (Angly, 2006; Dinsdale, 2008). In marine environments, environmental factors (e.g., light, temperature, nutrients) influence the microbial community composition (Falkowski, 1998; Fuhrman and Hagström, 2008). Given the large diversity of marine microbial assemblages (Fuhrman and Ouverney, 1998; Giovannoni and Rappé, 2000) and the high host dependence and specificity of viruses, it is reasonable to imagine that global marine viral genetic diversity is equally high.

Previous studies on viral diversity relied heavily on morphological data obtained by transmission electron microscopy (TEM) (Wommack and Colwell 2000, Weinbauer 2004). Although TEM provided valuable information into marine viral diversity, at the same time it underestimated diversity as morphology differences do not necessarily reflect genetic diversity. It was the application of molecular methods such as pulsed-field gel electrophoresis and metagenomic analysis that revealed the incredible diversity of marine viruses (Breitbart, 2002; Rohwer and Thurber, 2009).

'*Walk a mile in virus shoes*': The first metagenomic survey by Breitbart *et al.* (2002) identified several thousand viral genotypes in a 200 L surface seawater sample. A second viral survey, identified the viral metagenomes from four different oceanic environments contained a vast majority of uncharacterized viral genotypes, yet they appeared to share a common gene pool (Angly, 2006). In a subsequent 6000km transect study in the North Atlantic (from the Gulf of Maine to the North Sea), Rowe *et al* (2011) reported viruses infecting *Emiliania huxleyi* (EhVs) have

unprecedented diversity and few strains of similar EhVs were detected in some samples. The results suggested the existence of a shared marine viral gene pool despite extremely high levels of viral diversity (Breitbart, 2012).

In conclusion, it is increasingly evident from the studies conducted across vast oceanic environments that viruses are dynamic and diverse components of marine planktonic systems. More importantly, marine viruses represent the largest reservoir of genetic diversity on our green planet (Breitbart, 2012).

1.2 Virus life cycles – from predators to parasites

Prior to speculating on the role of viruses in the sea, it is important to understand how they locate and reproduce within their hosts. Viruses infect their host cells by passive diffusion or by random encounters. After infection, viruses attach to a specific host membrane receptor (making viruses host specific) and inject their viral nucleic acid into the host organism. Following infection, a virus can have potentially three reproductive lifestyles (Figure 1):

(i) Lytic, in which soon after infection, virus replication takes place by the synthesis of viral genetic material and proteins, followed by assembly and production of new viruses either in the host's cytoplasm or nucleus. The period between viral infection and cell lysis is called the latent period or latency. As a consequence of cell lysis, newly produced viruses together with host cellular material are released and can start a new lytic infection. The number of viruses released after cell lysis (burst size) is highly variable (from only a few to thousands) as it depends on the factors such as viral type, host cell size and host metabolism.

(ii) Lysogeny, where subsequent to infection, viral DNA is incorporated into the host cell genome, and does not enter the lytic cycle until stimulated to do so by either internal or external triggering events (Weinbauer and Suttle, 1999; Evans and Brussaard, 2012). Lysogenic viruses are called 'prophages'. It is speculated that lysogeny can act as a 'virus refuge' when host abundances are low (Paul, 2008).

(iii) The third lifestyle, chronic infection, is similar to lysogeny except that infected cells release viruses by budding or extrusion over many generations and the released viruses are sub-lethal (Fuhrman and Suttle, 1993; Williamson et al., 2001).

In marine environments, the lytic and lysogenic infections are the more commonly investigated forms of viral propagation. Hence, it can be generalised that lytic viruses are 'predators' of microbes, whereas lysogenic and chronic infections represent 'parasitic' interaction.

A lytic infection is commonly followed by the death of the host cells, thus represents an important source of mortality of marine microbes. Rough estimates suggest that viral lysis in surface waters removes 2-10% of the phytoplankton populations and 20–40% of the standing stock of prokaryotes daily (Fuhrman, 1999; Wilhelm and Suttle, 1999). Within the invisible forest of marine organisms (Falkowski, 2002), viruses are significant mortality agents for a wide variety of phytoplankton (Brussaard, 2004a; Brussaard, 2008; Nagasaki and Bratbak, 2010; Short, 2012) and bacterioplankton populations (Wommack and Colwell, 2000; Weinbauer, 2004; Breitbart, 2012). The current thesis aims to unravel the role of algal viruses influencing microbial community structure and associated biogeochemical cycles.

Lytic cycle

Latent period

Virus Attachment

Injection of viral genome

Viral synthesis

Viral package

Cell lysis

Lysogeny

Viral integration

Propagation with host

Trigger

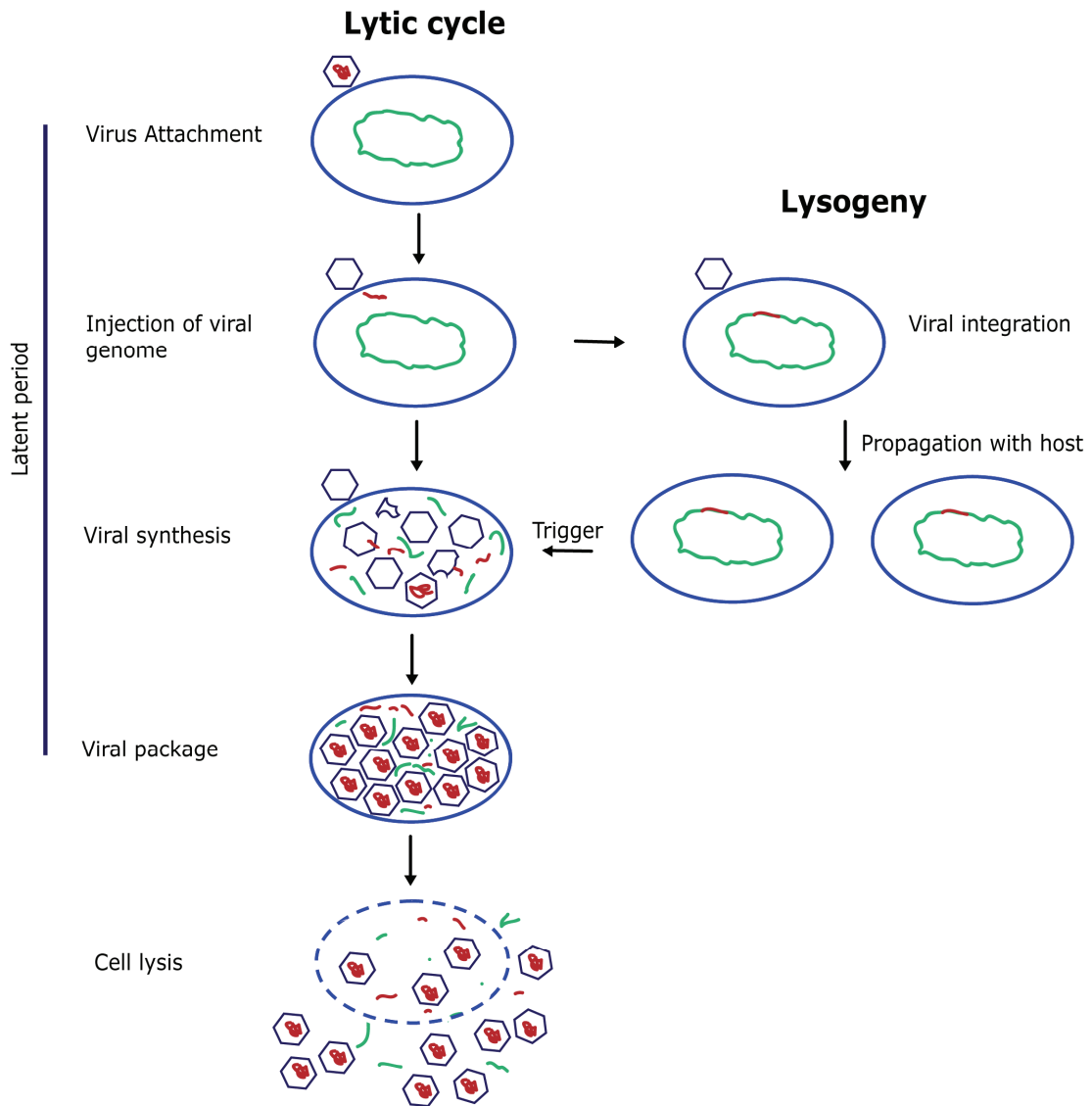**Figure 1: General schematic depiction of lytic and lysogenic reproductive life style of viruses. The green oval ring in a cell represents the host chromosome and the red coiled molecule in the virus represents viral genetic material. Up on injection of viral genetic material, a virus might enter lytic cycle or may integrate with host chromosome and undergo lysogeny. The image was adapted after Fuhrman and Suttle (1993).**

1.3 An introduction to algal viruses

The earliest observation of viruses infecting algal populations dates back to 1958, where the presence of intracellular virus-like particles were noted (described in a review by (Brown Jr, 1972)). More than 20 years later, the discovery and detailed study of the first successful cultivation of a virus infecting an eukaryotic algae, *Micromonas pusilla* was reported (Mayer and Taylor, 1979). Soon after, viruses that infect symbiotic *Chlorella* species (Van Etten et al., 1983; 1985) marked a second major breakthrough in algal virus research. Thus, these findings stimulated the idea that viruses could be significant mortality agents for algal populations and began a new era in the search of viruses infecting algal populations.

Algal viruses have larger genomes (400-560 kb) and the majority of characterized viruses possess double stranded (ds) DNA as genetic material, whereas, the presence of single stranded (ss) ssDNA, dsRNA and ssRNA viruses have also been reported (Brussaard and Martínez, 2008). Remarkably, the genome of a dsDNA virus infecting the green alga, *Pyramimonas orientalis,* (PoV) is similar in genome size to the smallest living microbe (Claverie et al., 2006). In contrast, some ssRNA and ssDNA algal viruses possess very small genomes (between 4 and 11 kb) (Nagasaki and Brussaard, 2008).

Typically, most of the dsDNA algal viruses belong to the family of *Phycodnaviridae*, which are 100-220 nm in diameter, lack an outer membrane and contain 5 or 6 faceted polyhedral capsid (Wilson et al., 2005). Phylogenetic analysis using the DNA polymerase gene revealed that the dsDNA algal viruses are more closely related to each other and form a distinct monophyletic group, yet the viral phylogeny diverges into different clades (Wilson et al., 2005; Brussaard and Martínez, 2008).

Despite the challenges associated with cultivation techniques, many studies have successfully isolated algal-virus systems from diverse marine habitats. A few examples of viruses infecting ecologically important bloom and non-bloom forming eukaryotic algae are listed in Table 1. Isolated viruses and hosts in culture provide a unique opportunity to study many of host-virus interactions. For example, the possible changes in the host viability during infection (Brussaard et al., 1999), and characterisation of different viruses infecting algal populations (Baudoux and Brussaard, 2005; Tomaru et al., 2012) could be studied on isolated strains of viruses and hosts.

1.3.1 The mortality imposed by algal viruses

A first vital step to comprehend the predatory role of algal viruses is to determine the extent of mortality they impose on host populations. The earliest and most convincing evidence that algal viruses were significant mortality agents emerged from field experiments. Concentrates of viruses from surface seawaters (2-200 nm in diameter) were added to whole water in order to increase the incidence of viruses (Suttle et al., 1990; Peduzzi and Weinbauer, 1993).

The examination of intracellular viruses by thin-sectioning (transmission electron microscopy) demonstrated the high frequency of viral infections on numerous bloom forming algal taxa: *Emiliania huxleyi* (Bratbak et al., 1993; Brussaard et al., 1996), *Aureococcus anophagefferens* (Gastrich et al., 2004) and *Heterosigma circularisquama* (Nagasaki et al., 2004). The high percentage of algal cells containing viral particles suggested that viral mediated lysis played an important role in the termination of algal blooms. Although these observations suggest that viruses were significant agents for bloom termination, the quantitative estimates remained unclear.

A recent quantitative approach to estimate virus mediated mortality was determined from the number of viruses produced divided by an empirical virus burst size (number of viruses produced per cell). For example, in a mesocosm study using the photosynthetic marine algae, *Phaeocystis globosa* as a model organism, Brussaard *et al* (2005a) determined a 7-100% of mortality of *P. globosa* cells was virally mediated. Using a classical dilution approach, during a spring bloom of *P. globosa*, Baudoux *et al* (2006) estimated that ∼ 66% of the *P. globosa* single cells were virally lysed.

The viral mediated mortality non-bloom forming algae have also been studied (Zingone et al., 1999). A prominent example is the photosynthetic picoeukaryote *Micromonas pusilla*, whose daily viral mediated lysis results in a 2-25% mortality of host standing stock (Cottrell and Suttle, 1995; Evans et al., 2003).

Our understanding of the global significance of viral lysis on phytoplankton mortality is emerging. In summary, studies conducted in the last years have made it increasingly evident that viruses infecting bloom and non-bloom forming eukaryotic algae are significant driving forces in algae population dynamics (Brussaard and Martínez, 2008; Short, 2012).

Table 1: Recent examples of algal hosts and viruses that were isolated and characterised in cultures. Modified after Brussaard *et al* (2008).

Algal host	Virus type	Latent period (h)*	Virus code	Principal references
Bloom-forming algae				
Raphidophytes				
Heterosigma akashiwoe	dsDNA	17	OIs1	(Lawrence et al., 2006)
Heterosigma akashiwoe	ssRNA	35	HaRNAV	(Tai, 2003)
Heterosigma akashiwoe	dsDNA	ND	HaV	(Nagasaki and Yamaguchi, 1997)
Prymnesiophytes				
Emiliania huxleyi	dsDNA	12-14	EhV	(Castberg et al., 2002)
Phaeocystis globosa	dsDNA	12-16	PgV-Group II	(Baudoux and Brussaard, 2005)
Phaeocystis globosa	dsDNA	8-12	PgV-Group I	(Baudoux and Brussaard, 2005)
Phaeocystis pouchetii	dsDNA	12-18	PpV	(Jacobsen et al., 1996)
Chrysochromulina ericina	dsDNA	14-19	CeV	(Sandaa et al., 2001)
Chrysochromulina brevifilum	dsDNA	ND	CbV	(Suttle et al., 1995)
Bacillariophytes				
Rhizosolenia setigerae	ssRNA	<24	RsRNAV	(Nagasaki et al., 2004)
Chaetoceros debilise	ssDNA	12-24	CdebDNAV	(Tomaru et al., 2008)
Asterionellopsis glacialis	ssRNA	ND	AglaRNAV	(Tomaru et al., 2012)
Thalassionema nitzschioides	ssDNA	ND	TnitDNAV	(Tomaru et al., 2012)
Dinophytes				
Heterocapsa circularisquamae	dsDNA	24	HcV	(e.g., (Tarutani et al., 2001))
Heterocapsa circularisquamae	ssRNA	ND	HcRNAV	(Tomaru et al., 2004b)
Non-bloom-forming algae				
Prasinophytes				
Micromonas pusilla	dsDNA	7-14	MpV	(Waters and Chan, 1982)
Micromonas pusilla	dsDNA	36	MpRVh	(Brussaard et al., 2004b)
Pyramimonas orientalis	dsDNA	14-19	PoV	(Sandaa et al., 2001)

ND: Not determined,
- **Time period between point of infection and cell lysis.**

1.3.2 Factors influencing viral infectivity

A successful infection depends on both the number of viruses present and the response of the host cells. A high number of viruses does not necessarily imply higher host mortality, rather mortality depends on how many viruses were infective at that period of time. The length of the lytic cycle and the number of infectious viruses produced after cell lysis critically influences the propagation of infection and subsequently the algal population dynamics (Brown et al., 2006). Although viruses impose significant mortality on host populations, algal blooms do occur.

Recent studies show evidence that temperature, UV radiation, presence of colloids or aggregates and grazing could result in the loss of viral infectivity (Kapuscinski and Mitchell, 1980; Suttle and Chen, 1992; Noble and Fuhrman, 1997; Jacquet and Bratbak, 2003; Brussaard et al., 2005a). Additionally, the response by the host cell to viral infection also affects the number of viruses available for infection (Brussaard and Martínez, 2008). The release of potential virucidal compounds by the host cell during viral infection can reduce the infection rates of other algal cells (Evans et al., 2003; Thyrhaug et al., 2003). It is hypothesized that prior to host cell lysis, the formation of flocs (**Figure 2**) in the alga, *Phaeocystis globosa,* increases viral attachment by up to 68% and ultimately leads to viral inactivation ((Sheik et al., 2012), Chapter 2).
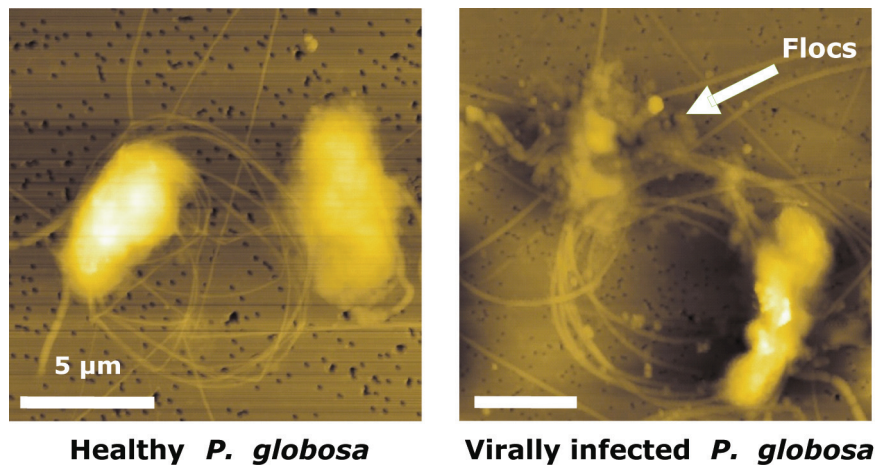

Healthy *P. globosa*   Virally infected *P. globosa*

Figure 2: Atomic force microscopy imaging of *Phaeocystis globosa* cells visualising flocculants prior to cell lysis (19 h post-infection).

Additionally, few algal hosts possess successful mechanisms or strategies for escaping viral infection. For example, *Phaeocystis sp.* has an interesting life history alternating between colonial and single cell stages (Schoemann et al., 2005). It has been suggested that the mucilaginous layer around colonial *Phaeocystis sp.* offers protection against viral infection (Bratbak et al., 1998b; Hamm et al., 1999). In response to viral infection, infected dinoflagellate cells (*Heterosigma akashiwo)* showed enhanced sinking rates (Lawrence et al., 2006). Viral infection in a coccolithophore, *Emiliania huxleyi,* triggered programmed cell death by the induction of host metacaspases as an escaping strategy (Bidle et al., 2007). The transition of *E. huxleyi* from diploid to the haploid phase of its life cycle appears to be another escape strategy, since haploid forms are resistant to viral infection (Frada et al., 2008).

Finally, resistance to viral infection is claimed as the ultimate escape from viral control. During an *E. huxleyi* bloom with a genetically diverse algal host and virus populations, Schroeder *et al* (2003) demonstrated that only a few viral genotypes were actually responsible for the bloom demise. Conversely, during blooms of *Heterocapsa akashiwo* (Tomaru et al., 2004a) and *H. circulisquama* (Tomaru et al., 2007), viral infections led to different host-virus combinations that varied year to year.

1.4 Ecological implications of algal viruses

Algal host cell death by viral infections, not only influences the algal population dynamics, but also regulates the microbial community structure and thereby drives global biogeochemical cycles. Using a theoretical modeling approach, Fuhrman *et al* (1992) predicted that viral lysis results in increased levels of bacterial activity (~27% increase in bacterial respiration and production rates) and reduces the transfer of organic matter to higher trophic levels (~37%) relative to a virus-free model. Thus, viral lysis can facilitate the availability of substrates for microbial-mediated processes and therefore direct food webs towards regenerative pathways (Fuhrman, 1999; Suttle, 2005). This section introduces the impact of algal viruses mediating the flow of biogeochemical elements, their regulation on the bacterial community structure and how the combination of these two factors influences the food web.

1.4.1 The impact of algal virus on biogeochemical cycles

Viruses are devoid of their own cellular machinery and depend on host resources for propagation. Most viruses infecting algal populations are reported to be lytic and can be characterised by their latent period (Table 1, (Brussaard and Martínez, 2008)). The infection period is a critical step for viral propagation, as the virus relies on host resources. Previous studies have shown that viral infection alters hosts cellular metabolism such as fatty acid and pigment composition (Llewellyn et al., 2007; Evans et al., 2009a), host DNA content (Brussaard et al., 1999), intracellular enzyme activity (Brussaard et al., 2001) and the production of cellular metabolites (Evans, 2007). Furthermore, as algae are photosynthetic, it is likely that viral infections can affect host physiology such as carbon assimilation. Previous studies have reported that viral infection either could lead to a rapid inhibition of host carbon assimilation (Van Etten et al., 1983; Seaton et al., 1995) or that assimilation could continue until cell lysis (e.g., (Bratbak et al., 1998b)). Very recently, the application of high resolution single cell techniques have demonstrated that viral infection of *P. globosa* affects the host carbon assimilation mainly by impeding the release of carbon enriched star-like structures ((Sheik et al., 2012), chapter 2). The alteration of host physiology during viral infection is an important consideration as it could influence the quality and quantity of organic matter released due to viral lysis and ultimately affects microbial communities and global biogeochemical cycles.

An initial attempt to assess the uptake of algal viral lysates by bacterial populations was carried out by Gobler *et al* (1997). Using radiotracer experiments, the authors found that viral lysis of a marine Chrysophyte *Aureococcous anophagefferens* causes a clear disparity between which elements are released as dissolved organic matter (DOM) and those which are retained in the particulate phase. Interestingly, viral lysis of *A. anophagefferens* released more than 50% of carbon and selenium compounds into the dissolved phase, where phosphorus and iron were retained within the particulate phase. Complementary to these observations, during viral lysis of *Phaeocystis* organic carbon was efficiently remineralised (Bratbak et al., 1998a; Brussaard et al., 2005a), enhancing bacterial utilization (Brussaard et al., 2005b). Recently, in a model ecosystem study using two autotrophic flagellates, *Phaeocystis pouchetii* and *Rhodomonas salina*, Haaber *et al* (2009) suggested that viral lysis of *P. pouchetii* had resulted in significant nitrogen (~78%) and phosphate (~26%) remineralization. Furthermore, the authors

emphasized the potential importance of the viral activity in supporting marine primary production as *P. pouchetii* lysates may have served as a nutrient link to non-infected *R. salina* propagation.

Consistent with laboratory studies, studies in the marine environment have concluded that algal viral lysates can act as an important source of carbon and nutrient elements. In the oligotrophic environments of the North Atlantic, viral lysis released ~ 21% of the total algal carbon production (Baudoux et al., 2007). Comparably in the South Pacific, highly variable amounts (9-96%) of the total dissolved nitrogen pool were regenerated daily due to viral lysis (Matteson et al., 2012).

1.4.2 The impact of algal viral lysis on bacterial community structure

In surface waters, prokaryotic communities are primarily comprised of eleven broad groups of marine picoplankton (Giovannoni and Rappé, 2000). Amongst them, the major bacterial groups of G*ammaproteobacteria*, *Alphaproteobacteria* and the *Bacteroidetes* constitute a significant proportion of picoplankton in most pelagic waters (Rappe et al., 1997; Giovannoni and Stingl, 2005; Kirchman et al., 2005). These bacterial members possess a suite of lifestyles to derive energy for survival such as autotrophy, heterotrophy, chemoautotrophy or mixotrophy (Kirchman, 2000; Venter et al., 2004).

In coastal environments, algal spring blooms are a prominent seasonal feature, leading to distinct successions of major bacterial groups (Alderkamp et al., 2007; Lamy et al., 2009; Teeling et al., 2012). Particularly, specific taxonomic groups, such as A*lteromonadaceae* (*Gammaproteobacteria*) and *Rhodobacteriaceae* (*Alphaproteobacteria*) which are normally rare can comprise a substantial proportion of bacterial communities for short periods of time during such seasonal algal blooms (Allers et al., 2007; Ferrera et al., 2011; Tada et al., 2011). Thus, sudden changes in the particulate organic matter (POM) and dissolved organic matter (DOM) during algal blooms may stimulate the growth of opportunistic bacterial populations (r-strategists). Consequently, r-strategists can represent much of the actively growing bacteria and therefore be responsible for major carbon and nutrient transformations in the ocean (Alonso and Pernthaler, 2006; Ferrera et al., 2011; Tada et al., 2011).

The quantity and the quality of the algal derived organic matter also regulates the bacterial community composition (Kirchman, 2000), which in turn, is a function of the composition of phytoplankton and their primary production (Falkowski et al.,

1997). Algal growth limiting conditions (such as nutrients and light) and community composition could result in the modifications of DOM concentration composition (Passow et al., 2007), thereby structuring the bacterial communities. To utilize varied compounds of algal derived DOM, a great diversity of uptake mechanisms and metabolic pathways have evolved among phylogenetically diverse bacteria (Teeling et al., 2012). Therefore the quality of algal derived compounds should be a strong selective force on bacterial community composition.

Algal-derived viral lysates consist of a variety of readily available (labile) substrates, which may sustain the coexistence of microbial populations with different ecological traits (Myklestad, 2000). An understanding of the mechanisms by which viral mediated algal mortality influences and regulates bacterial diversity is beginning to emerge. Previous studies documented the sharp increase in the bacterial abundance soon after viral-mediated decline of algal blooms (Gobler et al., 1997; Bratbak et al., 1998a; Castberg et al., 2001; Larsen et al., 2001; Haaber and Middelboe, 2009). However, very few studies have identified bacterial populations that resulted from viral lysis. For example, Castberg *et al* (2001) noted the changes in the bacterial community structure and related it to the viral induced mortality of *E. huxleyi*. In a mesocosm study, viral mediated lysis of *P. globosa* blooms led to rapid changes in the microbial community structure to one dominated by *Alphaproteobacteria* and *Bacteroidetes* members (Brussaard et al., 2005b).

Algal viruses vs. bacteriophages: Typically, in coastal environments, bacterial abundance is highest during and after the demise of an algal bloom and thus could also include bacteriophage mediated mortality among others (Weinbauer, 2004; Brussaard et al., 2007). Bacterial succession patterns can be moreover shaped by their selective mortality, e.g., bacteriophage mediated lysis.

Rough estimates suggest that 10-20% of the bacterioplankton is virally lysed daily (Suttle, 1994). The high host specificity of viruses can structure the relative proportions of different bacterial populations rather than solely affecting the total bacterial abundance (Thingstad, 2000). It is a general assumption that viruses help maintain bacterial diversity as explained by a density-dependent relationship referred to as 'Killing the winner' (Thingstad, 1997) **(Figure 3)**. It is a conceptual prey-predator model, with the assumption that dominant bacterial populations are more susceptible to lysis due to increased contact rates with their specific viruses and results in counteracting one bacterial population's dominance. Thus, the consequence maintains the species diversity within bacterial communities and allows rare bacterial

groups to compete for resources. If substantial bacterial phage lysis occurs, the availability of organic substrates should increase and help sustain other bacterial communities (Middelboe et al., 1996; 2006; 2006) or algal populations (Shelford et al., 2012). The 'Killing the winner' hypothesis partly explains Hutchinson's paradox (Hutchinson, 1961), which raises the question '*how many microbial populations can co-exist when resources are limiting*'.

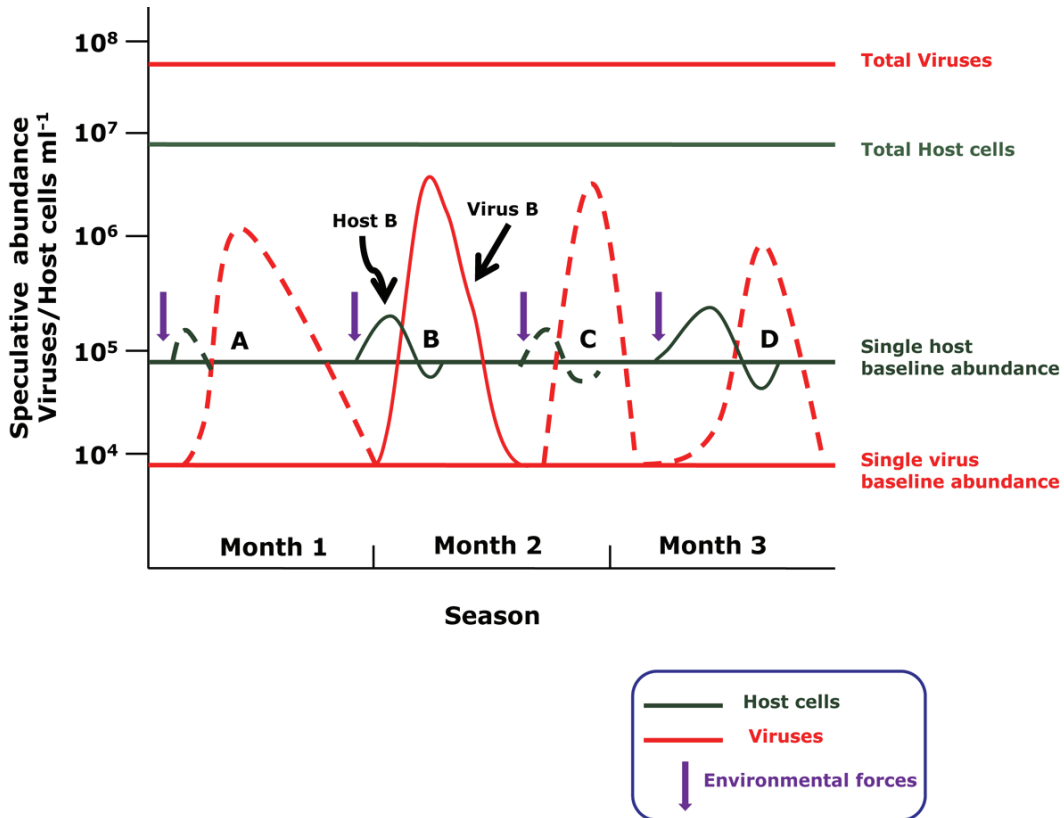**Figure 3: A hypothetical scenario to demonstrate the 'Kill the Winner' hypothesis showing how viruses control the host community diversity. An environmental factor stimulates the growth of a specific host. After reaching a critical host cell density, viral lysis causes the abundance of host cells to decline to baseline levels. The image was adapted and modified from Wommack and Colwell (2000).**

There is increasing evidence that viral lysis of algae and bacteria produces organic aggregates, potentially due to the release of 'sticky' lysis products (Suttle et al., 1990; Peduzzi and Weinbauer, 1993; Shibata et al., 1997; Brussaard et al., 2005b; Mari et al., 2005). Furthermore, these aggregates in turn could act as hot spots for bacterial communities (Azam, 1998). Aggregate-associated bacteria are often characterized by high abundances, enhanced enzymatic activities and growth rates relative to their free-living counterparts (e.g., (Simon et al., 2002)). However, due to their high bacterial abundance, it is estimated that ~37 % of the aggregate-associated bacteria may be killed by viral lysis (Proctor and Fuhrman, 1991). Therefore, determining the role of these individual groups in utilizing algal derived organic matter either due to viral lysis or exudation, is critical to understand their ecological roles and specific contributions to marine biogeochemical cycles.

1.4.3 Algal viruses: new players in the microbial loop

The eternal quest: *'Who are the trophic partners in the food web, how active are they, how elements are cycled in the microbial food web and how is this ecosystem controlled by external and by internal factors?'* (Thingstad et al., 1993).

In the last three decades, research in marine microbial ecology has undergone substantial changes in an attempt to fit together emerging puzzling pieces of new information to create a big picture (Fenchel, 2008). To begin with, the classical perception of marine food web suggested that bacteria were unable to derive resources from dissolved organic material (DOM) (Krogh, 1934; Sverdrup et al., 1942). Improvements in techniques for counting bacteria (Hobbie et al., 1977) together with the evidence that a substantial part of the bacterial communities is metabolically active (Hobbie et al., 1972; Meyer-Reil, 1978) indicated that marine bacteria in fact play a significant role in the transformation of organic matter and challenged the concept of the classical food web .

Later on, the term 'Microbial loop' (Azam et al., 1983) was introduced to describe how microbial communities e.g., unicellular algae, prokaryotes and grazers interact and influence each other. The conceptual framework was that phytoplankton populations being the primary producers at sea, sequester vast amounts of inorganic carbon and nutrients and transform them into organic material. The produced organic material is utilization in the upper ocean by bacteria. These bacteria are subsequently eaten by grazers, which in turn, are eaten by higher organisms. This

conventional view of the microbial loop, suggests that the primary source of DOM is phytoplankton exudation and sloppy feeding by zooplankton.

Now, our understanding of the microbial loop has added another box to the model, one composed of viruses as a new functional group. Viruses as small-sized particles do not add any new processes to the microbial loop. Instead, as significant mortality agents causing cell lysis e.g., for algal populations, contribute to elemental cycling by altering the availability of particulate and dissolved forms of organic matter. This process termed as 'viral shunt' (Wilhelm and Suttle, 1999), is the simplest approximation of how viruses may mediate global biogeochemical cycles. Thus, viral shunt (e.g., algal cell lysis), could lead to substrates becoming more available for microbial-mediated remineralisation, directing food webs towards regenerative pathways (Fuhrman, 1999; Suttle, 2005).

Algal virus activity also affects aggregate formation and degradation (Weinbauer, 2004; Weinbauer et al., 2011). The transfer of virally induced organic aggregates from the pelagic environment to the sea-floor may increase sinking rates. Thus, enhancing the biological carbon pump, which describes the biologically regulated transfer of particulate carbon from the euphotic zone to the deep-sea. Conversely, the high bacterial association with aggregates and their lysis by phages may increase dissolution of aggregates through the release of intracellular enzymes (Proctor and Fuhrman, 1991). Overall, algal viral lysis may influence biogeochemical cycles either by increasing the availability of organic substrates in the pelagic environment or by enhancing particle aggregation and their transfer into the deep sea (Brussaard et al., 2008).
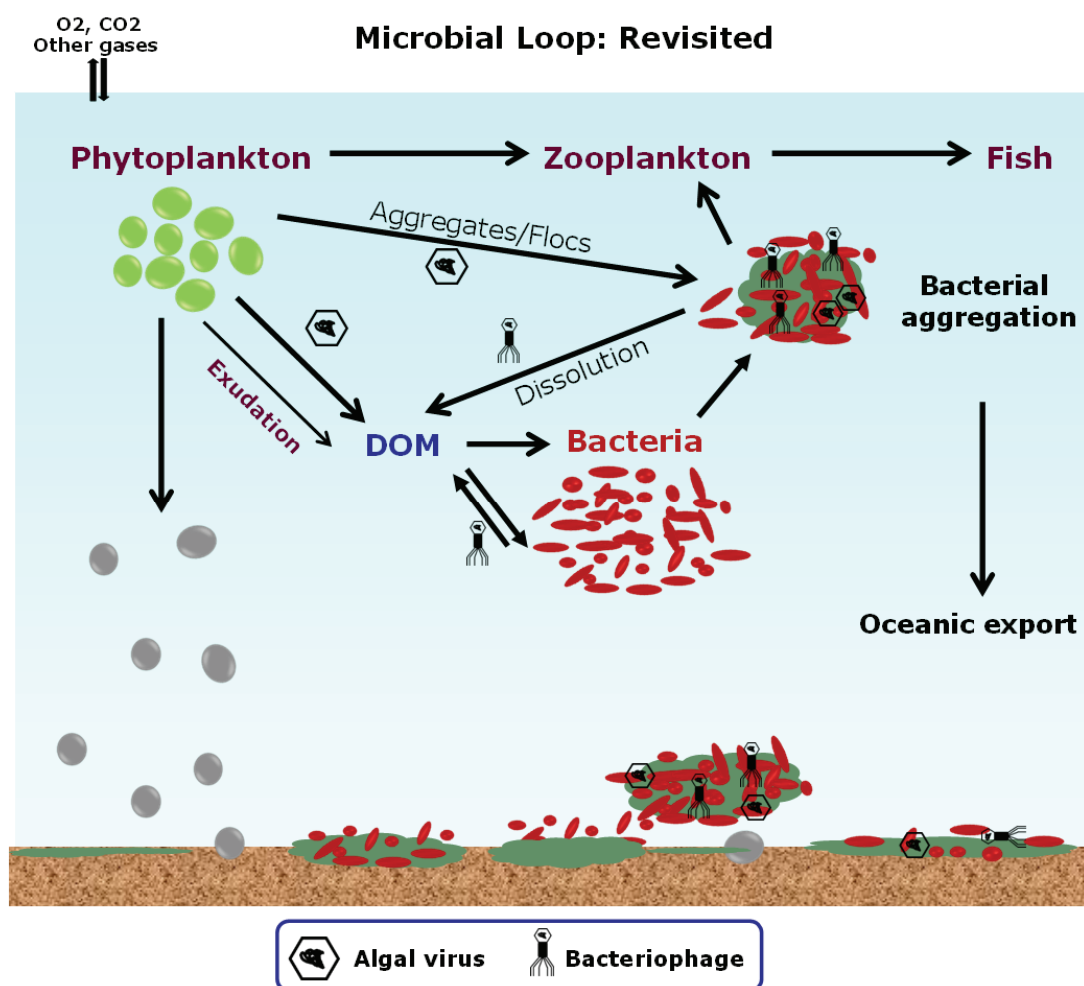
Figure 3: The conceptual model of the microbial loop illustrating the flow of carbon, nutrients and energy up the food chain. The transfer of senescence or dead algal biomass settling down to the sea-floor is depicted in grey. It represents a new schematic of microbial loop connecting bacteria, viruses and dissolved organic matter. Viral lysis of phytoplankton/algal populations diverts the particulate matter from the higher trophic levels and enhances the availability of dissolved organic matter (DOM) towards bacterial communities. For simplicity the term 'bacteria' is used to represent major bacterial groups observed in this thesis. Algal viral lysis forms aggregates (illustrated in dark green) could retain dense bacterial or viral communities. Depending on oceanic environments (coastal or open oceans) and the bacterial association, the fate of aggregates is decided whether it will be disintegrated enhancing the DOM in the euphotic zones or primes sinking enhancing biological carbon pump.

Given the abundance of microbial biomass in the oceans, it could also be expected that viruses, eukaryotic algal hosts and bacterial populations may impact our climate (Danovaro et al., 2011). The Intergovernmental Panel on Climate Change 2007 (Solomon, 2007) reported that the amount of oceanic organic carbon in DOM far exceeds the difference in atmospheric CO_2 concentrations observed between glacial and interglacial periods, and the amount released by anthropogenic activities. Thus, remineralisation of the oceanic organic carbon pool could considerably impact atmospheric carbon dioxide concentrations (Peltier et al., 2007), a process in which marine viruses have been implicated to play an important role. Additionally, few eukaryotic algae such as *Phaeocystis sp*. (Liss et al., 1994), *Micromonas sp*. (Richard et al., 1998) and *Emiliania sp.* (Malin et al., 1992) are known to produce a nonvolatile dimethylsulfide precursor, which is believed to enhance atmospheric cloud nucleation. Viral lysis of these algal blooms has been suggested to enhance the release of dimethylsulfide as gaseous form directly or indirectly (e.g., (Malin et al., 1998)).

As a final note, the sequence of algal blooms, their termination by virus attack, and the role of associated bacteria, can result in the distinct changes in the organic matter deposition over long geological scales and thus influences the micro-paleontological record of deep-sea sediments (Emiliani, 1993). However, the direct estimates of these virus-mediated activities in the geological past and present remain relatively uncertain and understudied. Understanding how the coupling between viruses and microbial communities occurs is an important subject to study as it directly influences microbial processes and as such determines the global ocean functioning.

1.5 Research motivation and thesis goals

Viruses are known to occur wherever life is documented and their occurrence in the sea causes tremendous mortality of varied life forms. As described above, attempts to integrate virally mediated process in to oceanic food web processes have increased significantly over the years. However, many challenges remain. For example, the direct evidence for and quantification of the impact of viruses on biogeochemical cycles in the microbial loop is still largely missing. The lack of straight forward and reliable techniques to quantify virus-mediated biogeochemical cycles has restricted our understanding of marine viruses (Suttle, 2007).

The studies described in this thesis investigated the impact of algal viral lysis on bacterial community structure, bacterial uptake of virally released organic compounds and oceanic biogeochemical carbon and nitrogen cycles. For the first time, we explored viral process occurring at a single cell level using atomic force microscopy (AFM) and nanometer-scale Secondary-Ion Mass Spectrometry (nanoSIMS).

We performed stable isotopic incubation experiments using the ecologically significant micro-algae, *Phaeocystis globosa*, a prominent bloom forming algae with its virus PgV-07T (Baudoux and Brussaard, 2005) and a non-blooming forming pico-algae *Micromonas pusilla* with its virus MpV-08T obtained from the culture collection of Royal Netherlands Institute for Sea Research (NIOZ). The bacterial populations used in this experiment were obtained from the Southern North Sea near Texel, The Netherlands. Changes in the bacterial community composition were monitored quantitatively by catalyzed reporter deposition fluorescent *in situ* hybridization (CARD-FISH) and qualitatively by amplicon pyrosequencing. The biogeochemical parameters were analysed using bulk measurements and single-cell substrate uptake measurements with nanoSIMS. Furthermore, changes in the cellular morphology of algal cells and algal-bacterial interactions were imaged using AFM.

The major goals of this study were

1. To investigate the impact of viral infection on host carbon and/or nitrogen assimilation (Chapters 2-4).

2. To investigate how viral infection interferes with the other cellular mechanisms such as the release of chitinous star-like structures of *P. globosa* single cells (Chapter 2).

3. To determine the impact of algal viral lysis on the bacterial community composition and diversity (Chapters 3 and 4).

4. To determine the subsequent bacterial uptake of virally released organic compounds and quantification of remineralised carbon pool (Chapters 3 and 4).

5. To quantify the extent of bacterial uptake of newly assimilated and previously incorporated algal biomass released by viral lysis (Chapter 4).

1.6 Publication overview

Chapter 2: Viral infection of *Phaeocystis globosa* impedes release of chitinous star-like structures: quantification using single cell approaches.
(Published as early view in the journal Environmental Microbiology, DOI: 10.1111/j.1462-2920.2012.02838.x)

A.R. Sheik[1], C.P.D. Brussaard[2], G. Lavik[1], R.A. Foster[1], N. Musat[1,3], B. Adam[1], M.M.M. Kuypers[1]

[1] Department of Biogeochemistry, Max Planck Institute for Marine Microbiology, Bremen, Germany.

[2] Department of Biological Oceanography, NIOZ - Royal Netherlands Institute for Sea Research, Texel, The Netherlands.

[3] Current address: Department of Isotope Biogeochemistry, Helmholtz Centre for Environmental Research – UFZ, Permoserstraße 15, Leipzig, Germany.

Chapter 3: Algal viral infection fuels bacterial substrate assimilation and drives community structure (In preparation)

A.R. Sheik[1], C.P.D. Brussaard[2], G. Lavik[1], P. Lam[1], N. Musat[1,3], A. Krupke[1], S. Littman[1], M.M.M. Kuypers[1]

[1] Department of Biogeochemistry, Max Planck Institute for Marine Microbiology, Bremen, Germany.

[2] Department of Biological Oceanography, NIOZ - Royal Netherlands Institute for Sea Research, Texel, The Netherlands.

[3] Current address: Department of Isotope Biogeochemistry, Helmholtz Centre for Environmental Research – UFZ, Permoserstraße 15, Leipzig, Germany.

Chapter 4: Viral infection of *Micromonas pusilla* hinders the new pyrenoid synthesis (starch and protein production) and regulates specific bacterial community structure. (In preparation)

A.R. Sheik[1], C.P.D. Brussaard[2], P. Lam[1], G. Lavik[1], B. Adam[1], S. Littman[1], M.M.M. Kuypers[1]

[1] Department of Biogeochemistry, Max Planck Institute for Marine Microbiology, Bremen, Germany.

[2] Department of Biological Oceanography, NIOZ - Royal Netherlands Institute for Sea Research, Texel, The Netherlands.

1.7 References

Alderkamp, A.C., Van Rijssel, M., and Bolhuis, H. (2007) Characterization of marine bacteria and the activity of their enzyme systems involved in degradation of the algal storage glucan laminarin. *FEMS microbiology ecology* **59**: 108-117.

Allers, E., Gómez-Consarnau, L., Pinhassi, J., Gasol, J.M., Šimek, K., and Pernthaler, J. (2007) Response of *Alteromonadaceae* and *Rhodobacteriaceae* to glucose and phosphorus manipulation in marine mesocosms. *Environmental Microbiology* **9**: 2417-2429.

Alonso, C., and Pernthaler, J. (2006) *Roseobacter* and SAR11 dominate microbial glucose uptake in coastal North Sea waters. *Environ. Microbiol.* **8**: 2022-2030.

Angly, F.E. (2006) The marine viromes of four oceanic regions. *PLoS Biol.* **4**: 2121-2131.

Azam, F. (1998) Microbial control of oceanic carbon flux: The plot thickens. *Science* **280**: 694-696.

Azam, F., Fenchel, T., Field, J.G., Gray, J.S., Meyer-Reil, L.A., and Thingstad, F. (1983) The ecological role of water-column microbes in the sea. *Mar Ecol Prog Ser* **10**: 257-263.

Baudoux, A.C., and Brussaard, C.P.D. (2005) Characterization of different viruses infecting the marine harmful algal bloom species *Phaeocystis globosa*. *Virology* **341**: 80-90.

Baudoux, A.C., Noordeloos, A.A.M., Veldhuis, M.J.W., and Brussaard, C.P.D. (2006) Virally induced mortality of *Phaeocystis globosa* during two spring blooms in temperate coastal waters. *Aquat. Microb. Ecol.* **44**: 207-217.

Baudoux, A.C., Veldhuis, M.J.W., Witte, H.J., and Brussaard, C.P.D.D. (2007) Viruses as mortality agents of picophytoplankton in the deep chlorophyll maximum layer during IRONAGES III. *Limnology and Oceanography* **52**: 2519-2529.

Bergh, O., Borsheim, K.Y., Bratbak, G., and Heldal, M. (1989) High abundance of viruses found in aquatic environments. *Nature* **340**: 467-468.

Bidle, K.D., Haramaty, L., Barcelos e Ramos, J., and Falkowski, P. (2007) Viral activation and recruitment of metacaspases in the unicellular coccolithophore, *Emiliania huxleyi*. *Proceedings of the National Academy of Sciences* **104**: 6049.

Boehme, J., Frischer, M.E., Jiang, S.C., Kellogg, C.A., Pichard, S., Rose, J.B. et al. (1993) Viruses, bacterioplankton, and phytoplankton in the southeastern Gulf of Mexico: distribution and contribution to oceanic DNA pools. *Marine Ecology-Progress Series* **97**: 1.

Borsheim, K.Y., Bratbak, G., and Heldal, M. (1990) Enumeration and biomass estimation of planktonic bacteria and viruses by transmission electron-microscopy. *Applied and Environmental Microbiology* **56**: 352-356.

Bratbak, G., Egge, J.K., and Heldal, M. (1993) Viral mortality of the marine alga *Emiliania huxleyi* (Haptophyceae) and termination of algal blooms. *Marine Ecology-Progress Series* **93**: 39-48.

Bratbak, G., Jacobsen, A., and Heldal, M. (1998a) Viral lysis of *Phaeocystis pouchetii* and bacterial secondary production. *Aquatic Microbial Ecology* **16**: 11-16.

Bratbak, G., Heldal, M., Norland, S., and Thingstad, T.F. (1990) Viruses as partners in spring bloom microbial trophodynamics. *Appl. Environ. Microbiol.* **56**: 1400-1405.

Bratbak, G., Heldal, M., Thingstad, T.F., and Tuomi, P. (1996) Dynamics of virus abundance in coastal seawater. *FEMS Microbiology Ecology* **19**: 263-269.

Bratbak, G., Jacobsen, A., Heldal, M., Nagasaki, K., and Thingstad, F. (1998b) Virus production in *Phaeocystis pouchetii* and its relation to host cell growth and nutrition. *Aquatic Microbial Ecology* **16**: 1-9.

Breitbart, M. (2002) Genomic analysis of uncultured marine viral communities. *Proc. Natl Acad. Sci. USA* **99**: 14250-14255.

Breitbart, M. (2012) Marine Viruses: Truth or Dare. *Annual Review of Marine Science* **4**: 425-448.

Brown, C.M., Lawrence, J.E., and Campbell, D.A. (2006) Are phytoplankton population density maxima predictable through analysis of host and viral genomic DNA content? *Journal of the Marine Biological Association of the UK* **86**: 491-498.

Brown Jr, R.M. (1972) Algal viruses. *Adv. Virus Res* **17**: 243-277.

Brussaard, C.P.D. (2004a) Viral control of phytoplankton populations - a review. *Journal of Eukaryotic Microbiology* **51**: 125-138.

Brussaard, C.P.D. (2004b) Optimization of procedures for counting viruses by flow cytometry. *Appl Environ Microbiol* **70**: 1506-1513.

Brussaard, C.P.D. (2009) Enumeration of bacteriophages using flow cytometry. *Methods Mol Biol* **501**: 97-111.

Brussaard, C.P.D., and Martínez, J.M. (2008) Algal bloom viruses. *Plant Viruses* **2**: 1-10.

Brussaard, C.P.D., Kuipers, B., and Veldhuis, M.J.W. (2005a) A mesocosm study of *Phaeocystis globosa* population dynamics: 1. Regulatory role of viruses in bloom. *Harmful Algae* **4**: 859-874.

Brussaard, C.P.D., Thyrhaug, R., Marie, D., and Bratbak, G. (1999) Flow cytometric analyses of viral infection in two marine phytoplankton species, *Micromonas pusilla* (Prasinophyceae) and *Phaeocystis pouchetii* (Prymnesiophyceae). *Journal of Phycology* **35**: 941-948.

Brussaard, C.P.D., Marie, D., Thyrhaug, R., and Bratbak, G. (2001) Flow cytometric analysis of phytoplankton viability following viral infection. *Aquatic Microbial Ecology* **26**: 157-166.

Brussaard, C.P.D., Short, S.M., Frederickson, C.M., and Suttle, C.A. (2004a) Isolation and phylogenetic analysis of novel viruses infecting the phytoplankton *Phaeocystis globosa* (Prymnesiophyceae). *Appl Environ Microbiol* **70**: 3700-3705.

Brussaard, C.P.D., Mari, X., Van Bleijswijk, J.D.L., and Veldhuis, M.J.W. (2005b) A mesocosm study of *Phaeocystis globosa* (Prymnesiophyceae) population dynamics - II. Significance for the microbial community. *Harmful Algae* **4**: 875-893.

Brussaard, C.P.D., Bratbak, G., Baudoux, A.C., and Ruardij, P. (2007) *Phaeocystis* and its interaction with viruses. *Biogeochemistry* **83**: 201-215.

Brussaard, C.P.D., Kempers, R.S., Kop, A.J., Riegman, R., and Heldal, M. (1996) Virus-like particles in a summer bloom of *Emiliania huxleyi* in the North Sea. *Aquatic Microbial Ecology* **10**: 105-113.

Brussaard, C.P.D., Noordeloos, A.A., Sandaa, R.A., Heldal, M., and Bratbak, G. (2004b) Discovery of a dsRNA virus infecting the marine photosynthetic protist *Micromonas pusilla*. *Virology* **319**: 280-291.

Brussaard, C.P.D., Wilhelm, S.W., Thingstad, F., Weinbauer, M.G., Bratbak, G., Heldal, M. et al. (2008) Global-scale processes with a nanoscale drive: the role of marine viruses. *ISME J* **2**: 575-578.

Brussaard, C.P.D.M., J. M. (2008) Algal Bloom Viruses. *Plant viruses, Global science books* **2 (1)**: 1-10.

Castberg, T., Thyrhaug, R., Larsen, A., Sandaa, R.A., Heldal, M., Van Etten, J.L., and Bratbak, G. (2002) Isolation and characterization of a virus that infects *Emiliania huxleyi* (Haptophyta). *Journal of Phycology* **38**: 767-774.

Castberg, T., Larsen, A., Sandaa, R.A., Brussaard, C.P.D.D., Egge, J.K., Heldal, M. et al. (2001) Microbial population dynamics and diversity during a bloom of the marine coccolithophorid *Emiliania huxleyi* (Haptophyta). *Marine Ecology-Progress Series* **221**: 39-46.

Claverie, J.M., Ogata, H., Abergel, C., Suhre, K., and Fournier, P.E. (2006) Mimivirus and the emerging concept of "giant" virus. *Virus research* **117**: 133-144.

Cochlan, W.P., Wikner, J., Steward, G.F., Smith, D.C., and Azam, F. (1993) Spatial distribution of viruses, bacteria and chlorophyll a in neritic, oceanic and estuarine environments. *Mar. Ecol. Prog. Ser.* **92**: 77-87.

Cottrell, M.T., and Suttle, C.A. (1995) Genetic diversity of algal viruses which lyse the photosynthetic picoflagellate *Micromonas pusilla* (Prasinophyceae). *Appl. Environ. Microbiol.* **61**: 3088-3091.

Danovaro, R., Dell'anno, A., Trucco, A., Serresi, M., and Vanucci, S. (2001) Determination of virus abundance in marine sediments. *Appl. Environ. Microbiol.* **67**: 1384-1387.

Danovaro, R., Dell/'Anno, A., Corinaldesi, C., Magagnini, M., Noble, R., Tamburini, C., and Weinbauer, M. (2008) Major viral impact on the functioning of benthic deep-sea ecosystems. *Nature* **454**: 1084-1087.

Danovaro, R., Corinaldesi, C., Dell'Anno, A., Fuhrman, J.A., Middelburg, J.J., Noble, R.T., and Suttle, C.A. (2011) Marine viruses and global climate change. *FEMS Microbiology Reviews* **35**: 993-1034.

De Corte, D., Sintes, E., Winter, C., Yokokawa, T., Reinthaler, T., and Herndl, G.J. (2010) Links between viral and prokaryotic communities throughout the water column in the (sub)tropical Atlantic Ocean. *ISME J* **4**: 1431-1442.

Dinsdale, E.A. (2008) Functional metagenomic profiling of nine biomes. *Nature* **452**: 629-632.

Duckworth, D. (1987) History and basic properties of bacterial viruses. In *Phage Ecology*. Goyal, S.M., Gerba, C.P., and Bitton, G. (eds). New York.
: John Wiley & Sons, pp. 1-44.

Emiliani, C. (1993) Extinction and viruses. *Biosystems* **31**: 155-159.

Evans, C. (2007) The relative significance of viral lysis and microzooplankton grazing as pathways of dimethylsulfoniopropionate (DMSP) cleavage: an *Emiliania huxleyi* culture study. *Limnol. Oceanogr.* **52**: 1036-1045.

Evans, C., and Brussaard, C.P.D. (2012) Regional variation in lytic and lysogenic viral infection in the Southern Ocean and its contribution to biogeochemical cycling. *Applied and Environmental Microbiology* **doi:10.1128/AEM.01388-12**

Evans, C., Pond, D.W., and Wilson, W.H. (2009a) Changes in *Emiliania huxleyi* fatty acid profiles during infection with *E. huxleyi* virus 86: physiological and ecological implications. *Aquatic Microbial Ecology* **55**: 219-228.

Evans, C., Pearce, I., and Brussaard, C.P.D. (2009b) Viral-mediated lysis of microbes and carbon release in the sub-Antarctic and Polar Frontal zones of the Australian Southern Ocean. *Environ Microbiol*.

Evans, C., Archer, S.D., Jacquet, S., and Wilson, W.H. (2003) Direct estimates of the contribution of viral lysis and microzooplankton grazing to the decline of a *Micromonas* spp. population. *Aquatic microbial ecology* **30**: 207-219.

Falkowski, P.G. (1998) Biogeochemical Controls and Feedbacks on Ocean Primary Production. *Science* **281**: 200.

Falkowski, P.G. (2002) The ocean's invisible forest. *Scientific American* **287**: 54-61.

Falkowski, P.G., Raven, J.A., and Laws, E.A. (1997) *Aquatic photosynthesis*: Blackwell Science London, UK.

Fenchel, T. (2008) The microbial loop-25 years later. *Journal of Experimental Marine Biology and Ecology* **366**: 99-103.

Ferrera, I., Gasol, J.M., Sebastian, M., Hojerova, E., and Koblizek, M. (2011) Comparison of growth rates of aerobic anoxygenic phototrophic bacteria and other bacterioplankton groups in coastal Mediterranean waters. *Applied and Environmental Microbiology* **77**: 7451.

Frada, M., Probert, I., Allen, M.J., Wilson, W.H., and de Vargas, C. (2008) The "Cheshire Cat" escape strategy of the coccolithophore *Emiliania huxleyi* in response to viral infection. *Proceedings of the National Academy of Sciences* **105**: 15944-15949.

Fuhrman, J.A. (1992) Bacterioplankton roles in cycling of organic matter: the microbial food web. In *Primary Productivity and Biogeochemical Cycles in the Sea* Falkowski, P.G. (ed): Plenum Press, New York, pp. 361-383.

Fuhrman, J.A. (1999) Marine viruses and their biogeochemical and ecological effects. *Nature* **399**: 541-548.

Fuhrman, J.A., and Suttle, C.A. (1993) Viruses in marine planktonic systems. *Oceanography* **6**: 51-63.

Fuhrman, J.A., and Ouverney, C.C. (1998) Marine microbial diversity studied via 16S rRNA sequences: cloning results from coastal waters and counting of native archaea with fluorescent single cell probes. *Aquatic Ecology* **32**: 3-15.

Fuhrman, J.A., and Hagström, Å. (2008) Bacterial and archaeal community structure and its patterns. *Microbial ecology of the oceans*: 45-90.

Gastrich, M.D., Leigh-Bell, J.A., Gobler, C.J., Roger Anderson, O., Wilhelm, S.W., and Bryan, M. (2004) Viruses as potential regulators of regional brown tide blooms caused by the alga, *Aureococcus anophagefferens*. *Estuaries and Coasts* **27**: 112-119.

Giovannoni, S., and Rappé, M. (2000) Evolution, diversity and molecular ecology of marine prokaryotes. . In *Microbial ecology of the oceans.* DL, K. (ed). New York: Wiley-Liss, pp. 47–84.

Giovannoni, S.J., and Stingl, U. (2005) Molecular diversity and ecology of microbial plankton. *Nature* **437**: 343-348.

Gobler, C.J., Hutchins, D.A., Fisher, N.S., Cosper, E.M., and Sanudo-Wilhelmy, S. (1997) Release and bioavailability of C, N, P, Se, and Fe following viral lysis of a marine Chrysophyte. *Limnol. Oceanogr.* **42**: 1492-1504.

Haaber, J., and Middelboe, M. (2009) Viral lysis of *Phaeocystis pouchetii*: Implications for algal population dynamics and heterotrophic C, N and P cycling. *Isme Journal* **3**: 430-441.

Hamm, C.E., Simson, D.A., Merkel, R., and Smetacek, V. (1999) Colonies of *Phaeocystis globosa* are protected by a thin but tough skin. *Marine Ecology Progress Series* **187**: 101-111.

Hennes, K.P., and Suttle, C.A. (1995) Direct counts of viruses in natural waters and laboratory cultures by epifluorescence microscopy. *Limnol. Oceanogr.* **40**: 1050-1055.

Hobbie, J.E., Daley, R.J., and Jasper, S. (1977) Use of nuclepore filters for counting bacteria by fluorescence microscopy. *Applied and environmental microbiology* **33**: 1225-1228.

Hobbie, J.E., Holm-Hansen, O., Packard, T.T., Pomeroy, L.R., Sheldon, R.W., Thomas, J.P., and Wiebe, W.J. (1972) A study of the distribution and activity of microorganisms in ocean water. *Limnology and oceanography*: 544-555.

Hutchinson, G.E. (1961) The paradox of the plankton. *Am Nat* **95**: 137.

Jacobsen, A., Bratbak, G., and Heldal, M. (1996) Isolation and characterization of a virus infecting *Phaeocystis pouchetii* (Prymnesiophyceae). *Journal of Phycology* **32**: 923-927.

Jacquet, S., and Bratbak, G. (2003) Effects of ultraviolet radiation on marine virus-phytoplankton interactions. *Fems Microbiology Ecology* **44**: 279-289.

Jiang, S.C., and Paul, J.H. (1994) Seasonal and diel abundance of viruses and occurrence of lysogeny/bacteriocinogeny in the marine environment. *Marine Ecology-Progress Series* **104**: 163.

Kapuscinski, R.B., and Mitchell, R. (1980) Processes controlling virus inactivation in coastal waters. *Water research* **14**: 363-371.

Kirchman, D.L. (2000) *Microbial ecology of the oceans*: Wiley-Liss, New York, N.Y.

Kirchman, D.L., Dittel, A.I., Malmstrom, R.R., and Cottrell, M.T. (2005) Biogeography of major bacterial groups in the Delaware Estuary. *Limnology and oceanography*: 1697-1706.

Krogh, A. (1934) Conditions of life in the ocean. *Ecological Monographs* **4**.

Lamy, D., Obernosterer, I., Laghdass, M., Artigas, F., Breton, E., Grattepanche, J.D. et al. (2009) Temporal changes of major bacterial groups and bacterial heterotrophic activity during a *Phaeocystis globosa* bloom in the eastern English Channel. *Aquatic Microbial Ecology* **58**: 95-107.

Larsen, A., Castberg, T., Sandaa, R.A., Brussaard, C.P.D.D., Egge, J., and Heldal, M. (2001) Population dynamics and diversity of phytoplankton, bacteria and viruses in a seawater enclosure. *Mar Ecol Prog Ser* **221**: 47-57.

Lawrence, J.E., Brussaard, C.P.D.D., and Suttle, C.A. (2006) Virus-specific responses of *Heterosigma akashiwo* to infection. *Applied and Environmental Microbiology* **72**: 7829-7834.

Liss, P.S., Malin, G., Turner, S.M., and Holligan, P.M. (1994) Dimethyl sulphide and *Phaeocystis*: a review. *Journal of Marine Systems* **5**: 41-53.

Llewellyn, C.A., Evans, C., Airs, R.L., Cook, I., Bale, N., and Wilson, W.H. (2007) The response of carotenoids and chlorophylls during virus infection of *Emiliania huxleyi* (Prymnesiophyceae). *Journal of Experimental Marine Biology and Ecology* **344**: 101-112.

Malin, G., Turner, S.M., and Liss, P.S. (1992) Sulfur: the plankton/climate connection. *Journal of phycology* **28**: 590-597.

Malin, G., Wilson, W.H., Bratbak, G., Liss, P.S., and Mann, N.H. (1998) Elevated production of dimethylsulfide resulting from viral infection of cultures of *Phaeocystis pouchetii*. *Limnol. Oceanogr.* **43**: 1389-1393.

Mari, X., Rassoulzadegan, F., Brussaard, C.P.D.D., and Wassmann, P. (2005) Dynamics of transparent exopolymeric particles (TEP) production by *Phaeocystis globosa* under N- or P-limitation: a controlling factor of the retention/export balance. *Harmful Algae* **4**: 895-914.

Marie, D., Partensky, F., Vaulot, D., and Brussaard, C. (2001) Enumeration of phytoplankton, bacteria, and viruses in marine samples. *Curr Protoc Cytom* **Chapter 11**: Unit 11 11.

Marie, D., Brussaard, C., Thyrhaug, R., Bratbak, G., and Vaulot, D. (1999) Enumeration of marine viruses in culture and natural samples by flow cytometry. *Appl Environ Microbiol* **65**: 45-52.

Matteson, A.R., Loar, S.N., Pickmere, S., DeBruyn, J.M., Ellwood, M.J., Boyd, P.W. et al. (2012) Production of viruses during a spring phytoplankton bloom in the South Pacific Ocean near of New Zealand. *FEMS Microbiology Ecology* **79**: 709-719.

Mayer, J.A., and Taylor, F.J.R. (1979) A virus which lyses the marine nanoflagellate *Micromonas pusilla*. *Nature* **281**: 299-301.

Meyer-Reil, L.A. (1978) Autoradiography and epifluorescence microscopy combined for the determination of number and spectrum of actively metabolizing bacteria in natural waters. *Applied and environmental microbiology* **36**: 506-512.

Middelboe, M., and Jorgensen, N.O.G. (2006) Viral lysis of bacteria: an important source of dissolved amino acids and cell wall compounds. *J. Mar. Biolog. Assoc. UK* **86**: 605-612.

Middelboe, M., Jorgensen, N.O.G., and Kroer, N. (1996) Effects of viruses on nutrient turnover and growth efficiency of noninfected marine bacterioplankton. *Applied and Environmental Microbiology* **62**: 1991.

Myklestad, S. (2000) Dissolved organic carbon from phytoplankton. *Marine Chemistry*: 111-148.

Nagasaki, K., and Yamaguchi, M. (1997) Isolation of a virus infectious to the harmful bloom causing microalga Heterosigma akashiwo (Raphidophyceae). *Aquat. Microb. Ecol.* **13**: 135-140.

Nagasaki, K., and Brussaard, C.P.D. (2008) Algal viruses (3rd Edn). In *Encyclopedia of Virology (5 Vols)*. Mahy, B.W.J., and Van Regenmortel, M.H.V. (eds). Oxford,: Elsevier, pp. 97-105.

Nagasaki, K., and Bratbak, G. (2010) Isolation of viruses infecting photosynthetic and nonphotosynthetic protests. In: Manual of Aquatic Viral Ecology, *American Society of Limnology and Oceanography*, pp. Chapter 10, 82-91.

Nagasaki, K., Tomaru, Y., Nakanishi, K., Hata, N., Katanozaka, N., and Yamaguchi, M. (2004) Dynamics of *Heterocapsa circularisquama* (Dinophyceae) and its viruses in Ago Bay, Japan. *Aquatic microbial ecology* **34**: 219-226.

Noble, R.T., and Fuhrman, J.A. (1997) Virus decay and its causes in coastal waters. *Applied and Environmental Microbiology* **63**: 77-83.

Noble, R.T., and Fuhrman, J.A. (1998) Use of SYBR Green I for rapid epifluorescence counts of marine viruses and bacteria. *Aquat. Microb. Ecol.* **14**: 113-118.

Parsons, R.J., Breitbart, M., Lomas, M.W., and Carlson, C.A. (2011) Ocean time-series reveals recurring seasonal patterns of virioplankton dynamics in the northwestern Sargasso Sea. *ISME J*.

Passow, U., De La Rocha, C., Arnosti, C., Grossart, H., Murray, A., and Engel, A. (2007) Microbial dynamics in autotrophic and heterotrophic seawater mesocosms. I. Effect of phytoplankton on the microbial loop. *Aquatic microbial ecology* **49**: 109-121.

Paul, J.H. (2008) Prophages in marine bacteria: dangerous molecular time bombs or the key to survival in the seas? *ISME J* **2**: 579-589.

Peduzzi, P., and Weinbauer, M.G. (1993) Effect of concentrating the virus-rich 2-200-nm size fraction of seawater on the formation of algal flocs (marine snow). *Limnology and Oceanography* **38**: 1562-1565.

Peltier, W.R., Liu, Y., and Crowley, J.W. (2007) Snowball Earth prevention by dissolved organic carbon remineralization. *Nature* **450**: 813-818.

Pienaar, R.N. (1976) Virus-like particles in three species of phytoplankton from San Juan Island, Washington. *Phycologia* **15**: 185-190.

Proctor, L.M., and Fuhrman, J.A. (1990) Viral mortality of marine bacteria and cyanobacteria. *Nature* **343**: 60-62.

Proctor, L.M., and Fuhrman, J.A. (1991) Roles of viral infection in organic particle flux. *Marine ecology progress series. Oldendorf* **69**: 133-142.

Rappe, M.S., Kemp, P.F., and Giovannoni, S.J. (1997) Phylogenetic diversity of marine coastal picoplankton 16S rRNA genes cloned from the continental shelf off Cape Hatteras, North Carolina. *Limnology and oceanography*: 811-826.

Richard, W.H., Bradley, A.W., Matthew, T.C., and John, W.H.D. (1998) Virus-mediated total release of dimethylsulfoniopropionate from marine phytoplankton: a potential climate process. *Aquatic Microbial Ecology* **14**: 1-6.

Rivers, T.M. (1937) Viruses and Koch's postulates. *Journal of Bacteriology* **33**: 1-12.

Rohwer, F., and Thurber, R.V. (2009) Viruses manipulate the marine environment. *Nature* **459**: 207-212.

Rowe, J.M., Fabre, M.F., Gobena, D., Wilson, W.H., and Wilhelm, S.W. (2011) Application of the major capsid protein as a marker of the phylogenetic diversity of *Emiliania huxleyi* viruses. *FEMS Microbiology Ecology* **76**: 373-380.

Rowe, J.M., Saxton, M.A., Cottrell, M.T., DeBruyn, J.M., Berg, G.M., Kirchman, D.L. et al. (2008) Constraints on viral production in the Sargasso Sea and North Atlantic. *Aquatic Microbial Ecology* **52**: 233-244.

Sandaa, R.A., Heldal, M., Castberg, T., Thyrhaug, R., and Bratbak, G. (2001) Isolation and characterization of two viruses with large genome size infecting *Chrysochromulina ericina* (Prymnesiophyceae) and *Pyramimonas orientalis* (Prasinophyceae). *Virology* **290**: 272-280.

Schoemann, V., Becquevort, S., Stefels, J., Rousseau, V., and Lancelot, C. (2005) *Phaeocystis* blooms in the global ocean and their controlling mechanisms: a review. *Journal of Sea Research* **53**: 43-66.

Schroeder, D.C., Oke, J., Hall, M., Malin, G., and Wilson, W.H. (2003) Virus succession observed during an *Emiliania huxleyi* bloom. *Applied and environmental microbiology* **69**: 2484-2490.

Seaton, G.G.R., Lee, K., and Rohozinski, J. (1995) Photosynthetic Shutdown in *Chlorella* NC64A associated with the infection cycle of *Paramecium bursaria Chlorella* virus-1. *Plant Physiol.* **108**: 1431-1438.

Sheik, A.R., Brussaard, C.P.D., Lavik, G., Foster, R.A., Musat, N., Adam, B., and Kuypers, M.M.M. (2012) Viral infection of *Phaeocystis globosa* impedes release of chitinous star-like structures: quantification using single cell approaches. *Environmental Microbiology* **DOI: 10.1111/j.1462-2920.2012.02838.x**.

Shelford, E.J., Middelboe, M., Møller, E.F., and Suttle, C.A. (2012) Virus-driven nitrogen cycling enhances phytoplankton growth. *Aquatic Microbial Ecology* **66**: 41-46.

Shibata, A., Kogure, K., Koike, I., and Ohwada, K. (1997) Formation of submicron colloidal particles from marine bacteria by viral infection. *Marine Ecology Progress Series* **155**: 303-307.

Short, S.M. (2012) The ecology of viruses that infect eukaryotic algae. *Environmental Microbiology* **DOI: 10.1111/j.1462-2920.2012.02706.x**.

Simon, M., Grossart, H.P., Schweitzer, B., and Ploug, H. (2002) Microbial ecology of organic aggregates in aquatic ecosystems. *Aquatic Microbial Ecology* **28**: 175-211.

Solomon, S. (2007) *Climate change 2007: the physical science basis: contribution of Working Group I to the Fourth Assessment Report of the Intergovernmental Panel on Climate Change*: Cambridge Univ Pr.

Spencer, R. (1955) A marine bacteriophage. *Nature* **175**: 690-691.

Suttle, C.A. (1994) The significance of viruses to mortality in aquatic microbial communities. *Microb. Ecol.* **28**: 237-243.

Suttle, C.A. (2005) Viruses in the sea. *Nature* **437**: 356-361.

Suttle, C.A. (2007) Marine viruses - major players in the global ecosystem. *Nat Rev Microbiol* **5**: 801-812.

Suttle, C.A., and Chen, F. (1992) Mechanisms and rates of decay of marine viruses in seawater. *Applied and Environmental Microbiology* **58**: 3721-3729.

Suttle, C.A., and Fuhrman, J.A. (2010) Enumeration of virus particles in aquatic or sediment samples by epifluorescence microscopy. *Manual of Aquatic Viral Ecology* **S.W. Wilhelm, M.G. Weinbauer, and C.A. Suttle [eds.]**: 145-153.

Suttle, C.A., Chan, A.M., and Cottrell, M.T. (1990) Infection of phytoplankton by viruses and reduction of primary productivity. *Nature* **347**: 467-469.

Suttle, C.A., Chan, A.M., and Cottrell, M.T. (1995) Viruses infecting the marine Prymnesiophyte *Chrysochromulina* spp.: isolation, preliminary characterization and natural abundance. *Marine ecology progress series. Oldendorf* **118**: 275-282.

Sverdrup, H.U., Johnson, M.W., and Fleming, R.H. (1942) *The Oceans: Their physics, chemistry and general biology*. Englewood Cliffs, NJ: Prentice-Hall, Inc.

Tada, Y., Taniguchi, A., Nagao, I., Miki, T., Uematsu, M., Tsuda, A., and Hamasaki, K. (2011) Differing Growth Responses of Major Phylogenetic Groups of Marine Bacteria to Natural Phytoplankton Blooms in the Western North Pacific Ocean. *Applied and Environmental Microbiology* **77**: 4055-4065.

Tai, V. (2003) Characterization of HaRNAV, a single-stranded RNA virus causing lysis of *Heterosigma akashiwo* (Raphidophyceae). *J. Phycol.* **39**: 343-352.

Tarutani, K., Nagasaki, K., and Yamaguchi, M. (2000) Viral impacts on total abundance and clonal composition of the harmful bloom-forming phytoplankton Heterosigma akashiwo. *Appl. Environ. Microbiol.* **66**: 4916-4920.

Tarutani, K., Nagasaki, K., Itakura, S., and Yamaguchi, M. (2001) Isolation of a virus infecting the novel shellfish-killing dinoflagellate *Heterocapsa circularisquama*. *Aquatic Microbial Ecology* **23**: 103-111.

Teeling, H., Fuchs, B.M., Becher, D., Klockow, C., Gardebrecht, A., Bennke, C.M. et al. (2012) Substrate-controlled succession of marine bacterioplankton populations induced by a phytoplankton bloom. *Science* **336**: 608-611.

Thingstad, T. (1997) A theoretical approach to structuring mechanisms in the pelagic food web. *Hydrobiologia* **363**: 59-72.

Thingstad, T.F. (2000) Elements of a theory for the mechanisms controlling abundance, diversity, and biogeochemical role of lytic bacterial viruses in aquatic systems. *Limnol. Oceanogr.* **45**: 1320-1328.

Thingstad, T.F., Heldal, M., Bratbak, G., and Dundas, I. (1993) Are viruses important partners in pelagic fend webs? *Trends in Ecology & Evolution* **8**: 209-213.

Thyrhaug, R., Larsen, A., Thingstad, T.F., and Bratbak, G. (2003) Stable coexistence in marine algal host-virus systems. *Marine Ecology-Progress Series* **254**: 27-35.

Tomaru, Y., Tarutani, K., Yamaguchi, M., and Nagasaki, K. (2004a) Quantitative and qualitative impacts of viral infection on a *Heterosigma akashiwo* (*Raphidophyceae*) bloom in Hiroshima Bay, Japan. *Aquat. Microb. Ecol.* **34**: 227-238.

Tomaru, Y., Shirai, Y., Suzuki, H., Nagumo, T., and Nagasaki, K. (2008) Isolation and characterization of a new single-stranded DNA virus infecting the cosmopolitan marine diatom *Chaetoceros debilis*. *Aqua Microbial Ecol* **50**: 103-112.

Tomaru, Y., Hata, N., Masuda, T., Tsuji, M., Igata, K., and Masuda, Y. (2007) Ecological dynamics of the bivalve-killing dinoflagellate *Heterocapsa circularisquama* and its infectious viruses in different locations of western Japan. *Environ Microbiol* **9**: 1376-1383.

Tomaru, Y., Toyoda, K., Kimura, K., Hata, N., Yoshida, M., and Nagasaki, K. (2012) First evidence for the existence of pennate diatom viruses. *ISME J* **6**: 1445-1448.

Tomaru, Y., Katanozaka, N., Nishida, K., Shirai, Y., Tarutani, K., Yamaguchi, M., and Nagasaki, K. (2004b) Isolation and characterization of two distinct types of HcRNAV, a single-stranded RNA virus infecting the bivalve-killing microalga *Heterocapsa circularisquama*. *Aquatic microbial ecology* **34**: 207-218.

Torrella, F., and Morita, R.Y. (1979) Evidence by electron micrographs for a high incidence of bacteriophage particles in the waters of Yaquina Bay, oregon: ecological and taxonomical implications. *Applied and environmental microbiology* **37**: 774-778.

Van Etten, J.L., Burbank, D.E., Xia, Y., and Meints, R.H. (1983) Growth cycle of a virus, PBCV-1, that infects *Chlorella*-like algae. *Virology* **126**: 117-125.

Van Etten, J.L., Burbank, D.E., Schuster, A.M., and Meints, R.H. (1985) Lytic viruses infecting a *Chlorella*-like alga. *Virology* **140**: 135-143.

Venter, J.C., Remington, K., Heidelberg, J.F., Halpern, A.L., Rusch, D., Eisen, J.A. et al. (2004) Environmental genome shotgun sequencing of the Sargasso Sea. *Science* **304**: 66-74.

Waters, R., and Chan, A. (1982) *Micromonas pusilla* virus: the virus growth cycle and associated physiological events within the host cells; host range mutation. *Journal of General Virology* **63**: 199.

Weinbauer, M.G. (2004) Ecology of prokaryotic viruses. *FEMS Microbiol. Rev.* **28**: 127-181.

Weinbauer, M.G., and Suttle, C.A. (1999) Lysogeny and prophage induction in coastal and offshore bacterial communities. *Aquatic microbial ecology* **18**: 217-225.

Weinbauer, M.G., Brettar, I., and Hofle, M.G. (2003) Lysogeny and virus-induced mortality of bacterioplankton in surface, deep, and anoxic marine waters. *Limnol. Oceanogr.* **48**: 1457-1465.

Weinbauer, M.G., Chen, F., and Wilhelm, S.W. (2011) Virus-mediated redistribution and partitioning of carbon in the global oceans. *Microbial carbon pump in the ocean*: 54-56.

Weinbauer, M.G., Fuks, D., Puskaric, S., and Peduzzi, P. (1995) Diel, seasonal, and depth-related variability of viruses and dissolved DNA in the northern Adriatic Sea. *Microbial Ecology* **30**: 25-41.

Wen, K., Ortmann, A.C., and Suttle, C.A. (2004) Accurate estimation of viral abundance by epifluorescence microscopy. *Appl. Environ. Microbiol.* **70**: 3862-3867.

Wilhelm, S.W., and Suttle, C.A. (1999) Viruses and nutrient cycles in the sea. *Bioscience* **49**: 781-788.

Williamson, S.J., McLaughlin, M.R., and Paul, J.H. (2001) Interaction of the ΦHSIC virus with its host: lysogeny or pseudolysogeny? *Applied and environmental microbiology* **67**: 1682-1688.

Wilson, W.H., Van Etten JL, Schroeder DC, Nagasaki K, Brussaard CPD, Delaroque N et al. (2005) Virus Taxonomy, Classification and Nomenclature of Viruses. In *Virus taxonomy: VIIIth report of the International Committee on Taxonomy of Viruses*. Fauquet, C.M., Mayo MA, Maniloff J, Desselberger U, and LA, B. (eds): Academic Press.

Winter, C., Herndl, G.J., and Weinbauer, M.G. (2004) Diel cycles in viral infection of bacterioplankton in the North Sea. *Aquat. Microb. Ecol.* **35**: 207-216.

Wommack, K.E., and Colwell, R.R. (2000) Virioplankton: viruses in aquatic ecosystems. *Microbiol. Mol. Biol. Rev.* **64**: 69-114.

Zingone, A., Sarno, D., and Forlani, G. (1999) Seasonal dynamics in the abundance of *Micromonas pusilla* (Prasinophyceae) and its viruses in the Gulf of Naples (Mediterranean Sea). *Journal of Plankton Research* **21**: 2143-2159.

Thesis chapters

Chapter 2: Viral infection of *Phaeocystis globosa* impedes release of chitinous star-like structures: Quantification using single cell approaches

A.R. Sheik[1*], C.P.D. Brussaard[2], G. Lavik[1], R.A. Foster[1],
N. Musat[1,3], B. Adam[1], M.M.M. Kuypers[1]

[1] Department of Biogeochemistry, Max Planck Institute for Marine Microbiology, Bremen, Germany

[2] Department of Biological Oceanography, NIOZ - Royal Netherlands Institute for Sea Research, Texel, The Netherlands.

[3] Current address: Department of Isotope Biogeochemistry, Helmholtz Centre for Environmental Research – UFZ, Permoserstraße 15, Leipzig, Germany

*Corresponding author.

Mailing address: MPI for Marine Microbiology, Celsiusstr.1, Bremen, Germany, D-28359.

Email: arsheik@mpi-bremen.de

Keywords: marine virus, PgV, *Phaeocystis globosa*, carbon uptake, stable isotope, atomic force microscope, nanoSIMS.

Running title: Single cell view on virally infected *P. globosa*.

Abstract:

Phaeocystis globosa is an ecologically important bloom-forming phytoplankton, which sequesters substantial amounts of inorganic carbon and can form carbon enriched chitinous star-like structures. Viruses infecting *P. globosa* (PgVs) play a significant regulatory role in population dynamics of the host species. However, the extent to which viruses alter host physiology and its carbon assimilation on single cell level is still largely unknown. This study demonstrates for the first time the impact of viral infection on carbon assimilation and cell morphology of individual axenic *P. globosa* cells using two single cell techniques: high resolution nanometer-scale Secondary-Ion Mass Spectrometry (nanoSIMS) approach and atomic force microscopy (AFM). Up until viral lysis (19 h post-infection), the bulk carbon assimilation by infected *P. globosa* cultures was identical to the assimilation by the non-infected cultures (33 µmol C L^{-1}). However, single cell analysis showed that viral infection of *P. globosa* impedes the release of star-like structures. Non-infected cells transfer up to 44.5 µmol C L^{-1} (36%) of cellular biomass in the form of star-like structures suggesting a vital role in the survival of *P. globosa* cells. We hypothesize that impediment of star-like structures in infected *P. globosa* cells may inactivate viral infectivity by forming flocculants after cell lysis. Moreover, we show that substantial amounts of newly produced viruses ($\sim$ 68%) were attached to *P. globosa* cells prior to cell lysis. Further, we speculate that infected cells become more susceptible for grazing which provides potential reasons for the sudden disappearance of PgVs in the environment. The scenarios of enhanced grazing is at odds to the current perspective that viral infections facilitates microbial mediated processes by diverting host material away from the higher trophic levels.

Introduction:

Marine phytoplankton form the base of marine food webs and are responsible for nearly half the global carbon-based net primary production (Falkowski *et al*., 1997). In recent years, numerous studies have demonstrated the potential role of marine viruses on phytoplankton mortality and population dynamics (Suttle, 1994, 2005; Brussaard, 2008; Nagasaki and Bratbak, 2010). Viral infection leads to host cell lysis and thereby diverts the carbon fluxes away from the higher trophic levels (Azam *et al*., 1983) towards microbe-mediated remineralization (Suttle, 2005; Brussaard *et al*., 2008). Since viruses are devoid of their own cellular machinery, it is likely that they affect host carbon assimilation and alter host physiology during the infection period. However, to date little is known on the impact of viral infection on the host carbon assimilation and how it interferes with the other cellular mechanisms.

In the southern North Sea, the prymnesiophyte, *Phaeocystis globosa*, are a dominant phytoplankton with the ability to generate high biomass spring blooms (Brussaard *et al*., 1996). A unique physiological feature of some motile *P. globosa* strains is the occurrence of filaments composed of chitin, a carbon polymer (Chrétiennot-Dinet *et al*., 1997). These chitinous filaments are synthesized within confined vesicles of the cell and are eventually dispersed to form typical star like structures (Chrétiennot-Dinet *et al*., 1997; Ogawa *et al*., 2010). The function of these chitin filaments is largely unresolved and speculated to provide mechanical support on solid surfaces (Chrétiennot-Dinet, 1999). The occurrence of high cell abundances and the ability to assimilate copious amounts of inorganic carbon makes *P. globosa* an ecologically important phytoplankton with a substantial impact on the coastal carbon cycle.

Cell lysis has been shown to be an important loss factor in *P. globosa* blooms, as well as grazing (Brussaard *et al*., 1996). Recently, viruses infecting *P. globosa* (PgVs) were isolated and brought into culture (Brussaard *et al*., 2004; Baudoux and Brussaard, 2005). Over the course of a *P. globosa* bloom, PgVs comprised up to 30% of the total viral abundance suggesting a significant role as mortality agents (Brussaard *et al*., 2005). In the coastal Dutch North Sea, viral mediated lysis of *P. globosa* accounts for up to 66% of the single cell mortality (Baudoux *et al*., 2006).

The viral dynamics in *Phaeocystis sp.* dominated ecosystems has been well documented (Brussaard *et al*., 2004; Brussaard *et al*., 2007). The presence of an active photosynthetic apparatus during infection is well known in *P. globosa* host-virus systems (Brussaard *et al*., 2007). However, to date nothing is known about

the *P. globosa* carbon assimilation during viral infection and the virus mediated impact on the host physiology (i.e. release of star-like structures). Biogeochemical implications of virus-host interactions are potentially cell specific, and by virtue require the ability to analyze carbon assimilation responses on a single cell level.

Recently, the high spatial resolution of atomic force microscopy (AFM) and high resolution nanometer-scale Secondary-Ion Mass Spectrometry (nanoSIMS) has been used independently to study microbial interactions on a single cell level. AFM provides three dimensional imaging of microbial communities with simultaneous measurements of cell diameter (Dufrene, 2002). The application of AFM on marine environmental samples has revealed fine structures of bacteria and provided new insights into bacteria-bacteria associations and their microscale networks (Malfatti *et al*., 2009). NanoSIMS provides quantitative elemental information (i.e. stable or radiotracers) and in addition, an image or elemental map of a cell of interest (Kuypers and Jørgensen, 2007). The application of NanoSIMS has contributed significantly to an improved understanding of the physiology on individual cells in cultures (e.g., Byrne *et al*., 2010) and in the environment (e.g., Foster *et al*., 2011).

Here, we report the results from laboratory experiments with axenic *P. globosa* strain Pg G (A) and its virus, PgV-07T. This study investigated the impact of viral infection on the host carbon assimilation using bulk measurements. Further, our study imaged and quantified for the first time the impact of viruses on host inorganic carbon assimilation at a single cell level using nanoSIMS. The combination of AFM and nanoSIMS was used to determine the response of the host morphology and physiology during viral infection.

Results:

Algal abundance and photosynthetic efficiency:

Cell abundances of *P. globosa* in non-infected and infected cultures remained stable at $\sim 1.5 \times 10^5$ ml^{-1} for the first 8 h (Fig. 1A). Subsequently, the cell abundance in infected cultures declined 24 h post-infection, whereas the non-infected control cultures increased in algal abundance. Preceding the decrease in cell abundance, a gradual decline of photochemical quantum yield (Fv/Fm) in the infected cultures was observed (12 h post-infection; Fig. 2B).

Temporal variation in viral abundance:

The extracellular viral abundance increased between 8 h and 12 h (during the latent period), with a viral maximum of $\sim 6.6 \times 10^7$ ml^{-1} at 48 h post-infection (Fig. 2C). From the net increase in extracellular viral abundance and the net decrease in algal abundance (~ 94 %) after 48 h post-infection, we estimated a burst size (number of viruses released per cell lysed) of 425 PgV cell^{-1}.

In order to estimate the number of viruses attached to *P. globosa* (lysing) cells, we applied scanning electron microscopy (SEM), AFM and epifluorescence microscopy with SYBR GREEN I staining. SEM visualized extracellular viruses while using AFM viruses appeared surrounding *P. globosa* cells (Figs. 2A-B). However, by SYBR GREEN I staining, we visualized and quantified viruses attached onto *P. globosa* cells (Fig. 2C). There was no virus-association of *P. globosa* cells for the first 8 h post-infection as cell lysis had not started yet (Fig. 2D, E). The number of virus-associated cells (Fig. 2D) and attached viruses (Fig. 2E) increased significantly (P=0.002, n=107) from 8 to 12 h, and a maximum was observed at 19 h post-infection.

When we pool the abundance of attached viruses and the net increase in the number of extra-cellular viruses by 19 h, the attached viruses account for ~ 68 % of the total newly produced viruses and ~ 39 % of the total virus abundance (Fig. 2E). It should be noted that the abundance of attached viruses embedded within cytoplasm can not be easily visualized with SYBR GREEN I staining. It could be speculated that this attachment of viruses on *P. globosa* cells was a filtration artifact. However, this is unlikely as the attached viruses on *P. globosa* cells covered only ~ 1.2 % of the total filter area.
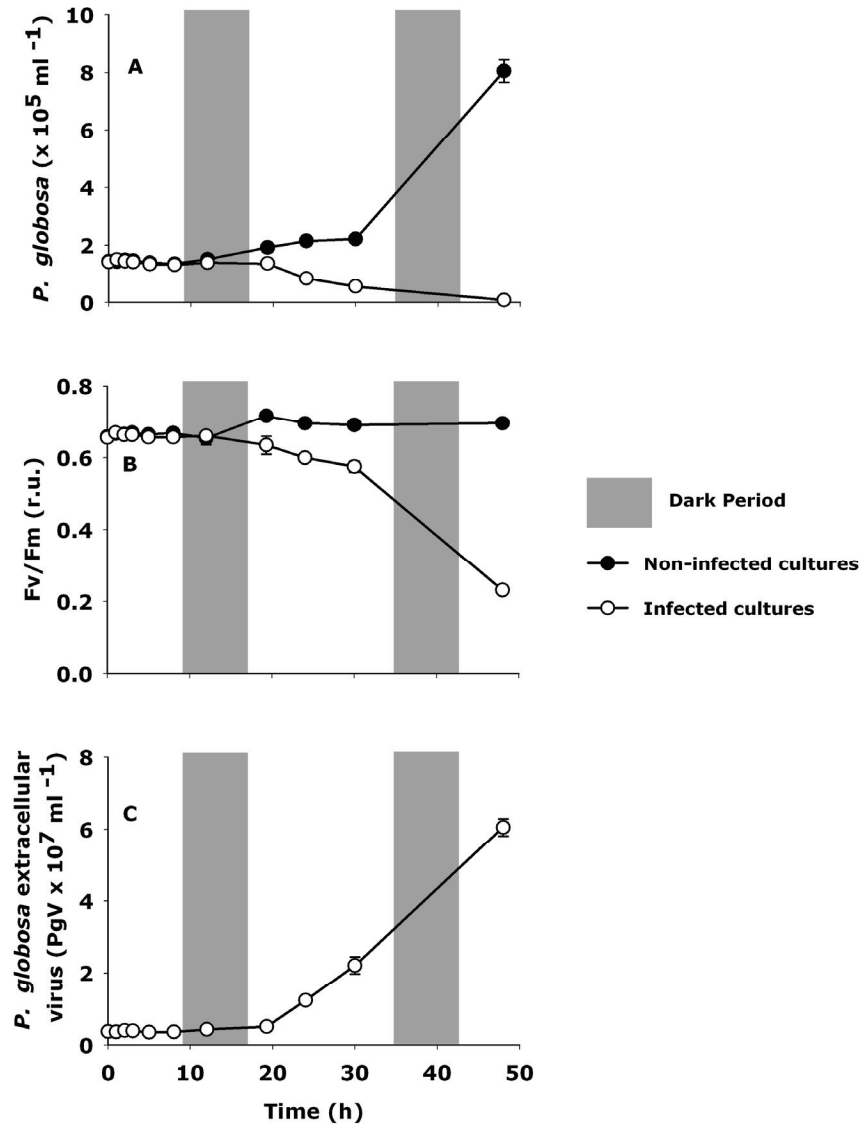
Figure 1. Viral infection dynamics of *P. globosa. (*A) algal abundance, (B) photosynthetic efficiency Fv/Fm, and (C) extracellular viral abundance. Grey bars indicate 8 hours of dark periods. Error bars indicate standard error of mean (SM).
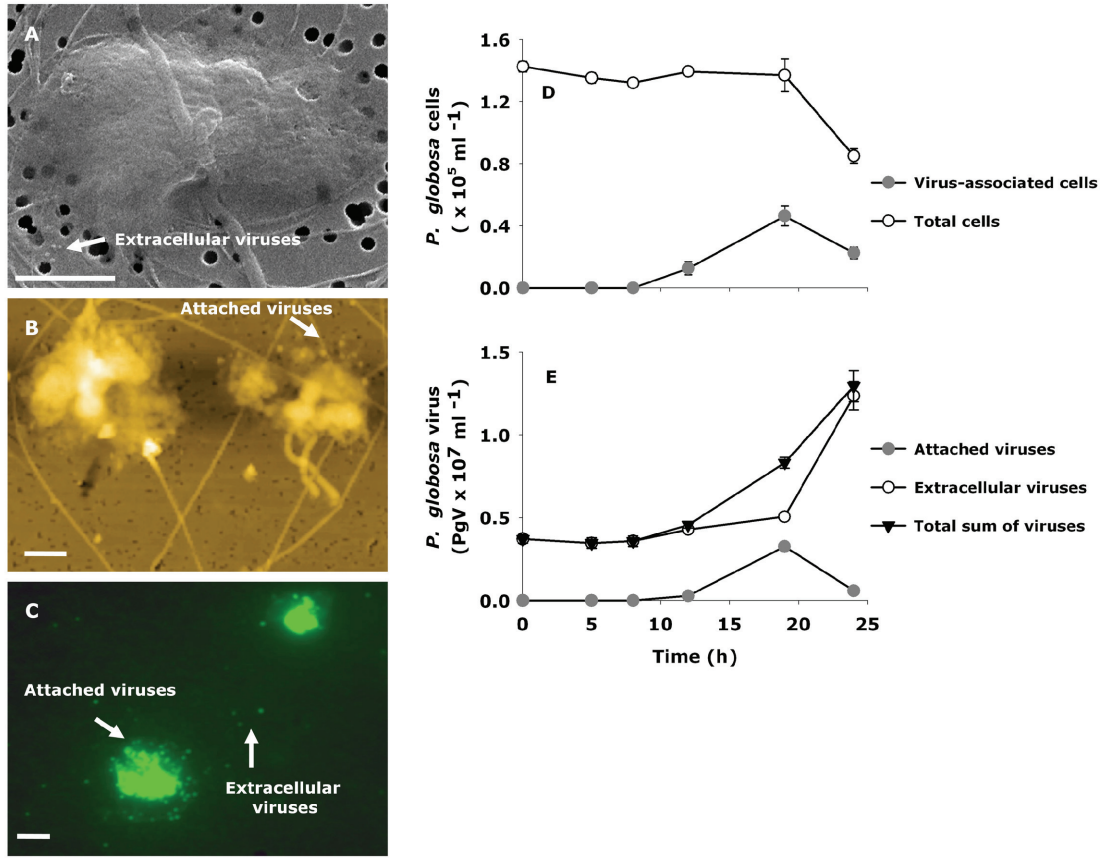
Figure 2. Visualization of *P. globosa* cells from the infected cultures using scanning electron microscopy (A), atomic force microscopy (B) and SYBR GREEN I staining (C). Scale bar = 2 µm. The abundance of virus-associated *P. globosa* cells (D) and the abundance of attached, extracellular and total sum of the viruses (E). Error bars indicate SM.

P. globosa *star-like structures and particles:*

Using AFM we found the abundance of filaments, junctions (will be referred to as star-like structures) and particles in both non-infected and infected cultures at 0 h to be ~ 2.23×10^5 ml^{-1}, ~ 3.3×10^4 ml^{-1} and ~ 1.7×10^5 ml^{-1}, respectively (Fig. 3). Thereafter, viral infection of *P. globosa* had a significant negative effect on the abundance of particles (P=<0.019, n=200) and star-like structures (P=<0.001, n=150). For example, the abundance of star-like structures (Figs. 3A-B) and particles (Fig. 3C) in the infected cultures decreased after 5 h post-infection. In contrast, the abundance of star-like structures and particles in non-infected cultures increased. Further, there was no change in the dimensions of star-like structure and particles over time from both non-infected and infected cultures (Table 1).

Table 1: The average dimensions of star-like structures (filaments and junctions) and particles (mean ± SM).

Filaments (length, diameter in µm)	Junctions (diameter in µm)	Particles (diameter in µm)
12.62 ± 0.43, 0.23 ± 0.08	0.91 ± 0.028	0.63 ± 0.04

Carbon assimilation:

The rates of bulk carbon assimilation in non-infected and infected cultures were already detectable at 1 h post-infection (Fig. 4A). For the first 8 h of the light period, carbon assimilation in non-infected and infected cultures increased linearly with a net maximum of 33 µmol C L^{-1} (Fig. 4A). Subsequently, after 19 h post-infection and with the onset of the dark period, carbon assimilation in non-infected and infected cultures leveled off. The carbon assimilation between non-infected and infected cultures differed after 19 h post-infection. The carbon assimilation in non-infected cultures increased sharply until the end of the experiment (~230 µmol C L^{-1} by 48 h), whereas the infected cultures only showed a slight net increase in carbon assimilation until 30 h post-infection (~93 µmol C L^{-1}).

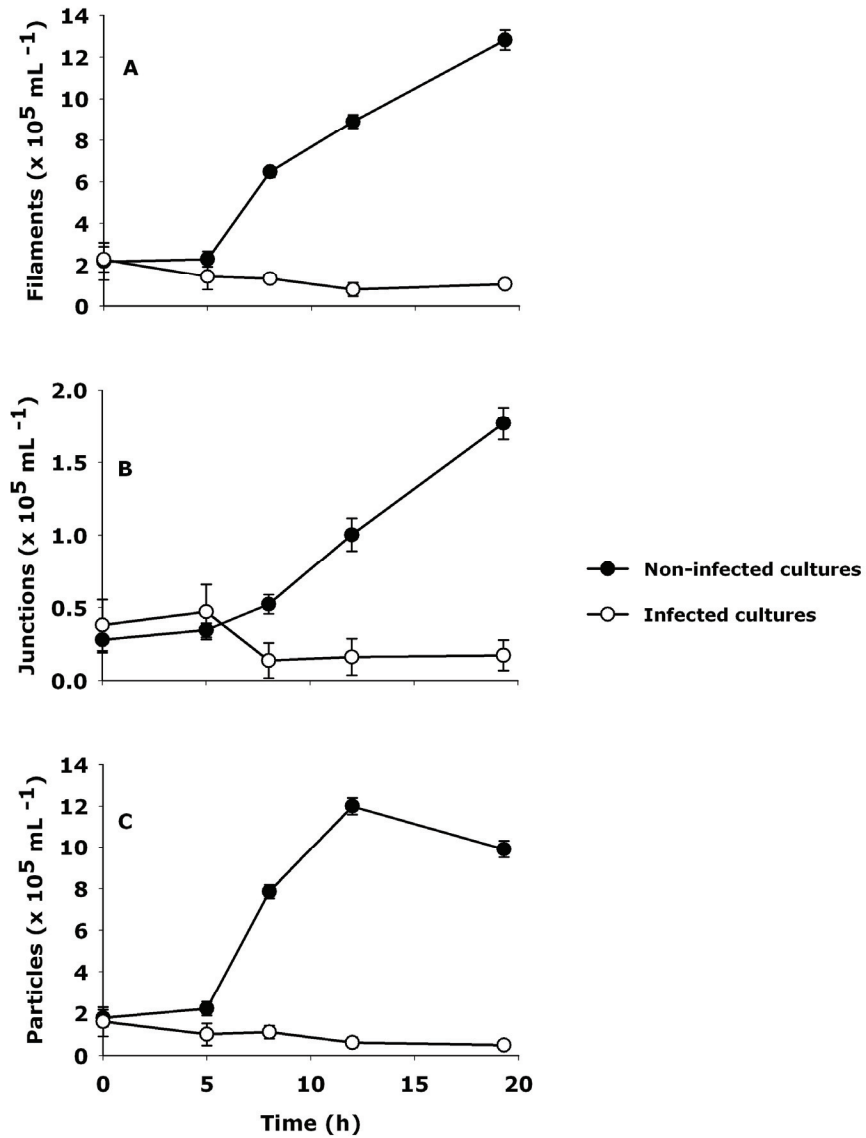**Figure 3. The abundance of star-like structures (filaments (A) and junctions (B)) and particles (C) of non-infected and infected *P. globosa* cultures as measured by AFM. Viruses were introduced at 0 h time interval. Error bars indicate SM.**

The ^{13}C enrichment of cells, star-like structures and particles from both non-infected and infected cultures increased substantially with time (Figs. 4 and 5). The

number of *P. globosa* cells analyzed by nanoSIMS from the non-infected and infected cultures is presented in Table 2. Using nanoSIMS on individual cells, the ^{13}C enrichment in non-infected cells increased significantly after 8 h post-infection compared to the ^{13}C enrichment in infected cells (Fig. 4B; P =< 0.001, n<=35). Interestingly, our nanoSIMS analysis revealed that the *P. globosa* cells from the non-infected cultures were substantially more enriched in ^{13}C than the bulk biomass (two-fold at 19 h post-infection; Fig. 4B). The nanoSIMS measurements on *P. globosa* cells from the infected cultures did not differ from the ^{13}C enrichment in the bulk analysis (Fig. 4B). Meanwhile, there were significant differences in the ^{13}C enrichment of star-like structures from both non-infected and infected cultures (Figs. 5 E-G). Moreover, the ^{13}C enrichment of particles from non-infected cultures increased linearly, whereas after 8 h post-infection the ^{13}C enrichment of particles from infected cultures decreased.

Table 2: Number of *P. globosa* single cells analyzed using NanoSIMS.

	Number of *P. globosa* cells	
Time (h)	**Non-Infected**	**Infected**
0	Bulk Measurements*	Bulk Measurements
5	28	31
8	35	30
12	36	29
19	17	11

* The 0 h time interval was taken from the bulk measurements as the ^{13}C At % enrichment was the natural abundance. Further, nanoSIMS analyses at our facility is not precise to determine the natural abundance of samples.
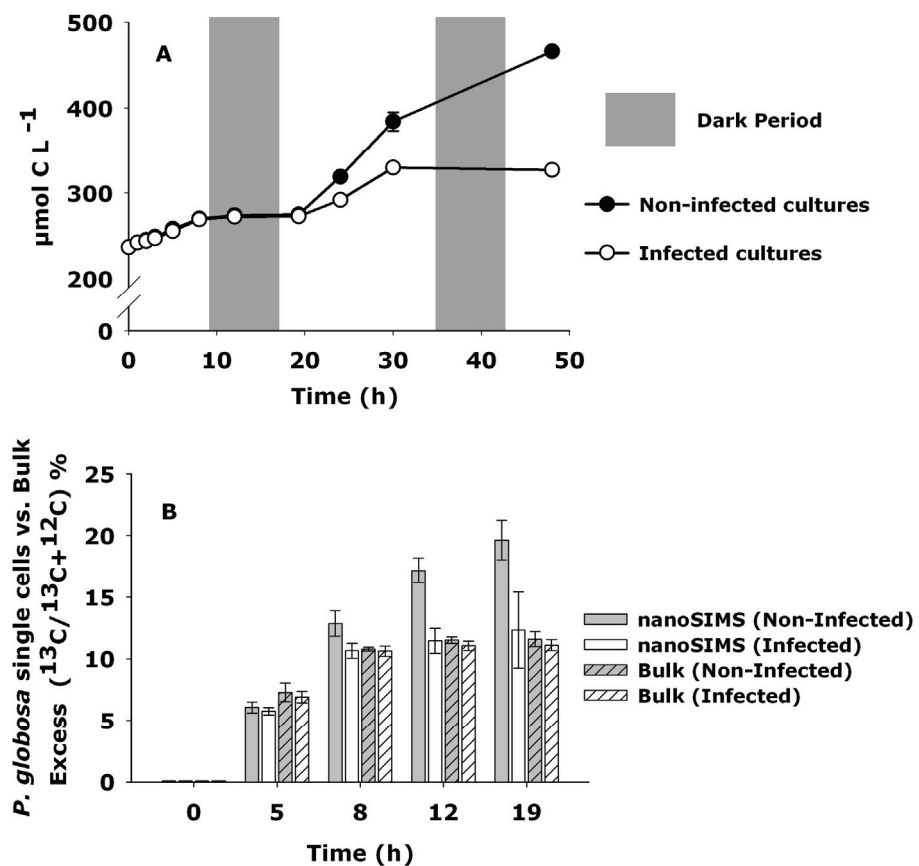
Figure 4. Bulk carbon assimilation of non-infected and infected *P. globosa* cultures as determined by bulk measurements (A). Comparison of ^{13}C enrichment by bulk measurements and single cell nanoSIMS analysis (B). Error bars indicate SM.
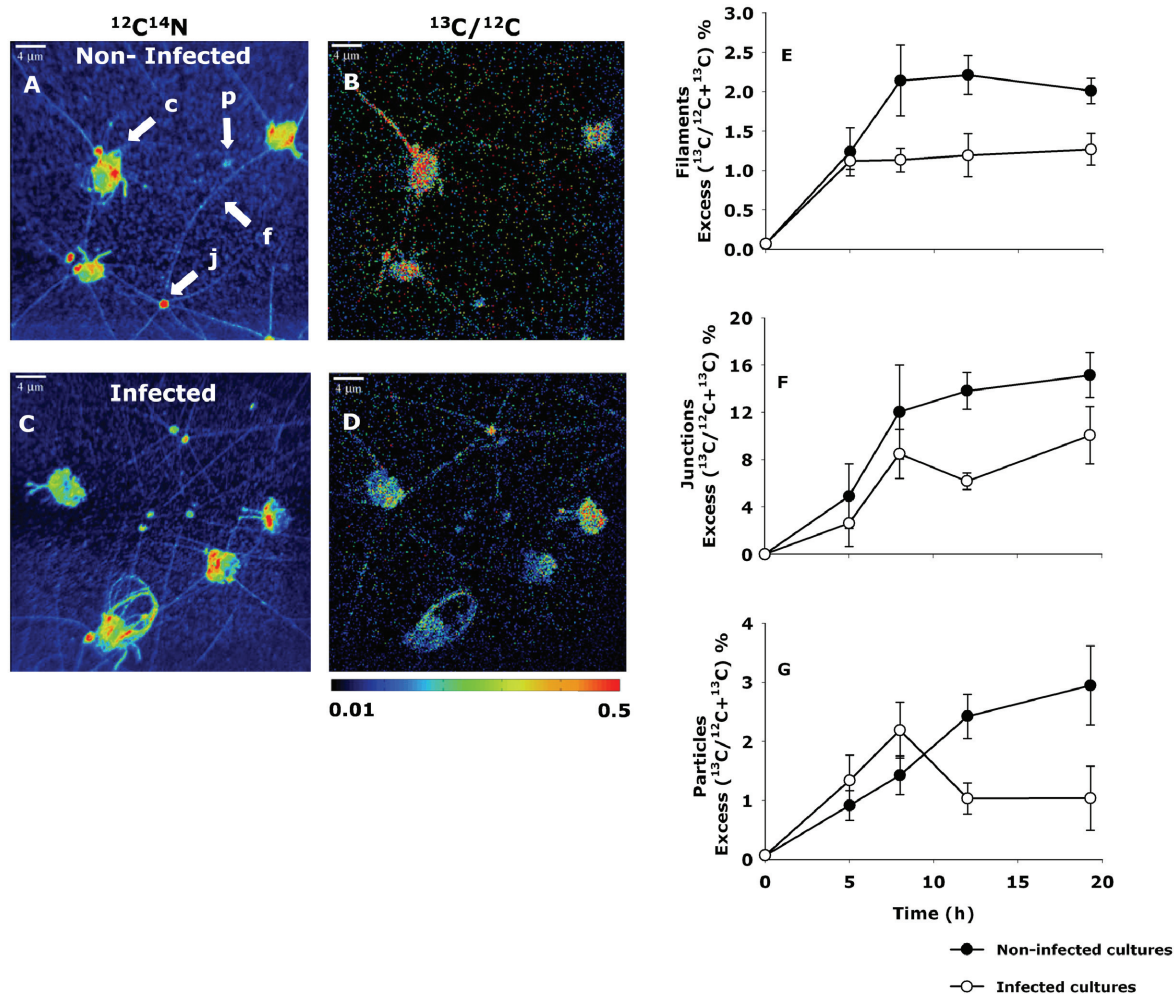
Figure 5. NanoSIMS imaging of non-infected (A-B) and infected (C-D) *P. globosa* cultures at 19 h of incubation. The ^{13}C enrichments of star-like structures and particles (E-F). Error bars indicate SM.

In order to estimate the amount of carbon biomass comprised in the star-like structures and particles in the non-infected and infected cultures of *P. globosa* we made a few basic assumptions and measurements (Fig. 6). The estimation was based on biovolume measurements over the incubation time, a chitin dry density of 1.425 g cm^{-3} (Carlström, 1957), and consider that carbon accounts for 47.3% based on the empirical formula of chitin ($C_8H_{13}NO_5$). Further, we estimated the amount of carbon in the cells by assuming 10 pg C per *P. globosa* cell (Schoemann *et al*., 2005), cellular biovolume at 0 h time interval and the rate of bulk ^{13}C incorporation for the first 8 h of the experiment. The *P. globosa* cellular bound carbon was

corrected for the amount of carbon released by star-like structures and particles at the respective time intervals analyzed (Fig. 6). The total sum of the carbon content within cells, star-like structures and particles deviated slightly to our calculated bulk carbon assimilation. This underestimation could have been due to the assumption of carbon conversion factors or underestimating the abundances of star-like structures and particles.
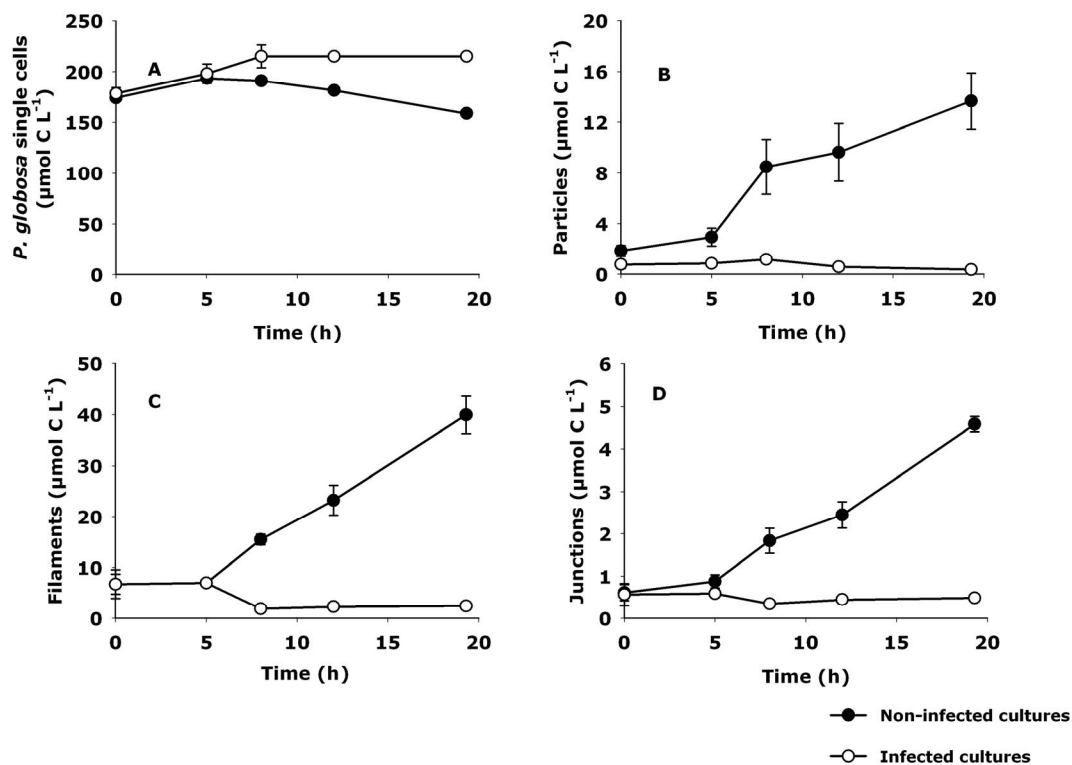
Figure 6. The estimated amount of carbon that was bound to cells (A), particles (B) and star-like structures (filaments (C) and junctions (D)). Error bars indicate SM.
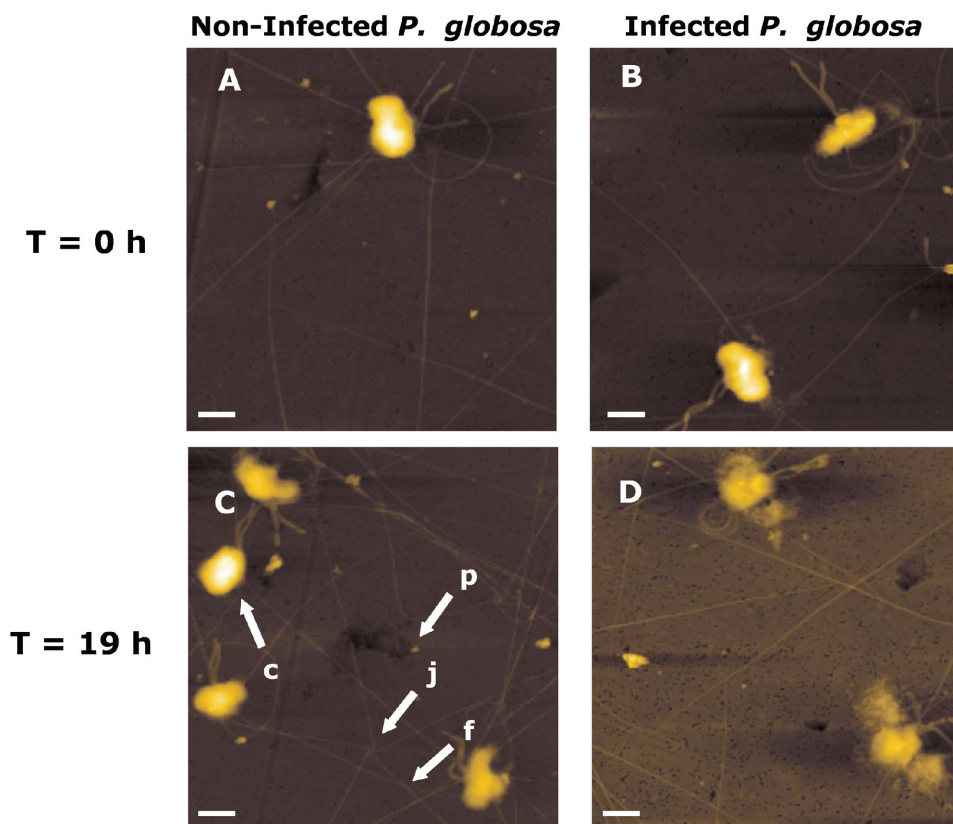
Figure 7. A 20x20 μm resolution scan by atomic force microscopic of non-infected cells (A-C) and infected cells (B-D) at time intervals of 0 h and 19 h, respectively. Images visualizing single cells of *P. globosa* (c) with star-like structures consisting of filaments (f) originating from junctions (j). Besides, we noticed presence of particles (p). Scale bar = 4 μm.

Discussion:

Bulk biomass and single cell ^{13}C-enrichment:

Intriguingly, *P. globosa* single cells in the non-infected cultures showed higher ^{13}C enrichment than the bulk biomass. Moreover, the increase in ^{13}C enrichment of *P. globosa* cells in non-infected cultures at 12 h of incubation was unexpected since this is the time interval where the cultures were in the dark and photosynthesis should be low. This increasing cellular ^{13}C enrichment could be due to loss of ^{13}C depleted cellular material during the dark period. The *P. globosa* strain used in this study has the ability to produce C-rich chitinous filaments, which are synthesized within intracellular disc like vesicles and are eventually released to form star-like structures

(Chrétiennot-Dinet *et al.*, 1997; Ogawa *et al.*, 2010). Using AFM, we observed an increase in the abundances of extracellular star-like structures (filaments and junctions). We, furthermore, noted the presence of particles, whose origin and identity is not clear at this moment. These particles did not stain with SYBR Green I indicating that they do not represent gametes or viruses (data not shown). The nanoSIMS imaging clearly shows the star-like structures and particles were depleted in ^{13}C relative to the single cells. Combined, results of AFM and nanoSIMS on the non-infected cultures indicate that the release of ^{13}C depleted star-like structures and particles led to a gradual increase in ^{13}C enrichment of *P. globosa* single cells with time.

On the other hand, single cell measurements of ^{13}C enrichments from the infected cultures up to 19 h post-infection did not diverge from the bulk biomass. This is supported by the observation that the abundance of star-like structures and particles declined quickly at 5 h post-infection. The latter AFM observations and nanoSIMS imaging indicate that viral infection of *P. globosa* cells impeded the release of new star-like structures.

Quantifying the impact of viral infection on host carbon content:

One of the key aspects of this study was to quantify the amount of carbon bound within the cellular biomass of *P. globosa* and in addition, in the released star-like structures and particles. As can be expected from our AFM observations and nanoSIMS imaging, non-infected *P. globosa* cultures had contributed significant amounts of cellular biomass for the production of star-like structures and particles. The amount of cellular bound carbon in the non-infected *P. globosa* cultures decreased linearly, corresponding to the increasing abundances of star-like structures and particles. Therefore we concluded that a substantial amount of host cellular carbon was utilized for the production of star-like structures and particles. When quantified, ~ 44.5 µmol C L^{-1} and ~ 13.7 µmol C L^{-1} of *P. globosa* biomass in the non-infected cultures was comprised of star-like structures and particles, respectively, at 19 h of incubation, which constitutes ~ 36 % of the total cellular biomass.

In the infected *P. globosa* cultures, since viral infection impeded the release of new star-like structures and particles, much of the assimilated carbon was localized within the cellular biomass. Viral infection of *P. globosa* cells had significantly allocated less carbon (~ 2.91 µmol C L^{-1} and 0.37 µmol C L^{-1}) to the release of star-like structures and particles, respectively. Assuming a carbon conversion factor of

0.2 fg C virus^{-1} (Kepner *et al*., 1998) and a net viral increase of 5.7 × 10^7 ml^{-1}, we estimated that a minimal amounts of (∼ 0.95 μmol C L^{-1}, 1.4 %) *P. globosa* bulk carbon assimilation was utilized for the viral production. Thus the viral infection of *P. globosa* mainly affected the host carbon assimilation by impeding the release of star-like structures and particles.

Ecological implications:

The biological function of star-like structures in *P. globosa* is still unknown. It is speculated that they serve as anchors for attachment on solid surfaces or on co-existing diatoms for colony development (Chrétiennot-Dinet, 1999) or may provide protection against grazers (Zingone *et al*., 1999). Considering that non-infected *P. globosa* cells use about 36% of their cellular biomass for the formation of star-like structures and particles rather than investing in their cell division, they must play an important role in the survival of *P. globosa* cells.

A general perception during viral infection is the shutdown of host non-essential cellular machinery and the subsequent redirection towards viral synthesis. Since this is the first observation of the impairment of the release of star-like structures in the infected *P. globosa*, we can only speculate on the ecological implications. In *P. globosa*, the vesicles containing chitinous filaments exist in a fluid state before they are released as star-like structures (Chrétiennot-Dinet *et al*., 1997). The consequence of viral infection is cell lysis, thereby releasing the fluidic chitinous material to the environment. This chitinous material might undergo a phase transition resulting in the formation of hydrated flocculants (Chin *et al*., 2004). Therefore, we speculate that the viral lysis of *P. globosa* cells leads to the formation of flocculants, which are characterized by substantial attachment of newly produced viruses (up to 68% attached to lysing host cells) and could function in viral inactivation and removal.

Additionally, we speculate that the impairment of infected *P. globosa* cells to release new chitinous star-like structures may make the cells more prone to grazing. Given the fact that production of chitin filaments increases defensive capacity against grazers (Verity and Villareal, 1986), we hypothesize that viral infection of *P. globosa* enhances grazing on the cells that are unable to release new star-like structures. The combination of viral attachment on flocculants and grazing of the infected *P. globosa* cells, offers a potential explanation of the sudden decline in PgV abundance observed in the field (Brussaard *et al*., 2005). In the case of enhanced grazing, much of the host assimilated carbon will be diverted away from the microbial mediated processes.

This is in sharp contrast to the current view that viral infections divert the organic carbon transfer from higher trophic levels (e.g., grazers).

Viruses are very diverse with respect to how they affect and overrule host metabolism. This study reports a rare and unique insight into the impairment of the release of the star-like structures of virally infected *P. globosa*. To our knowledge, this is the first report of an intriguing finding that viral infection affects cellular mechanism of the host. The independent application of high resolution single cells techniques using AFM and nanoSIMS visualized the unique host morphological feature due to viral infection. Further, application of single cell techniques enables us to quantify the impact of viral infection on the host carbon assimilation that was not obtained by bulk measurements alone. Given the ubiquitous distribution of *P. globosa*, further study is necessary to elucidate the biogeochemical consequences of the impediment of the star-like structures in infected cells and its persistence in the environment.

Experimental Procedures:

Culturing:

Axenic cultures of *Phaeocystis globosa* strain Pg G (A) obtained from the culture collection of Royal Netherlands Institute for Sea Research (NIOZ) was grown in a modified 1:1 mixture of f/2 medium (Guillard, 1975) and nutrient enriched artificial seawater (ESAW) (Cottrell and Suttle, 1991). Nutrients were added to the media to a final concentration of 1mM HCO_3^- and 80 µM of NO_3^-. The cultures were grown under 95 µmol quanta $m^{-2}\,s^{-1}$ irradiance with a light to dark regime of 16:8 hours and at a temperature of 15 ± 1°C. The lytic *Phaeocystis globosa* virus, PgV-07T (Baudoux and Brussaard, 2005) from the virus culture collection at NIOZ, was produced using exponentially growing host cultures.

Experimental Setup:

A 1 L culture of exponential growing *P. globosa* Pg G (A) of 1.5 x 10^5 mL^{-1} was split into four batch cultures and each was transferred to a fresh 2 L ESAW medium (10% v/v) containing approximately 1 mM $H^{13}CO_3^-$ (as a sodium salt, 99 atom%, ISOTEC). Two of these batch cultures were infected with pre-filtered PgV-07T virus (0.2 µm pore-size, cellulose acetate, Whatmann) at an initial virus to alga ratio of 26:1. The other two cultures served as non-infected control cultures and received medium instead of viral lysate in equal amount. The experiment was conducted during the mid light phase of the light to dark regime. Sampling for algae and virus abundance, photosynthetic efficiency, isotopic carbon assimilation and single cell

analyses was performed directly after the addition of viral lysate at regular time intervals for up to 48 h post-infection.

Abundances:

Algal abundance was monitored by flow cytometry (FCM) using a Beckman Coulter EPICS XL-MCL benchtop flow cytometer (Veldhuis and Kraay, 2000), which was equipped with a laser with an excitation wavelength of 488 nm (15 mW) and emission bands for the chlorophyll autofluorescence (> 630 nm). The 1 mL samples taken at each time point were diluted up to 10-fold in sterile sea water. The flow cytometer trigger was set on the red chlorophyll autofluorescence.

The abundance of *P. globosa* virus PgV-07T was enumerated using a Becton-Dickson FACSCalibur flow cytometer (Brussaard, 2004). Samples of 1 mL at every time point were fixed with 25% glutaraldehyde (0.5% final concentration, EM grade, Sigma-Aldrich, St Louis, MO, USA) for 15 to 30 minutes at 4°C, flash frozen in liquid nitrogen and stored at -80°C until analysis. The thawed samples were diluted 50 to 1,000-fold in sterile TE-buffer (pH 8.0) and stained with the nucleic acid-specific dye SYBR Green I (Invitrogen-Molecular Probes, Eugene, OR, USA) at a final concentration of 0.5×10^{-4} of the commercial stock for 10 min at 80°C. The flow cytometer trigger was set on the green fluorescence. All listmode files were analyzed as described by Brussaard *et al* (2010).

SYBR Green I staining was performed as described by Lunau *et al* (2005) to quantify the attachment of PgV-07T virus on *P. globosa* cells from the infected cultures. Further, SYBR Green I staining was used to investigate the presence of genomic material in particles from both non-infected and infected cultures. Samples taken at each time interval were fixed with 1% paraformaldehyde (PFA) (for 1 h at room temperature or overnight at 4°C), filtered on to gold-palladium pre-sputtered polycarbonate filters (GTTP type; pore-size 0.22 μm; diameter 25 mm; Millipore), washed with 5-10 mL of 1× Phosphate Buffer Saline (PBS), air dried and stored at -20°C until analysis. The filter samples were embedded onto glass slides in a mounting mixture containing 5 μL of SYBR Green I commercial stock solution (Invitrogen-Molecular Probes, Eugene, OR, USA), 200 μL of Moviol solution (Fluka, Switzerland) and 5 μL of 1M ascorbic acid. Subsequently, all SYBR Green I stained samples were imaged and quantified by epifluorescence microscopy under green excitation (510-560 nm) (Axioplan II Imaging epifluorescence microscope, Zeiss, Jena, Germany). The area of *P. globosa* cells associated with viruses was measured

on the micrographs using the software AxioVision Rel. 4.8 (Carl Zeiss). About 100 *P. globosa* cells (10–20 view fields) were enumerated.

The abundance of star-like structures (filaments and junctions) and particles were visualized and measured with atomic force microscope imaging (AFM; NT-MDT Co., Moscow, Russia) in a semi-contact mode. At each time point 2-5 mL of the samples were fixed with 1% PFA for 1 hour at room temperature or overnight at 4°C. Subsequently, PFA fixed samples were filtered on to gold-palladium pre-sputtered polycarbonate filters (GTTP type; pore-size 0.22 μm; diameter 25 mm; Millipore) using a gentle vacuum, washed with 5-10 mL of 1×PBS, air dried and stored at -20°C until analysis. AFM analysis was performed in air and images were acquired in AC mode at scan rates between 0.5 and 1 Hz. We used semi-contact "golden" coated silicon cantilever (NSG10; NT-MDT) with a spring constant of 11.8 Nm^{-1}. Images were acquired at a scan resolution of 50 x 50 μm which enabled us to visualize star-like structures and particles at a given filter field. About 10 - 15 images were acquired at random filter fields at each time interval. Surface topography of cells and compartments were acquired by height channel and images were processed with flatten correction function of the software (Nova P9, version 2.1.0.828, NT-MDT, Moscow, Russia). The number of star-like structures and particles (at least 100 per filter) were counted manually. The abundance of star-like structures and particles was estimated based on the filter diameter, area of the field of analyses (50 x 50 μm), the number of star-like structures and particles and the amount of sample volume filtered.

Scanning electron microscopy:

Scanning electron microscopy (SEM) was performed on samples from infected *P. globosa* cultures at the 19 h post-infection. Samples that were 1% PFA fixed and filtered on gold-palladium pre-sputtered polycarbonate filters (GTTP type; pore-size 0.22 μm; diameter 25 mm; Millipore) were analyzed by a ZEISS SUPRA40 scanning electron microscope.

Photosynthetic efficiency:

Photosynthetic efficiency (F_v/F_m) of the algal cultures was measured by PHYTO-ED system (Walz, Effeltrich, Germany). Five mL of culture was sub-sampled at each time point and dark acclimated for 30 minutes. The natural fluorescence (F_o) and maximal fluorescence (F_m) of the sample was measured in a glass cuvette with a WATER-ED Emitter-Detector Unit. The variable fluorescence (F_v) was deduced as $F_v = F_m - F_o$. The

photochemical quantum yield (F_V/F_M) of the algal cultures was measured as F_V normalized to F_M.

Carbon Measurements:

For determination of bulk carbon assimilation, 30-50 mL of the cultures were filtered onto a pre-combusted GF/F filters (Whatmann, 25 mm diameter) using a hydraulic jet pump (Vacsafe 15, Labgene, Denmark), freeze dried and stored at room temperature until analysis. The ^{13}C-bicarbonate incorporation into biomass was determined as CO_2 released by flash combustion in excess oxygen at 1050°C, with caffeine as standards. An automated elemental analyzer (Thermo Flash EA, 1112 Series) coupled to a Delta Plus Advantage mass spectrometer (Finnigan Delta^{plus} XP, Thermo Scientific) was used to determine particulate organic material concentrations and ^{13}C enrichments, respectively. Over the course of the experiment, ^{13}C-bicarbonate in the medium escaped due to atmospheric CO_2 exchange. We corrected this exchange by measuring ^{13}C isotopic abundances in the medium as described by Assayag *et al* (2006) using gas chromatography-isotope ratio monitoring mass spectrometry (VG Optima, Micromass, Manchester, UK).

For single cell carbon analyses using nanoSIMS, 2-5 ml of the samples were fixed as described above with a final concentration of 1% PFA for 1 hour at room temperature or overnight at 4°C. Fixed samples were filtered on to gold-palladium pre-sputtered polycarbonate filters (GTTP type; pore-size 0.22 μm; diameter 25 mm; Millipore), washed with 5-10 ml of 1× PBS, air dried and stored at -20°C until analysis.

Enrichment of the ^{13}C in algal cells, star-like structures and particles were analyzed with NanoSIMS 50 L (CAMECA, Paris, France). The primary ion beam had a nominal size of ~ 150 nm and the sample was sputtered with a dwelling time of 6 ms per pixel. The primary current was 20-30 nA Cs$^+$ during acquisition for most images. For each analysis, we recorded simultaneously secondary-ion images of naturally abundant ^{12}C (measured as ^{12}C$^-$) and ^{14}N atoms (measured as ^{12}C^{14}N$^-$) for the localization of biomass and similarly, of ^{13}C for the uptake quantification.

NanoSIMS data-sets were analyzed using the Look@NanoSIMS software (Polerecky *et al.*, 2012). To obtain good visual contrast per pixel, all nanoSIMS images were graphically displayed in a false-color scale from black (natural abundance of C) to red (adjusted maximum intensity). The different scans of each image were realigned to correct for any drift during acquisition. Regions of interest (ROI) around individual cells, star like structures and particles were defined manually

using the $^{12}C^{14}N$ image. The isotope ratio (r= $^{13}C/^{12}C$) was calculated for each ROI based on the total $^{13}C^-$ and $^{12}C^-$ counts for each pixel. Subsequently, the ^{13}C enrichments were calculated in terms of absolute abundance, defined as A = $^{13}C/(^{13}C+^{12}C)$, was calculated as A = r/(r+1).

Biovolume calculations:

Using AFM (Fig. 7) and nanoSIMS (Fig. 5), we observed the presence of star-like structures (s) consisting of filaments (f) emerging from junctions (j), along with particles (p) in non-infected and infected cultures. For the ease of abundance and biovolume calculations using AFM and the deduction of ^{13}C enrichment using nanoSIMS, we classified star-like structures into filaments and junctions. Assuming cells, particles and junctions as spheres and filaments as straight-sided rods with hemispherical ends, we calculated the biovolume of cells (v_c, μm^3 mL^{-1}), particles (v_p), filaments (v_f) and junctions (v_j) at 0, 5, 8, 12 and 19 h of the experiment.

Statistical analysis:

Kolmogorov-Smirnov normality test was performed to check whether the data (^{13}C enrichments of cells and abundances of star-like structures) were normally distributed. When normality test was passed, analyses of differences between single cell ^{13}C enrichments abundances of star-like structures of infected and non-infected cells were made using t-test. All analyses were carried out using the Sigmastat version 3.5 software package.

Acknowledgments:

References:
Assayag, N., Rivé, K., Ader, M., Jézéquel, D., and Agrinier, P. (2006) Improved method for isotopic and quantitative analysis of dissolved inorganic carbon in natural water samples. *Rapid communications in mass spectrometry* **20**: 2243-2251.

Azam, F., Fenchel, T., Field, J.G., Gray, J.S., Meyer-Reil, L.A., and Thingstad, F. (1983) The ecological role of water-column microbes in the sea. *Mar Ecol Prog Ser* **10**: 257-263.

Baudoux, A.C., and Brussaard, C.P.D. (2005) Characterization of different viruses infecting the marine harmful algal bloom species *Phaeocystis globosa*. *Virology* **341**: 80-90.

Baudoux, A.C., Noordeloos, A.A.M., Veldhuis, M.J.W., and Brussaard, C.P.D. (2006) Virally induced mortality of *Phaeocystis globosa* during two spring blooms in temperate coastal waters. *Aquat. Microb. Ecol.* **44**: 207-217.

Brussaard, C.P.D. (2004) Optimization of procedures for counting viruses by flow cytometry. *Appl. Environ. Microbiol.* **70**: 1506-1513.

Brussaard, C.P.D., Kuipers, B., and Veldhuis, M.J.W. (2005) A mesocosm study of *Phaeocystis globosa* population dynamics: 1. Regulatory role of viruses in bloom. *Harmful Algae* **4**: 859-874.

Brussaard, C.P.D., Gast, G.J., vanDuyl, F.C., and Riegman, R. (1996) Impact of phytoplankton bloom magnitude on a pelagic microbial food web. *Mar Ecol Prog Ser* **144**: 211-221.

Brussaard, C.P.D., Short, S.M., Frederickson, C.M., and Suttle, C.A. (2004) Isolation and phylogenetic analysis of novel viruses infecting the phytoplankton *Phaeocystis globosa* (Prymnesiophyceae). *Appl Environ Microbiol* **70**: 3700-3705.

Brussaard, C.P.D., Bratbak, G., Baudoux, A.C., and Ruardij, P. (2007) *Phaeocystis* and its interaction with viruses. *Biogeochemistry* **83**: 201-215.

Brussaard, C.P.D., Wilhelm, S.W., Thingstad, F., Weinbauer, M.G., Bratbak, G., Heldal, M.   *et al*. (2008) Global-scale processes with a nanoscale drive: the role of marine viruses. *ISME J* **2**: 575-578.

Brussaard, C.P.D., J. P. Payet, C. Winter, and M. G. Weinbauer. (2010) Quantification of aquatic viruses by flow cytometry. *In S. W. Wilhelm, M. G. Weinbauer, and C. A. Suttle [eds.], Manual of Aquatic Viral Ecology. ASLO.* : p. 102–109.

Brussaard, C.P.D.M., J. M. (2008) Algal Bloom Viruses. *Plant viruses, Global science books* **2 (1)**: 1-10.
Byrne, M.E., Ball, D.A., Guerquin-Kern, J.L., Rouiller, I., Wu, T.D., Downing, K.H.   *et al*. (2010) *Desulfovibrio magneticus* RS-1 contains an iron-and phosphorus-rich organelle distinct from its bullet-shaped magnetosomes. *Proceedings of the National Academy of Sciences* **107**: 12263.

Carlström, D. (1957) The crystal structure of α-chitin (poly-N-acetyl-D-glucosamine). *The Journal of Biophysical and Biochemical Cytology* **3**: 669-683.

Chin, W.-C., Orellana, M.V., Quesada, I., and Verdugo, P. (2004) Secretion in Unicellular Marine Phytoplankton: Demonstration of Regulated Exocytosis in *Phaeocystis globosa*. *Plant Cell Physiol.* **45**: 535-542.

Chrétiennot-Dinet, M.J. (1999) An enigma in marine nanoplankton. The role of star-like structures produced by *Phaeocystis*. *Enigmatic microorganisms and life in extreme environments*: 207.

Chrétiennot-Dinet, M.J.P., Giraud-Guille, M.M., Vaulot, D., Putaux, J.L., Saito, Y., and Chanzy, H. (1997) The chitinous nature of filaments ejected by *Phaeocystis*. *Journal of Phycology* **33**: 666-672.

Cottrell, M.T., and Suttle, C.A. (1991) Wide-spread occurrence and clonal variation in viruses which cause lysis of a cosmopolitan, eukaryotic marine phytoplankter, *Micromonas pusilla*. *Mar Ecol Prog Ser* **78**: 1-9.

Dufrene, Y.F. (2002) Atomic force microscopy, a powerful tool in microbiology. *Journal of bacteriology* **184**: 5205.

Falkowski, P.G., Raven, J.A., and Laws, E.A. (1997) *Aquatic photosynthesis*: Blackwell Science London, UK.

Foster, R.A., Kuypers, M.M.M., Vagner, T., Paerl, R.W., Musat, N., and Zehr, J.P. (2011) Nitrogen fixation and transfer in open ocean diatom-cyanobacterial symbioses. *ISME J* **5**: 1484-1493.

Guillard, R.R.L. (1975) Culture of phytoplankton for feeding marine invertebrates. *Smith, Walter L. and Matoira H. Chanley (Ed.). Culture of Marine Invertebrate Animals. Conference, Greenport, N.Y., Oct., 1972. Viii+338p. Illus. Plenum Press: New York, N.Y., U.S.A.; London, England. Isbn 0-306-30804-5*: 29-60.

Kepner, R.L., Wharton, R.A., and Suttle, C.A. (1998) Viruses in Antarctic lakes. *Limnol Oceanogr* **43**: 1754-1761.

Kuypers, M.M.M., and Jørgensen, B.B. (2007) The future of single cell environmental microbiology. *Environ Microbiol* **9**: 6-7.

Lunau, M., Lemke, A., Walther, K., Martens-Habbena, W., and Simon, M. (2005) An improved method for counting bacteria from sediments and turbid environments by epifluorescence microscopy. *Environ Microbiol* **7**: 961-968.

Malfatti, F., Samo, T., and Azam, F. (2009) High-resolution imaging of pelagic bacteria by Atomic Force Microscopy and implications for carbon cycling. *ISME J* **4**: 427-439.

Nagasaki, K., and Bratbak, G. (2010) Isolation of viruses infecting photosynthetic and nonphotosynthetic protists. In: Manual of Aquatic Viral Ecology, *American Society of Limnology and Oceanography*, pp. Chapter 10, 82-91.

Ogawa, Y., Kimura, S., Wada, M., and Kuga, S. (2010) Crystal analysis and high-resolution imaging of microfibrillar α-chitin from *Phaeocystis*. *Journal of Structural Biology* **171**: 111-116.

Polerecky, L., Adam, B., Milucka, J., Musat, N., Vagner, T., and Kuypers, M.M.M. (2012) Look@NanoSIMS – a tool for the analysis of nanoSIMS data in environmental microbiology. *Environ Microbiol* **14**: 1009-1023.

Schoemann, V., Becquevort, S., Stefels, J., Rousseau, V., and Lancelot, C. (2005) *Phaeocystis* blooms in the global ocean and their controlling mechanisms: a review. *Journal of Sea Research* **53**: 43-66.

Suttle, C.A. (1994) The significance of viruses to mortality in aquatic microbial communities. *Microb. Ecol.* **28**: 237-243.

Suttle, C.A. (2005) Viruses in the sea. *Nature* **437**: 356-361.

Veldhuis, M.J.W., and Kraay, G.W. (2000) Application of flow cytometry in marine phytoplankton research: current applications and future perspectives. *Scientia Marina* **64**: 121-134.

Verity, P.G., and Villareal, T.A. (1986) The relative food value of diatoms, dinoflagellates, flagellates, and cyanobacteria for tintinnid ciliates. *Archiv für Protistenkunde* **131**: 71-84.

Zingone, A., Chrétiennot Dinet, M.J., Lange, M., and Medlin, L. (1999) Morphological and genetic characterization of *Phaeocystis cordata* and *P. jahnii* (Prymnesiophyceae), two new species from the Mediterranean Sea. *Journal of phycology* **35**: 1322-1337.

Chapter 3: Algal viral infection fuels bacterial substrate assimilation and drives community structure

A.R. Sheik[1], C.P.D. Brussaard[2], G. Lavik[1], P. Lam[1], N. Musat[1,3], A. Krupke[1], S. Littman[1], M.M.M. Kuypers[1]

[1] Department of Biogeochemistry, Max Planck Institute for Marine Microbiology, Celciusstraße 1, Bremen, Germany.

[2] Department of Biological Oceanography, NIOZ – Royal Netherlands Institute for Sea Research, Texel, The Netherlands.

[3] Current address: Department of Isotope Biogeochemistry, Helmholtz Centre for Environmental Research – UFZ, Permoserstraße 15, Leipzig, Germany.

Keywords: marine viruses, *Phaeocystis globosa*, *Alteromonas* and *Roseobacter*, pyrosequencing, carbon remineralisation, nanoSIMS.

Running title: Single-cell bacterial assimilation of algal lysates

Abstract:

Algal cell lysis due to viral infections is thought to be the significant process how lytic viruses structure bacterial communities and affect biogeochemical fluxes. Here, using ^{13}C and ^{15}N-labelled *Phaeocystis globosa* biomass and the North Sea bacterioplankton (0.8 µm pre-filtered), we show that instead, the leakage or excretion by infected yet intact algal cells is mainly responsible for shaping bacterial community structure and enhanced bacterial substrate assimilation. The application of secondary-ion mass spectrometry (nanoSIMS) showed a high transfer of infected *P. globosa* biomass towards *Alteromonas* cells indicating leakage or excretion of algal cells, which stimulated its initial doubling in abundance, attachment to algal cell surroundings 'phycosphere' and consisted of an individual phylotype. Following algal viral lysis, temporal succession of bacterial populations consisted of *Alteromonas* and *Roseobacter* cells with distinct phylotypes (Day 2). When quantified, the total ^{13}C-carbon and ^{15}N-Nitrogen uptake of *Alteromonas* represented ~35% and *Roseobacter* cells ~6% of both the bulk particulate organic ^{13}C-carbon and ^{15}N-Nitrogen, respectively, emphasizing an efficient utilisation of *P. globosa* viral lysates by these specific bacterial members. The sharp increase of these two genera, which occurred in aggregate-association, was followed by rapid decline in abundance due to plausible phage mediated lysis. Aggregate dissolution due to potential phage lysis appeared to be responsible for regeneration of dissolved inorganic carbon (55% of the particulate ^{13}C-organic carbon) and generation of plentiful recalcitrant organic carbon. These findings reveal a previously unrecognized role of viruses such as algal leakage during infection, which appears to be responsible for substantial alterations in the ecosystem process such as bacterial community structure and carbon availability.

Introduction:

Marine viruses are the most abundant entities and dynamic components of the microbial loop (Bergh et al 1989, Suttle 2005). Through the 'viral shunt' (Wilhelm and Suttle 1999), viral release of dissolved forms of carbon and nutrients from the particulate pool is increased, and thus more substrates become available for microbially mediated processes (Fuhrman 1999, Suttle 2005). Thereby, viruses can have a significant impact on biogeochemical cycling in the world's oceans (Brussaard et al 2008, Suttle 2007). Studies conducted in the last years have made it increasingly evident that viruses are significant driving forces in algal (Short 2012) and bacterioplankton populations dynamics (Breitbart 2012).

The genus *Phaeocystis globosa* is a widespread algae and can be dominant in temperate and tropical oceans (Schoemann et al 2005). Few strains of *P. globosa* single cells have the potential in the formation of carbon enriched chitinous star-like structures by investing substantial amounts of their cellular biomass (Sheik et al 2012). Viruses infecting *P. globosa* populations (PgVs) can control *Phaeocystis* population dynamics and even bloom formation (Baudoux and Brussaard 2005). In the southern North Sea, viral mediated lysis of *P. globosa* accounts for up to 66% of the single cell mortality (Baudoux et al 2006). Hence, *P. globosa* is an ideal species to study the impact of viruses structuring bacterial communities and in turn the transfer of algal biomass towards microbial communities affecting coastal biogeochemical fluxes.

In the coastal North Sea waters, during the course of algal blooms, the bacterioplankton communities are mainly dominated by *Alphaproteobacteria, Gammaproteobacteria* and *Bacteroidetes* (Alderkamp et al 2007, Lamy et al 2009, Teeling et al 2012). In particular, bacterioplankton belonging to these specific taxonomic groups exhibit distinctive successive patterns most likely in relation to the changes in the organic matter composition in course of the algal blooms (Eilers et al 2000). The gammaproteobacterial *Alteromonadaceae* (referred to as *Alteromonas* cells henceforth) and Alphaproteobacterial *Rhodobacteriaceae* (will be referred to as *Roseobacter* cells) can become very abundant in such seasonal algal blooms (Pernthaler et al 2001).

The majority of marine pelagic bacteria exists as free-living, but also its occurrence as attached to algal surfaces and aggregates is common (Azam et al 1983). Aggregate-associated bacteria are often characterized by high abundance, growth rate and enzymatic activity relative to their free-living counterparts (Simon et

al 2002). Viral mediated algal lysis could induce aggregate formation due to the released lysis products and can be associated with dense bacterial abundances (Peduzzi and Weinbauer 1993). Due to high incidence of host cells within aggregates, it is estimated that ~37% of the aggregate-associated bacteria may be killed by viral lysis and could mediate aggregate dissolution (Proctor and Fuhrman 1991). Consequently, by assisting the retention of dissolved substances (e.g., carbon) within the euphotic zone, viruses might alter the efficiency of the biological carbon pump, which describes the biologically regulated transfer of particulate carbon from the euphotic zone to the deep-sea (Azam and Long 2001).

Moreover, viral mediated algal lysis could stimulate the growth of heterotrophic bacteria and consequently heterotrophic mediated nutrient cycling (Brussaard et al 1996, Brussaard et al 2005, Gobler et al 1997, Haaber and Middelboe 2009). To date, using varied algal-virus host systems, most virus ecology studies have largely focused on the overall changes in bacterial abundance due to algal viral mediated lysis and subsequent bacterial production by the uptake of radio-active substrates ((Jacquet et al 2010) and references therein). However, how viral lysis shapes the bacterial community structure and subsequently bacterial uptake of virally released organic compounds, thereby mediating oceanic biogeochemical fluxes remains poorly understood.

In the current study using the natural bacterial assemblages from the North Sea (0.8 µm pre-filtered), we investigated the uptake of carbon and nitrogen released from infected to virally lysed ^{13}C and ^{15}N labelled *P. globosa* biomass by specific bacterial cells. The combination of fluorescent *in situ* hybridisation (CARD-FISH) and amplicon pyrosequencing was used to examine the changes in the bacterial composition and diversity. The application of high-resolution single cell techniques enabled us to visualise the occurrence of bacterial populations as aggregate-associated and/or free-living (atomic force microscopy imaging, AFM) and precisely quantify the single-cell bacterial substrate assimilation using nanometer-scale secondary-ion mass spectrometry approach (nanoSIMS). Furthermore, we quantified the organic carbon remineralisation.

Materials and Methods:

Generation of ^{13}C and ^{15}N labelled algal biomass: Axenic cultures of *Phaeocystis globosa* strain Pg G (A) were obtained from the culture collection of Royal Netherlands Institute for Sea Research (NIOZ). The ^{13}C and ^{15}N labelled *P. globosa* biomass was generated from exponentially growing axenic *P. globosa* culture grown in enriched artificial seawater (ESAW, (Cottrell and Suttle 1991)) containing 1mM $H^{13}CO_3^-$ and 80 µM of $^{15}NO_3^-$ (as sodium salts, 99 atom %, ISOTEC) for a period of 2 days. The cultures were grown under 95 µmol quanta $m^{-2} s^{-1}$ irradiance with a light to dark regime of 16:8 hours and at a temperature of 15 ± 1°C. On day 3, cultures were centrifuged at 1500 x *g* (with a swing rotor) for 10 minutes to remove unincorporated ^{13}C and ^{15}N labelled substrates from the media. Algal cell pellets formed after centrifugation were washed twice and re-suspended in an ESAW media without nutrient loadings.

P. globosa *virus culturing and bacterial inoculum:* The lytic *P. globosa* virus, PgV-07T (Baudoux and Brussaard 2005) used in this study was produced using exponentially growing *P. globosa* cultures. The bacterial populations used in this experiment were obtained from Southern North Sea near Texel, The Netherlands (December 2008). Prior to the bacterial inoculation (10% v/v), sea water was filtered through 0.8 µm pore size filters (45 mm in diameter; Millipore, Eschborn, Germany) to minimise heterotrophic nanoflagellates and other zooplankton.

Experimental Setup: The ^{13}C and ^{15}N labelled *P. globosa* culture was split into 4 subcultures and each was transferred (10% v:v) to a fresh 3 L 1:1 mixture of f/2 (Guillard 1975) and ESAW media. Two of these subcultures were infected with pre-filtered PgV-07T virus (0.2 µm pore-size, cellulose acetate, Whatman, Maidstone, England) at an initial virus to algae ratio of 17:1. The other two cultures served as non-infected control cultures and received medium instead of viral lysate in equal amount. The experiment was conducted during the mid light phase of the light to dark regime. At regular time intervals, samples for algae and virus abundance, bulk particulate ^{13}C and ^{15}N- measurements, catalyzed reporter deposition-fluorescence *in situ* hybridization analyses (CARD-FISH) and for single cell analyses i.e., AFM and nanoSIMS were taken for up to 7 days post-infection and analyzed as described in the following.

Abundances: Algal abundance was monitored by flow cytometry using a Beckman Coulter EPICS XL-MCL benchtop flow cytometer, equipped with an 15 mW 488 nm

argon laser (Veldhuis and Kraay 2000). The 1 mL samples taken at each time point were diluted up to 10-fold in sterile seawater (0.2 µm filtered and autoclaved). The flow cytometer trigger was set on the red chlorophyll autofluorescence (emission >630 nm). The abundance of *P. globosa* viruses and bacteriophages were enumerated using a 15 mW 488 nm argon laser Becton-Dickson FACSCalibur flow cytometer (Brussaard 2004). Samples of 1 mL were fixed with 25% glutaraldehyde (0.5% final concentration, EM grade, Sigma- Aldrich, St Louis, MO, USA) for 15 to 30 minutes at 4°C, flash frozen in liquid nitrogen and stored at -80°C until analysis. The thawed samples were diluted 50 to 1,000-fold in sterile TE-buffer (pH 8.0) and stained with the nucleic acid-specific dye SYBR Green I (Invitrogen-Molecular Probes, Eugene, OR, USA) at a final concentration of 0.5×10^{-4} of the commercial stock for 10 min at 80°C. The flow cytometer trigger was set on the green fluorescence and data files were analyzed as described by Brussaard *et al* (2010).

CARD-FISH and HISH-SIMS analyses: CARD-FISH analyses was performed to identify and quantify the bacterial populations as described by Pernthaler et al (2004). Subsamples taken at each time interval were fixed with paraformaldehyde (PFA, 1% final concentration) for 1 h at room temperature or overnight at 4°C. Subsamples were filtered onto white polycarbonate membrane filters (GTTP, 0.2 µm pore size, 25 mm in diameter, Millipore, Eschborn, Germany), washed with 5-10 ml of 1× phosphate buffer saline (PBS), air-dried and stored at -20°C until analysis. Samples were hybridised with the following probes: Gamma42a for *Gammaproteobacteria* together with Beta42a competitor (Manz et al 1992), CF319a for *Bacteroidetes* (Manz et al 1996), ALF986 for *Alphaproteobacteria* (Amann et al 1997), Alt1413 for *Alteromonas* cells (Eilers et al 2000), Ros593 for *Roseobacter* cells (Eilers et al 2001). Hybridised filters were counterstained with 1 µg ml^{-1} of 4,6-diamidino-2-phenylindole (DAPI). Subsequently, all DAPI-stained and hybridised cells were quantified by epifluorescence microscopy (Axioplan II Imaging epifluorescence microscope, Zeiss, Jena, Germany).

Similarly, Halogen *In-Situ* Hybridization assay coupled to nanoSIMS (HISH-SIMS) (Musat et al 2008) was performed to quantify the substrate assimilation of individual *Alteromonas* (probe Alt1413) and *Roseobacter* (probe Ros593) cells with ^{19}F containing tyramides.

Bulk Carbon and Nitrogen Measurements: For the determination of bulk particulate ^{13}C and ^{15}N- measurements, 30-80 mL of the experimental cultures were filtered onto pre-combusted glass fiber filters (GF/F, 25 mm diameter, Whatman, Maidstone, England) freeze-dried and stored at room temperature until analysis. The C- and N- isotopic composition of particulate organic matter was determined as CO_2 and N_2 released by flash combustion in an automated elemental analyzer (Thermo Flash EA, 1112 Series) coupled to an isotope ratio mass spectrometer (Finnigan Delta^{plus} XP, Thermo Scientific).

Carbon remineralisation: Carbon remineralisation was measured as dissolved inorganic ^{13}C-carbon (^{13}C-DIC) from labeled biomass released within the plankton community in our incubation experiments. Subsamples (5 mL) were poisoned with saturated mercuric chloride solution. The isotopic component of DIC was then determined after acidifying with 1% final concentration of hypo-phosphoric acid as described by Assayag *et al* (2006) and was analyzed on a gas chromatography-isotope ratio monitoring mass spectrometry (Optima Micromass, Manchester, UK).

Atomic force microscopy: Atomic force microscopy (NT-MDT Co., Moscow, Russia) was performed in a semi-contact mode as described by Sheik *et al* (2012). Briefly, 5-10 mL of the samples were fixed with 1% PFA for 1 hour at room temperature or overnight at 4°C. Subsequently, PFA fixed samples were filtered on to gold-palladium sputtered polycarbonate membrane filters (GTTP type; pore-size 0.22 µm; diameter 25 mm; Millipore) using a gentle vacuum, washed with 5-10 ml of 1× PBS, air-dried and stored at -20°C until analysis. AFM analysis was performed in air and images were acquired in alternating current mode at scan rates between 0.5 and 1 Hz. We used a semi-contact golden coated silicon cantilever (NSG10; NT-MDT) with a spring constant of 11.8 Nm^{-1}. Surface topography of cells and compartments were acquired by height channel and images were processed with flatten correction function of the software (Nova P9, version 2.1.0.828, NT-MDT, Moscow, Russia).

NanoSIMS analyses: Enrichment of the ^{13}C and ^{15}N in the specific probe hybridised bacterial cells (Alt1413 and Ros593) were analyzed with NanoSIMS 50 L (CAMECA, Paris, France). The primary ion beam had a nominal size of approximately 150 nm and the sample was sputtered with a dwelling time of 6 ms per pixel. The primary current was 20-30 nA Cs^+ during acquisition for most images. For each analysis, we recorded simultaneously secondary-ion images of naturally abundant ^{12}C (measured as $^{12}C^-$), ^{14}N (measured as $^{12}C^{14}N^-$) and similarly, ^{19}F for the identification of specific

probe hybridised bacterial cells, ^{13}C and ^{15}N for the uptake quantification. NanoSIMS data-sets were analyzed using the Look@NanoSIMS software (Polerecky et al 2012). Regions of interest (ROI) around individual bacterial cells were defined manually using ^{19}F image. The isotope ratio ($r = {}^{13}C/{}^{12}C$ or $^{15}N/{}^{14}N$) was calculated for each ROI based on the total $^{13}C^{-}$ and $^{12}C^{-}$ counts for each pixel. Subsequently, the ^{13}C and ^{15}N ratios were calculated in terms of absolute abundance, defined as $^{13}C/({}^{13}C+{}^{12}C)$ and $^{15}N/({}^{15}N+{}^{14}N)$ respectively.

Calculations of biovolume and single cell assimilation of ^{13}C and ^{15}N: Epifluorescence microscopy images taken during CARD-FISH analyses and before nanoSIMS analyses were used to determine the dimensions of *Alteromonas* and *Roseobacter* cells. Assuming cells as rotational ellipsoids, we deduced the biovolume of *Alteromonas* and *Roseobacter* cells at the 5 h (*Alteromonas* cells only), day 2 and day 7 of the experiment (Table 1).

Table 1: Biovolume (based on cell abundances) of *Alteromonas* and *Roseobacter* cells from non-infected and infected *P. globosa* cultures.

Time	*Alteromonas* cells		*Roseobacter* cells	
	Non-infected cultures	Infected Cultures	Non-infected cultures	Infected Cultures
5 h	1.03 ± 0.11	1.51 ± 0.11	N.D*	N.D
Day 2	0.87± 0.04	0.48 ± 0.03	0.58± 0.06	0.59± 0.07
Day 7	0.66 ± 0.06	0.43 ± 0.04	0.36 ± 0.03	1.05 ± 0.06

*N.D = not determined

We quantified the ^{13}C and ^{15}N substrate assimilation (fmol per cell^{-1}) within single cells of *Alteromonas* and *Roseobacter* due to *P. globosa* viral lysis, relative to non-infected *P. globosa* cells). This estimation was based on the ^{13}C and ^{15}N enrichments of *Alteromonas* and *Roseobacter* cells, calculated biovolume and assuming bacterial carbon conversion factor of 350 fg C μm^{-3} with C:N ratio of 4 (Lee and Fuhrman 1987).

DNA extraction and amplicon pyrosequencing:

DNA extraction was performed as described by Zhou *et al* (Zhou et al 1996) on samples that were filtered (100-200 mL) onto white polycarbonate membrane filters (GTTP, 0.2 μm pore size, 25 mm in diameter, Millipore, Eschborn, Germany) and stored at -20°C until analysis. The extracted DNA was further purified using

Wizard® DNA Clean-Up System (Promega Corporation, Madison, USA) as per manufacturer's instructions. The bacterial 16S rRNA genes were amplified and sequenced using amplicon pyrosequencing at the Research and Testing Laboratories (Lubbock, Texas). The pyrosequencing was performed at 6h, day 2 and 7 of the experiment from the infected and non-infected cultures targeting *Gammaproteobacteria* (forward primer 5'- CMATGCCGCGTGTGTGAA-3', reverse primer 5'- ACTCCCCAGGCGGTCDACTTA-3'), *Alphaproteobacteria* (forward primer 5'-ARCGAACGCTGGCGGCA-3', reverse primer 5'- TACGAATTTYACCTCTACA-3') and *Bacteroidetes* (forward primer 5'- AACGCTAGCTACAGGCTT-3', reverse primer 5'-CAATCGGAGTTCTTCGTG-3'). The generated sequences were processed and taxonomically identified as per company's standard procedure (Sun et al 2011), to the species level according to the >97% sequence identity of 16S rRNA genes. Thereafter, the species percentage composition of each major bacterial group was based on the relative abundance information within and among the individual samples and relative numbers of reads (S.I. Table 1).

MEGAN 4, a metagenome analysing software was used to construct the heat plot of 16S rRNA amplicon sequence dataset (S.I. Figure 1, (Huson et al 2011)). Amplicon sequences were clustered with >97% sequence identity and BLASTN was used to compare clustered sequences against the SILVA rRNA database (http://www.arb-silva.de). The output of this comparison was then parsed by MEGAN4 and mapped onto the NCBI taxonomy. The BLASTN comparison shown that *Bacteroidetes* 16S rRNA amplicon sequences targeted mostly uncultured *Bacteroidetes* species and hence not described further in the text.

Statistical analyses: One-way analyses of variance (ANOVAs) was used to test for differences in the bacterial numbers and single cell ^{13}C and ^{15}N enrichments of *Alteromonas* and *Roseobacter* cells in infected and non-infected *P. globosa* cultures at different time intervals. Pearson Product Moment Correlation was used to determine the correlation between algal cell numbers, particulate ^{13}C-carbon and ^{13}C-DIC. All analyses were carried out using the Sigmastat version 3.5 software package.

Results:

Dynamics of P. globosa and PgV abundances:

While the *P. globosa* cell abundance in non-infected cultures increased by 10-fold in 4 days (from 0.22 to 2.26 x 10^6 cells ml^{-1}; Fig. 1A), viral infection led to a decline of *P. globosa* cell abundance from 18 h post-infection onwards (1.91 x 10^3 cells ml^{-1} by day 4). Correspondingly, the abundance of PgV in infected cultures increased between 12 h and 18 h post-infection, with a viral maximum of ~ 2.33 × 10^7 ml^{-1} after 2 days (Figure 1B).
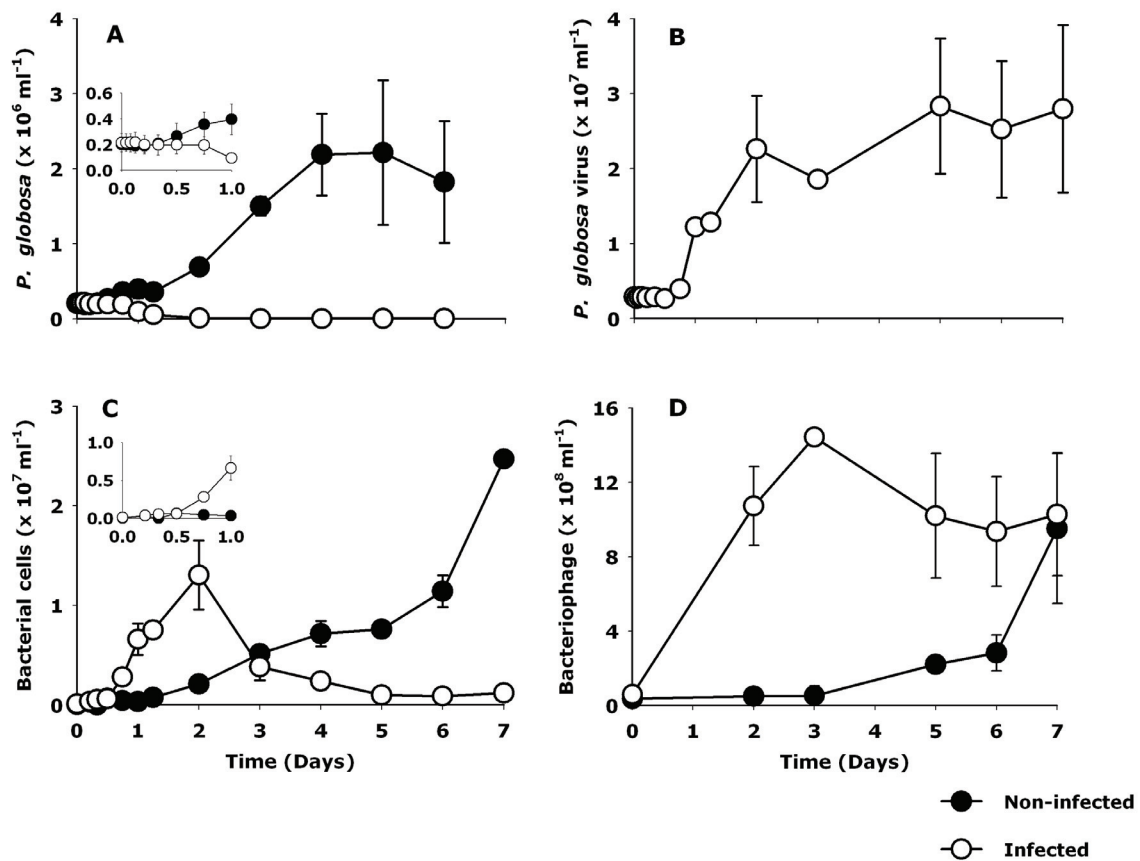

Figure 1: Microbial population dynamics due to viral infection of *P. globosa* relative to non-infected cultures. *(A)* algal abundance, (B) *P. globosa* virus (PgV-07T) abundance, and (C) total microbial abundance as DAPI-stained cells, and (D) bacteriophage dynamics. Error bars indicate standard deviation from duplicate batch cultures (STDEV).

*C*hanges in bacterial community composition:

The bacterial abundance in non-infected *P. globosa* cultures increased steadily throughout the 7-day experiment (Figure 1C). In infected cultures, bacterial abundance increased rapidly from the point of *P. globosa* cell lysis (18 h) reaching a maximum by day 2, but dropped sharply right afterwards until a stable abundance was reached after day 4 ($\sim$ 6.93 x 10^5 cells ml^{-1}, Figure 1C). The sharp decline in the bacterial numbers coincided with an increase in the number of bacteriophages (Figure 1D).

In the non-infected cultures, catalyzed reporter deposition- fluorescence *in situ* hybridization (CARD-FISH) analysis revealed dominance by *Bacteroidetes* and *Alphaproteobacteria* by day 7, accounting for $\sim$ 56% and $\sim$ 34% of the total microbial populations, respectively (Figure 2A). Viral mediated *P. globosa* lysis did not affect *Bacteroidetes* populations which remained of relatively minor importance with stable low cell abundance throughout the experiment ($\sim$ 1.49 x 10^5 cells ml^{-1}, Figure 2B). Within *Alphaproteobacteria*, *Roseobacter* cells reached their highest abundance in the non-infected cultures on day 7 ($\sim$ 6.31 x 10^6 cells ml^{-1}) but on day 2 in the infected cultures ($\sim$ 2.5 x 10^6 cells ml^{-1}). The majority of the *Alphaproteobacteria* phylotypes as per amplicon pyrosequencing analysis belonged to *Roseobacter* cells (Figure 3, Supplementary Table 1). Alphaproteobacterial phylotypes in the non-infected cultures showed *Leisingera sp.* dominance, where as in infected cultures showed higher species diversity and evenness (Figure 3, Supplementary Table 2).

Even more striking were the changes in the gammaproteobacterial populations (Figure 2). Amongst them, substantial growth of *Alteromonas* cells was stimulated shortly after *P. globosa* viral infection. At 5 and 8 h post-infection, yet prior to cell lysis of *P. globosa*, the abundance of *Alteromonas* cells has already increased significantly (ANOVA, n=25, P = <0 0.001) and in fact dominated the *Gammaproteobacteria* as identified in amplicon pyrosequencing analysis (Figure 3). *Alteromonas* cells showed the highest abundance on day 3 in the control cultures ($\sim$ 2.88 x 10^5 cells ml^{-1}) and in the infected cultures at day 2 ($\sim$ 8.52 x 10^6 cells ml^{-1}; Figure 2C). Epifluorescence microscopy imaging revealed that *Alteromonas* cells from the infected *P. globosa* cultures formed (micro)aggregates soon after *P. globosa* cell lysis, with increasing percentage of cellular aggregation until day 2 of the experiment

(Table 2). In combination with atomic force microscopy imaging, we confirmed the presence of aggregates in infected *P. globosa* cultures (Figure 4). Thereafter, gammaproteobacterial populations and similarly *Alteromonas* cells in infected *P. globosa* cultures dropped until day 5 maintaining stable cell abundances. Interestingly, amplicon pyrosequencing analysis indicated that only a single phylotype, *Alteromonas* sp., dominated the gammaproteobacterial populations due to *P. globosa* viral lysis which persisted throughout the experiment (Figure 3, Supplementary Table 1). However, in non-infected cultures, phylotypes of *Alteromonas* cells were diverse, for example, *Galciecola* sp. dominated at day 2 and *Amphritea atlantica* at day 7 (Figure 3, Supplementary Table 2).
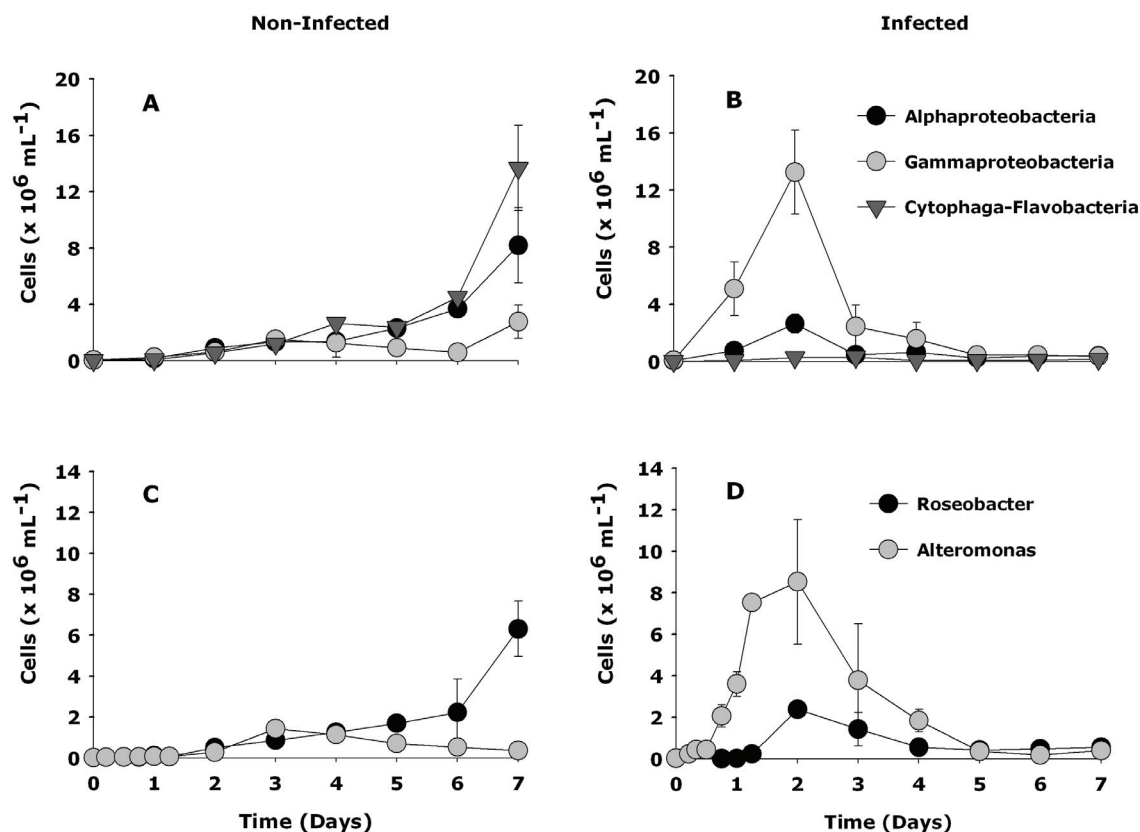
Figure 2: Temporal changes in the abundance of major bacterial groups *Alphaproteobacteria, Gammaproteobacteria* and the *Bacteroidetes* (A-B), *Alteromonas* and *Roseobacter* cells (C-D) due to growing non-infected *P. globosa* cells and due to *P. globosa* viral lysis. Please note the different y-axis scale. Error bars indicate STDEV.

Table 2: Percentage of *Alteromonas* and *Roseobacter* cells as free-living and aggregate associated.

		Alteromonas cells						
		Non-infected Cultures			Infected Cultures			
Time	n	Free-living (mean ± SE)	n	Aggregate-associated (mean ± SE)	n	Free-living (mean ± SE)	n	Aggregate-associated (mean ± SE)
0 h	15	100 ± 0	0	0	24	100 ± 0	0	0
5 h	21	100 ± 0	0	0	35	78 ± 2.5	26	22 ± 3.9
18 h	19	100 ± 0	0	1 ± 0	324	49 ± 3.6	335	51 ± 2.6
Day 2	67	81.3 ± 2.7	15	18.6 ± 2.4	168	12.2 ± 2.1	1196	87.7 ± 5.2
Day 4	91	74.7 ± 2.8	31	25.8 ± 3.1	200	40.9 ± 5.2	290	59.1 ± 6.3
Day 7	45	83.3 ± 3.5	29	16.6 ± 3.9	69	70.8 ± 4.5	45	29.1 ± 3.5

		Roseobacter cells						
		Non-infected Cultures			Infected Cultures			
Time	n	Free-living (mean ± SE)	n	Aggregate-associated (mean ± SE)	n	Free-living (mean ± SE)	n	Aggregate-associated (mean ± SE)
0 h	15	100 ± 0	0	0	15	100 ± 0	0	0
5 h	17	100 ± 0	0	0	35	100 ± 0	0	0
18 h	19	95.6 ± 1.7	6	4.4 ± 2.6	17	98.2 ± 3.2	6	1.7 ± 2.8
Day 2	166	83.1 ± 2.5	33	16.9 ± 5.7	172	67.8 ± 1.8	82	32.2 ± 1.2
Day 4	214	67.3 ± 6.3	104	32.7 ± 4.6	59	41.8 ± 4.4	90	58.1 ± 3.6
Day 7	603	55.1 ± 3.1	459	44.95 ± 4.0	50	27.8 ± 4.6	131	72.1 ± 4.8

n = total number of cells per microscopic field.

Gammaproteobacteria

Alphaproteobacteria

Figure 3: The percentage of diverse phylotypes belonging to Gamma and Alpha-proteobacterial as deduced from amplicon pyrosequencing analysis.
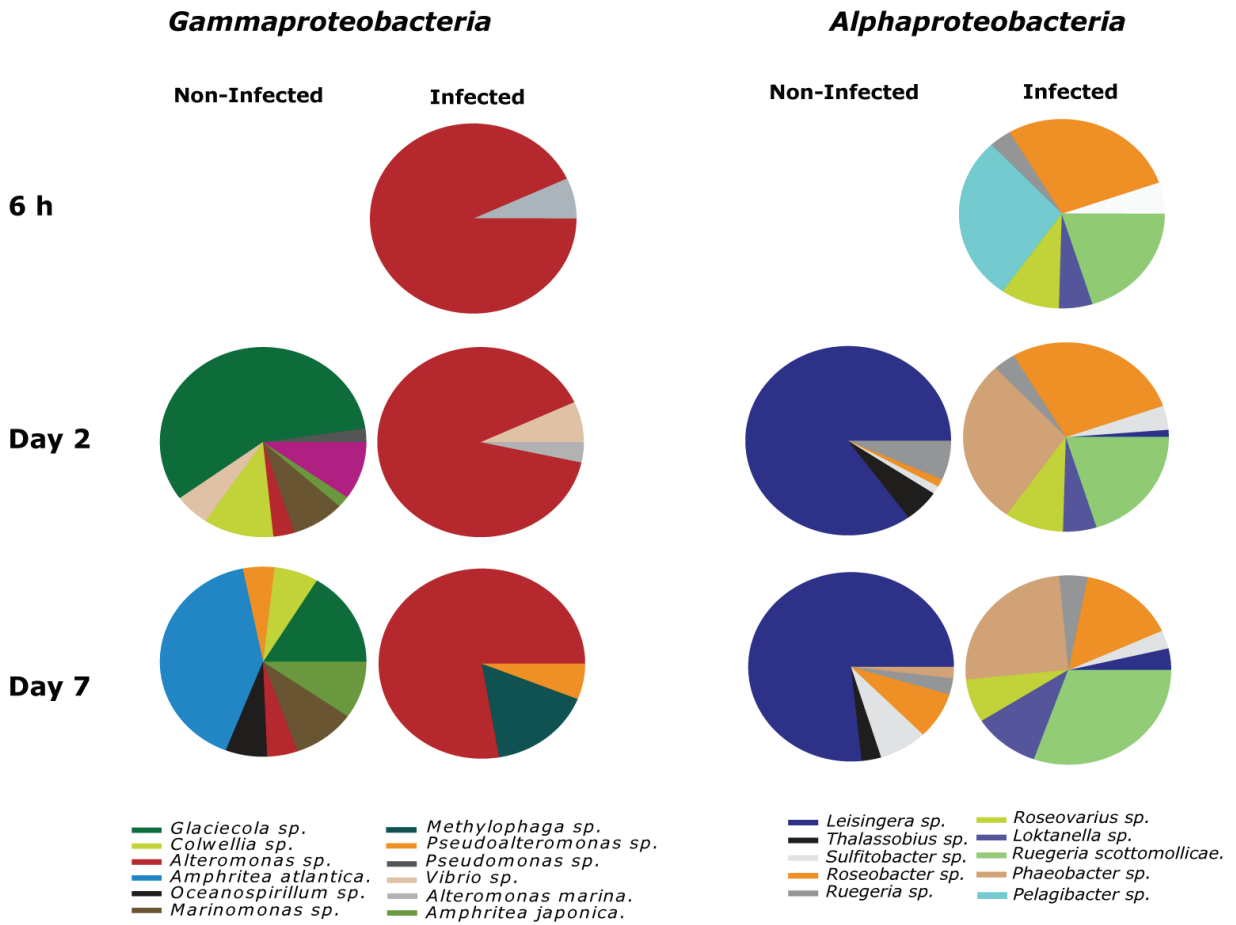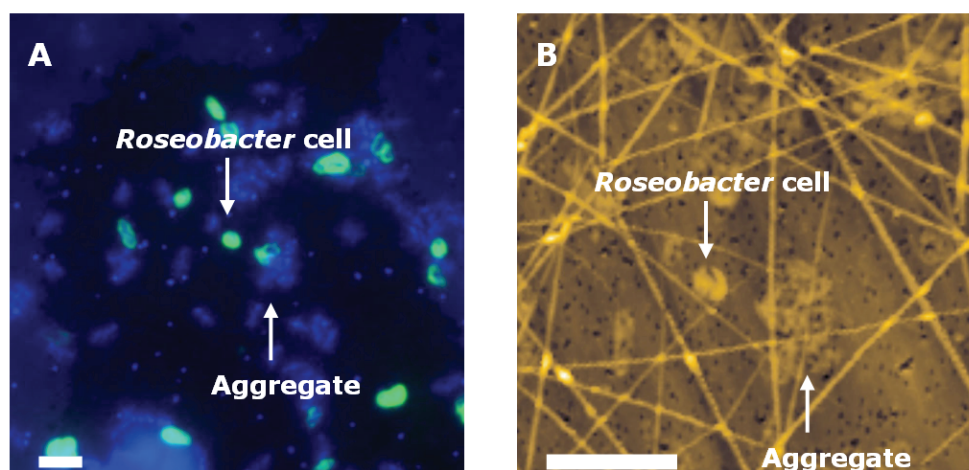
Figure 4: Visualisation of aggregates using epifluorescence imaging (A) and its corresponding atomic force microscope image (B) in the infected *P. globosa* cultures at day 2. Green cells represent CARD-FISH hybridization of *Roseobacter* cells. Scale bar = 5μm

Carbon remineralization:

There was no significant change in the particulate organic ^{13}C-carbon (^{13}C -POC) and particulate organic ^{15}N-nitrogen (^{15}N -POC) with time in the control cultures (Figure 5A-B). As expected, however, viral lysis of *P. globosa* led to a marked decline in the amount of ^{13}C -POC, which correlated strongly to the declining cell abundances (Pearson Product Moment Correlation, R= -0.947, P= <0.001, Figure 4A). Based on the net decline of the ^{13}C -POC by day 7 of the experiment, ~ 74 % of the *P. globosa* biomass from the infected cultures appears to be diverted towards dissolved forms (Figure 5A-B). Meanwhile, there was no significant decline in ^{15}N -POC (ANOVA, P = 0.004, Figure 5B). The decrease in the ^{13}C -POC in infected *P. globosa* cultures was strongly correlated to the amount of organic carbon remineralized to ^{13}C-DIC (R= -0.991, P= <0.001, Figure 5C). By day 1 of the experiment, the amount of carbon mineralised in the infected cultures differed substantially relative to the non-infected cultures (ANOVA, P = <0.001). Comparing the net amount of ^{13}C -POC declined and the net increase in the ^{13}C-DIC, ~ 22.5 μ mol ^{13}C l^{-1}, equivalent to 55 % of the shunted particulate ^{13}C-carbon has been remineralized by day 7 (Figure 5C). In contrast, ^{13}C-DIC showed no significant change in the amount of carbon remineralized in the non-infected cultures until day 6 when a small increase in ^{13}C-DIC was observed. Throughout the experiment, there was no detectable ammonium in both the non-infected and infected *P. globosa* cultures (data not shown).
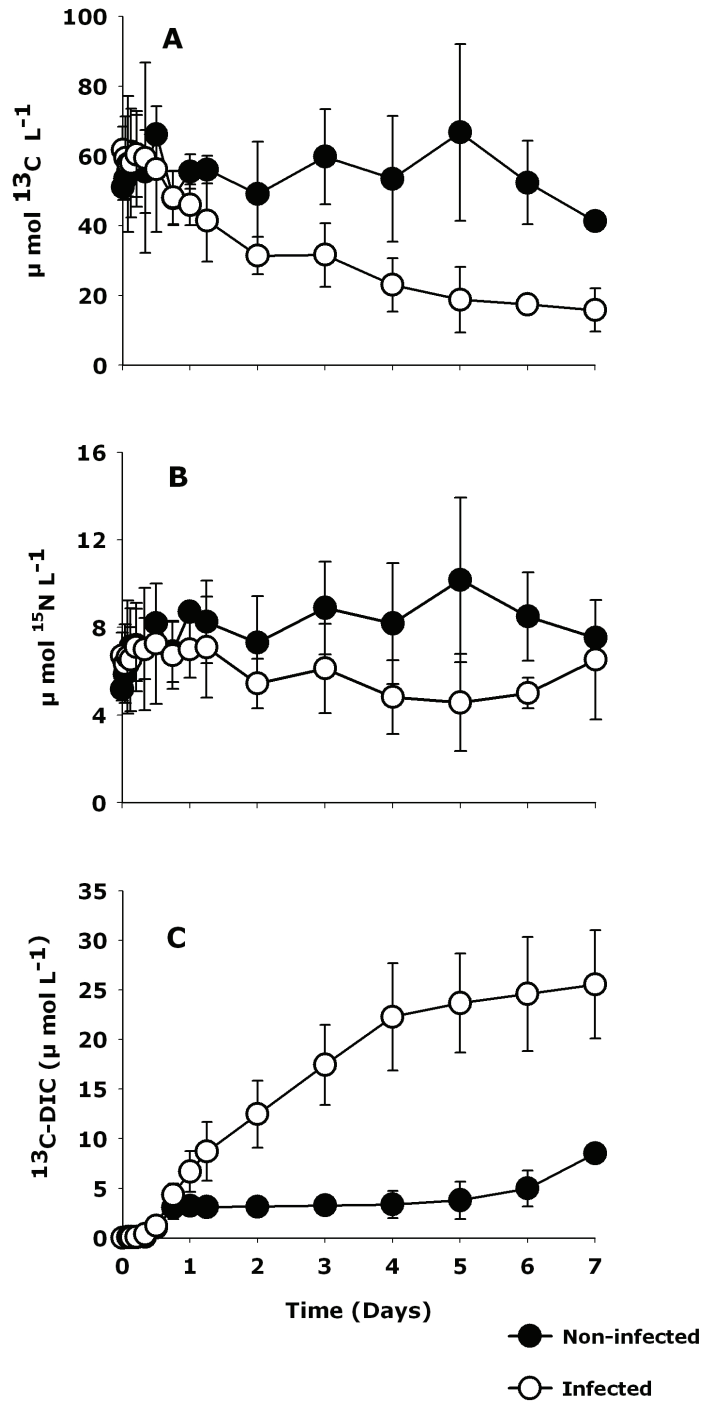
Figure 5: Quantification of the viral mediated shunt and the extent of the bacterial mediated carbon remineralization using bulk measurements. Error bars indicate from duplicate batch cultures STDEV.

Effect of viral lysis on algal C and N transfer to specific bacterial groups:

By combining CARD-FISH and HISH-SIMS, we measured the ^{13}C and ^{15}N enrichments of the *Alteromonas* and *Roseobacter* cells from the non-infected and infected *P. globosa* cultures using nanoSIMS (Figures 6-7). In the non-infected *P. globosa* cultures, by 5 h, the ^{13}C and ^{15}N enrichment (Figures 6A and C) and hence, substrate assimilation of *Alteromonas* cells was minimal (Table 3). In contrast, already by 5 h, *Alteromonas* cells from the infected *P. globosa* cultures were characterized by significant enrichment in ^{13}C and ^{15}N (Figures 7A and C), with calculated substrate assimilation of 2.14 fmol ^{13}C per cell and ~ 0.65 f mol ^{15}N per cell (P = <0.001, Table 3), respectively. A maximum substrate assimilation of *Alteromonas* and *Roseobacter* cells from the non-infected was noticed at day 2 of the experiment. The ^{13}C and ^{15}N substrate assimilation of *Alteromonas* from the infected cultures *P. globosa* cultures decreased by day 7 relative to day 2, while substrate assimilation of *Roseobacter* cells increased from day 2 to day 7 (Table 3).
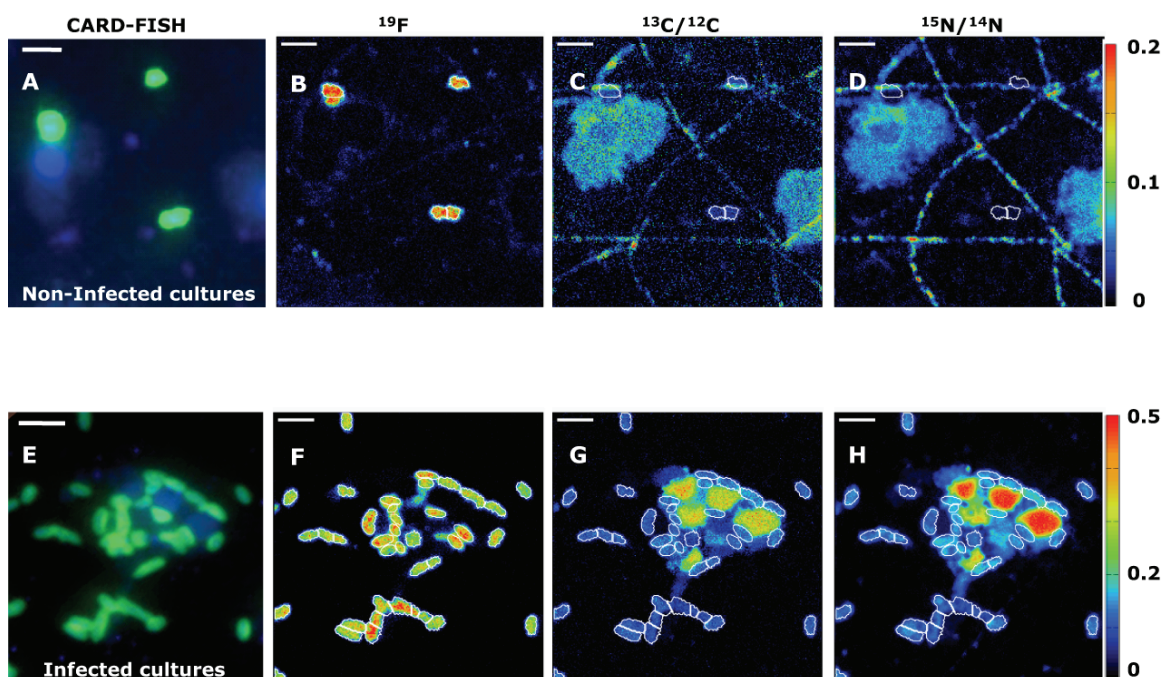
Figure 6: Comparison of *Alteromonas* cells nanoSIMS imaging in non-infected cultures (upper panel) and infected *P. globosa* cultures (lower panel) at day 2 of the experiment. First column (A, E) illustrates the CARD-FISH image taken before nanoSIMS analyses. The corresponding cells were located by the ^{19}F signal during nanoSIMS (B, F) and their respective ^{13}C (C, G) and ^{15}N enrichments (D, H).
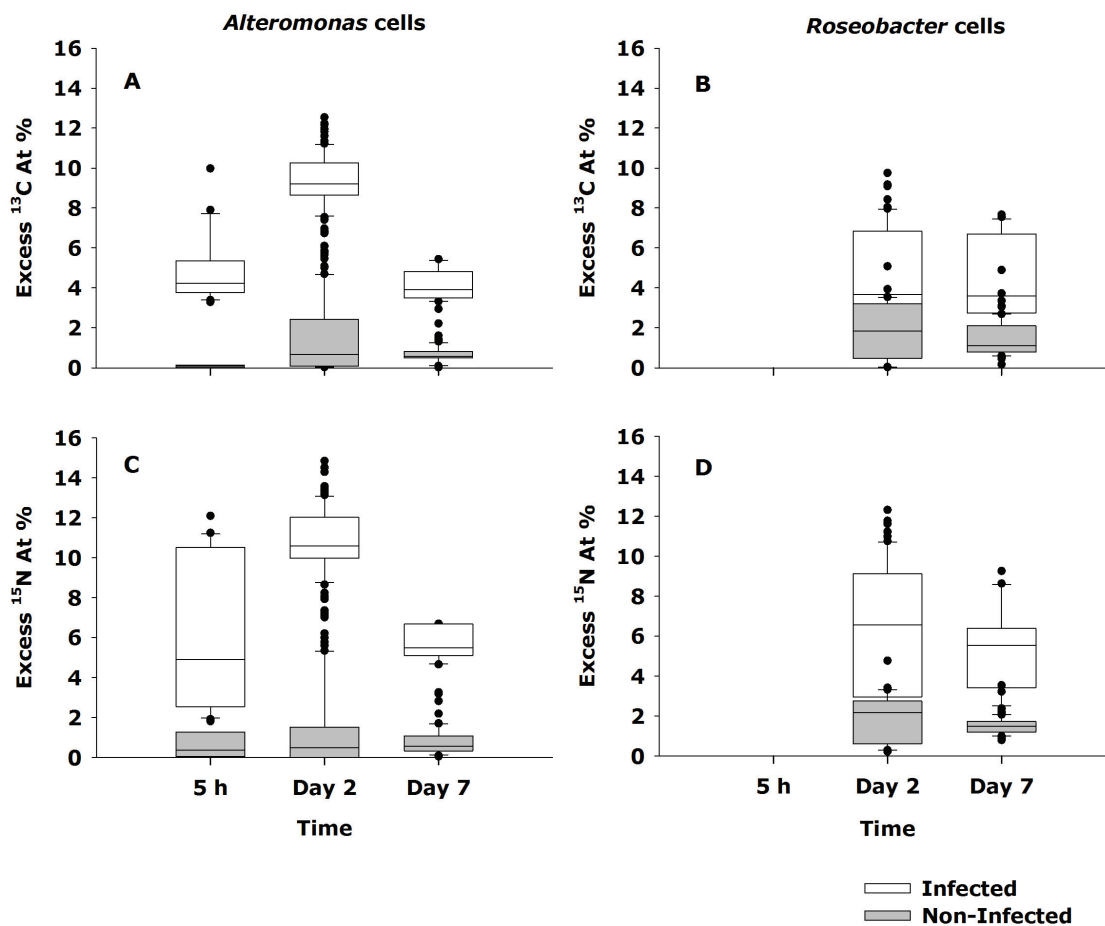
Figure 7: ^{13}C and ^{15}N enrichments within single cells of *Alteromonas* and *Roseobacter* as deduced from nanoSIMS analyses.

Table 3: Single cell ^{13}C and ^{15}N substrate assimilation of *Alteromonas* and *Roseobacter* cells (f mol per cell) at various temporal stages of *P. globosa* viral lysis relative to non-infected *P. globosa* cells.

| | *Alteromonas* cells | | | | | *Roseobacter* cells | | | | |
| | Non-Infected cultures | | | Infected cultures | | Non-Infected cultures | | | Infected cultures | |
Time	n	f mol ^{13}C cell^{-1} (mean ± SE)	f mol ^{15}N cell^{-1} (mean ± SE)	n	f mol ^{13}C cell^{-1} (mean ± SE)	f mol ^{15}N cell^{-1} (mean ± SE)	n	f mol ^{13}C cell^{-1} (mean ± SE)	f mol ^{15}N cell^{-1} (mean ± SE)	n	f mol ^{13}C cell^{-1} (mean ± SE)	f mol ^{15}N cell^{-1} (mean ± SE)
0 h	8	0	0	12	0	0	N.D	-	-	N.D	-	-
5 h	12	0.03± 0.01	0.03 ± 0.02	21	2.14 ± 0.16	0.05 ± 0.04	N.D	-	-	N.D	-	-
Day 2	87	0.56 ± 0.08	0.07 ± 0.01	82	1.32 ± 0.02	0.22 ± 0.005	41	0.32 ± 0.04	0.05 ± 0.01	63	0.76 ± 0.06	0.16 ± 0.01
Day 7	46	0.13 ± 0.01	0.02 ± 0.002	36	0.53 ± 0.23	0.10 ± 0.004	21	0.16 ± 0.01	0.02 ± 0.002	46	1.38 ± 0.15	0.24 ± 0.02

n = number of single cells analysed by nanoSIMS

N.D = not determined

Discussion:

Role of algal viral lysis in structuring bacterial community composition:

The distinct temporal patterns in the major bacterial groups show that *P. globosa* viral lysis led to significant and very rapid changes in the bacterial community composition. Furthermore, viral mediated *P. globosa* lysis promoted the growth of opportunistic *Gamma-* and *Alphaproteobacteria* (r-strategists) relative to slow growing competitive bacteria (e.g., *Bacteroidetes*, K-strategists) (Fuchs et al 2000). The bacterial community composition also changed in association with senescing *P. globosa* cells from non-infected cultures. However, these communities were distinct from those in the infected cultures. The predominance of *Alphaproteobacteria* and *Bacteroidetes* observed in the non-infected cultures is in congruence with studies of the progression of naturally occurring *P. globosa* blooms (Alderkamp et al 2006, Lamy et al 2009).

Within specific taxonomic groups, viral infections of *P. globosa* enhanced the rapid development of *Alteromonas* cells as observed by its initial doubling during the *P. globosa* infection cycle and dominated bacterial communities soon after *P. globosa* viral lysis. In contrast to the development of *Alteromonas* abundance, the relative contribution of *Roseobacter* cells rose slowly. The initial proliferation of *Alteromonas* and *Roseobacter* cells is consistent with previous phytoplankton incubation studies (Allers et al 2007, Sandaa et al 2009). The observation of rapid development of *Alteromonas* cells coinciding with increasing bacteriophage abundance indicates that potential phage lysis was not able to prevent the initial *Alteromonas* bloom.

Additionally, we observed substantial phylotype diversity among *Gammaproteobacteria* and *Alphaproteobacteria,* which exhibited diverse patterns due to viral lysis and growing cells of *P. globosa* (S:I. Figure 1). Remarkably, *Alteromonas* populations in infected cultures mainly consisted of one individual phylotype, *Alteromonas* sp., which showed a clear dominance during initial doubling of *Alteromonas* abundance and remained to be a major phylotype throughout the experiment. On the other hand, gammaproteobacterial phylotypes in the non-infected cultures were diverse. At day 2, *Glaciecola* sp. represented the majority of the gammaproteobacterial phylotypes and diminished in phylotype dominance by day 7. The development of *Methylophaga* sp., a known dimethylsulfide (DMS) degrader (Schäfer 2007), by day 7 in the infected cultures could be related to the occurrence of *P. globosa* derived DMS compounds (Liss et al 1994). Moreover, within *Alphaproteobacteria*, viral lysis of *P. globosa* triggered the development of several

individual phylotypes, most of which belonged to *Roseobacter* cells. Interestingly, alphaproteobacterial phylotypes in the non-infected cultures mainly consisted of one individual phylotype, *Leisingera* sp. (affiliated to *Roseobacter* cells), which persisted and remained to be a major phylotype throughout the experiment. Overall, our results indicate that algal viral lysis structures bacterial community composition by favouring distinct bacterial phylotypes.

In the coastal North Sea, the *P. globosa* blooms are often associated with aggregates that are formed due to the disintegration of *P. globosa* colonies and/or cell lysis (Brussaard et al 2005, Lancelot et al 1994, Mari et al 2005, Verity et al 2007). Despite the presence of *P. globosa* single cells in this study, both the atomic force and epifluorescence microscopy revealed that the initial increasing abundances of *Alteromonas* and to a lesser extent *Roseobacter* cells were aggregate-associated. Recently, we showed that viral infection of *P. globosa* single cells impeded the release of star-like structures and that subsequent release of the intracellular fluidic pre-stage of the star-like structures might stimulate (micro) aggregate formation (Sheik et al 2012). Furthermore, phage lysis products might have also enhanced the formation of aggregates (Shibata et al 1997). The aggregate formation could partly inactivate viruses such as PgVs from surrounding waters (Brussaard et al 2005, Sheik et al 2012).

The dense bacterial association within aggregates could enhance the bacterial contact to its specific phage, thereby leading to efficient viral lysis. Indeed, the declining cell abundance of *Alteromonas* and *Roseobacter* cells, which were mostly aggregate associated in *P. globosa* infected cultures coincided with an increase in ambient bacteriophage abundances. Assuming a burst size (number of viruses produced per cell) of 50 (Parada et al 2006), the net decrease in the abundances of *Alteromonas and Roseobacter* cells matched the net increase in the number of ambient bacteriophages. Under natural conditions, an initial increase in *Alteromonas* and *Roseobacter* cellular abundances followed by disproportional decline due to predation and viral lysis was reported from the North Sea (Beardsley et al 2003). However, as we pre-filtered (0.8 μm) the North Sea water which was used as bacterial inocula, the potential presence of grazers can be excluded. Therefore, in our study, it seems that bacteriophages were the significant and sole mortality agents of *Alteromonas and Roseobacter* cells.

Viral driven carbon and nitrogen flow:

It is generally conceived that viruses facilitate the microbial substrate assimilation through the lysis of the host cells. A prominent finding of this study based on nanoSIMS imaging was a substantial carbon and nitrogen substrate assimilation of *Alteromonas* cells from infected *P. globosa* cultures by 5 h post-infection, prior to *P. globosa* viral induced cell lysis. Indeed, the presence of intact *P. globosa* cells (Figure 8), no decrease in the cellular abundance of *P. globosa* or an increase in the PgVs suggests that *P. globosa* viral lysis at 5 h time interval was unlikely. Therefore, the isotopic enrichment in *Alteromonas* cells would have to come from the leakage or enhanced excretion of organic compounds from the infected but still intact *P. globosa* host cells. The leakage or enhanced excretion of infected algal cells to the best of our knowledge so far represents an undocumented mechanism of viruses facilitating bacterial substrate assimilation.

At day 2, *P. globosa* viral lysis specifically enhanced the single cell ^{13}C and ^{15}N assimilation of *Alteromonas* cells by ~ 2.5 fold relative to *Roseobacter* cellular substrate assimilation. The observed differences in substrate assimilation were most likely due to different metabolic activities of these two genera. The *Alteromonas* cells are capable of utilising a high diversity of organic compounds for energy acquisition ranging from low molecular weight organics such as hexoses (Gómez-Consarnau et al 2012) to complex substrates such as coral mucus (Allers et al 2008). On the other hand, *Roseobacter* cells are known to prosper on the phytoplankton derived material such as algal osmolytes and monomers such as amino acids (Tada et al 2011, Zubkov et al 2001). Thus, the cell abundances attained by *Alteromonas* and *Roseobacter* and their ^{13}C and ^{15}N substrate assimilation by day 2, confirms that early stages of *P. globosa* viral lysis favours the development of opportunistic bacteria, such as *Alteromonas*.

We determined the total uptake of ^{13}C-carbon and ^{15}N-Nitrogen (in µ mol L^{-1}) for *Alteromonas* and *Roseobacter* cells by multiplying their average single-cell ^{13}C-carbon and ^{15}N-Nitrogen substrate assimilation with their respective cell abundances. When quantified, the total ^{13}C-carbon and ^{15}N-Nitrogen uptake of *Alteromonas* represented ~35% and *Roseobacter* cells ~6% of both the bulk particulate organic ^{13}C-carbon and ^{15}N-Nitrogen, respectively. The high relative contribution of *Alteromonas* and to a lesser extent *Roseobacter* cells to bulk particulate carbon and nitrogen suggests an efficient transfer of *P. globosa* viral lysates towards these specific bacterial members. However, the single cell substrate assimilation of

Alteromonas and *Roseobacter* cells from the non-infected cultures and similarly, its bulk contribution was minimal. Therefore it seems that much of the *P. globosa* biomass in the non-infected cultures was particulate bound and might have been utilised in the host physiological processes such as release of star-like structures (Sheik et al 2012).

The composition and contribution of the virally released *P. globosa* organic matter due to bacterial utilization might change with time, from readily available organic substrates to more refractory compounds (Brussaard et al 2005). Given the high enzymatic activity of aggregate-associated bacteria (Proctor and Fuhrman 1991), we speculate that potential phage mediated lysis might have facilitated the enzymatic dissolution of aggregates leading to enhanced organic carbon remineralisation rates. Based on our estimates, ~55 % of the particulate ^{13}C organic carbon was remineralized to dissolved inorganic carbon by day 7, with the rest potentially constituting of recalcitrant particulate organic carbon forms such as cellular debris and *P. globosa* star-like structures. In fact, the development of *Pseudoalteromonas* sp., an algal polysaccharide decomposer (Ivanova et al 2002), indicates the formation of refractory material.

In infected *P. globosa* cultures, the decreased single-cell substrate assimilation of *Alteromonas* cells by day 7 was consistent with its decreased cell abundance (Figure 2D, Table 3). In contrast, the carbon and nitrogen assimilation of *Roseobacter* cells was highest at day 7. The presence of higher substrate assimilation of *Roseobacter* cells during the times of its low contribution to the total bacterial abundances is in accordance with the previous observations conducted during naturally occurring *P. globosa* blooms (Alderkamp et al 2006, Lamy et al 2009). The delayed increase in *Roseobacter* cellular abundance during initial stages of *P. globosa* viral lysis and increased substrate assimilation by day 7 suggests that organic material released due to potential *Alteromonas* phage lysis partly favoured the enhanced substrate assimilation of *Roseobacter* cells. Thus, it appears that bacteriophage mediated lysis of a dominant bacterial species generates substrates, which may in turn facilitate the growth of other bacterial species.

We did not observe significant changes in the particulate ^{15}N-nitrogen from the *P. globosa* viral shunt. Although the adsorption of ammonium compounds on aggregates (Shanks and Trent 1979) could have interfered with our sampling procedure (0.2 μm syringe filtration), we did not notice the regeneration of ammonium as reported previously (Haaber and Middelboe 2009, Shelford et al

2012). The *Gammaproteobacteria* from the North Sea habitats (Eilers et al 2001) and some *Roseobacter* sp. (Moran et al 2007) are known for the rapid uptake of ammonium. The dominance of *Alteromonas* and *Roseobacter* cells indicates that ammonium or particulate organic nitrogen uptake could have occurred very rapidly.
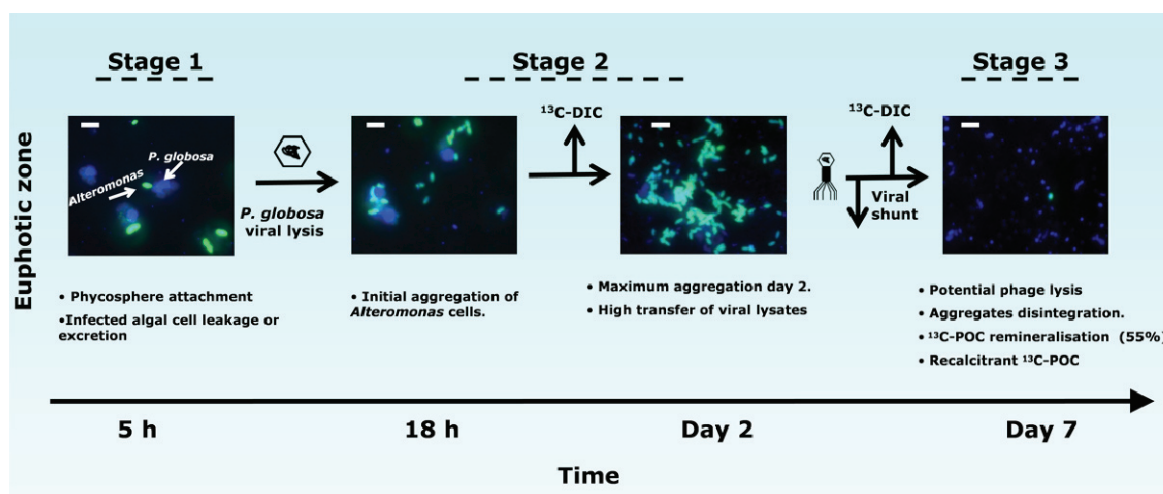
Figure 8: Conceptual diagram illustrating the observed temporal microbial regulation and associated biogeochemical processes due to *P. globosa* viral lysis using *Alteromonas* CARD-FISH images as an example.

Conclusions and implications:

Based on our combined results, we propose the following stages of viral mediated algal lysis structuring bacterial community composition and diversity, which in turn mediated the flow of carbon and nitrogen (Figure 8).

During early hours of viral infection, *P. globosa* cells leaked or excreted substantial amounts of organic matter not only stimulated substrate assimilation by *Alteromonas* cells but also triggered its attachment to the infected algal host (stage 1). The surroundings of algal-associated bacteria, the phycosphere (Bell and Mitchell 1972), is a microenvironment for a diverse set of bacterial populations. The phycosphere formation has been attributed to various environmental factors (Gomez-Pereira et al 2010, Teeling et al 2012, Tittel et al 2012). However, viral infections stimulating algal leakage or excretion and promoting the growth of phycosphere-associated is a previously undocumented finding. The bacterial attachment with infected phycosphere prior to algal cell lysis signifies interactions such as commensalism or mutualism can occur.

Our observations indicate that viral lysis of *P. globosa* single cells resulted in the formation of aggregates which were colonised densely with bacteria (stage 2). The bacterial response to algal viral infections was very rapid and consisted of a temporal succession of distinct populations with distinct phylotypes. Differences in the size of aggregates, bacterial colonisation, time of occurrence and environmental factors (e.g., nutrients (Mari et al 2005)) will determine whether or not aggregate formation enhances or impedes the biological pump. Aggregate dissolution due to potential phage lysis on one hand appeared to be responsible for regeneration of dissolved inorganic carbon (stage 3). On the other hand, development of specific bacterial phylotypes and bulk measurements indicated the presence of plentiful recalcitrant organic carbon. The sudden appearance of r- strategists and their rapid demise signifies the efficiency of potential phage mediated lysis and offers a potential explanation to their rarity in the environment (Allers et al 2007). The possibility that leakage or enhanced excretion of infected algal cells as a dominant process structuring bacterial diversity and mediating carbon and nitrogen flow should be now further explored.

Acknowledgments:

References:

Alderkamp AC, Sintes E, Herndl GJ (2006). Abundance and activity of major groups of prokaryotic plankton in the coastal North Sea during spring and summer. *Aquatic microbial ecology* **45:** 237-246.

Alderkamp AC, Van Rijssel M, Bolhuis H (2007). Characterization of marine bacteria and the activity of their enzyme systems involved in degradation of the algal storage glucan laminarin. *FEMS microbiology ecology* **59:** 108-117.

Allers E, Gómez-Consarnau L, Pinhassi J, Gasol JM, Šimek K, Pernthaler J (2007). Response of *Alteromonadaceae* and *Rhodobacteriaceae* to glucose and phosphorus manipulation in marine mesocosms. *Environmental Microbiology* **9:** 2417-2429.

Allers E, Niesner C, Wild C, Pernthaler J (2008). Microbes enriched in seawater after addition of coral mucus. *Appl Environ Microbiol* **74:** 3274-3278.

Amann R, Glöckner FO, Neef A (1997). Modern methods in subsurface microbiology: in situ identification of microorganisms with nucleic acid probes. *FEMS microbiology reviews* **20:** 191-200.

Assayag N, Rivé K, Ader M, Jézéquel D, Agrinier P (2006). Improved method for isotopic and quantitative analysis of dissolved inorganic carbon in natural water samples. *Rapid communications in mass spectrometry* **20:** 2243-2251.

Azam F, Fenchel T, Field JG, Gray JS, Meyer-Reil LA, Thingstad F (1983). The ecological role of water-column microbes in the sea. *Mar Ecol Prog Ser* **10:** 257-263.

Azam F, Long RA (2001). Sea snow microcosms. *Nature* **414:** 495-498.

Baudoux AC, Brussaard CPD (2005). Characterization of different viruses infecting the marine harmful algal bloom species *Phaeocystis globosa*. *Virology* **341:** 80-90.

Baudoux AC, Noordeloos AAM, Veldhuis MJW, Brussaard CPD (2006). Virally induced mortality of *Phaeocystis globosa* during two spring blooms in temperate coastal waters. *Aquat Microb Ecol* **44:** 207-217.

Beardsley C, Pernthaler J, Wosniok W, Amann R (2003). Are readily culturable bacteria in coastal North Sea waters suppressed by selective grazing mortality? *Applied and environmental microbiology* **69:** 2624.

Bell W, Mitchell R (1972). Chemotactic and growth responses of marine bacteria to algal extracellular products. *Biological Bulletin* **143:** 265-277.

Bergh O, Borsheim KY, Bratbak G, Heldal M (1989). High abundance of viruses found in aquatic environments. *Nature* **340:** 467-468.

Breitbart M (2012). Marine Viruses: Truth or Dare. *Annual Review of Marine Science* **4:** 425-448.

Brussaard CPD, Gast GJ, vanDuyl FC, Riegman R (1996). Impact of phytoplankton bloom magnitude on a pelagic microbial food web. *Mar Ecol Prog Ser* **144:** 211-221.

Brussaard CPD (2004). Optimization of procedures for counting viruses by flow cytometry. *Appl Environ Microbiol* **70:** 1506-1513.

Brussaard CPD, Mari X, Van Bleijswijk JDL, Veldhuis MJW (2005). A mesocosm study of *Phaeocystis globosa* (Prymnesiophyceae) population dynamics - II. Significance for the microbial community. *Harmful Algae* **4:** 875-893.

Brussaard CPD, Wilhelm SW, Thingstad F, Weinbauer MG, Bratbak G, Heldal M *et al* (2008). Global-scale processes with a nanoscale drive: the role of marine viruses. *ISME J* **2:** 575-578.

Brussaard CPD, J. P. Payet, C. Winter, and M. G. Weinbauer. (2010). Quantification of aquatic viruses by flow cytometry. *In S W Wilhelm, M G Weinbauer, and C A Suttle [eds], Manual of Aquatic Viral Ecology ASLO* p. 102–109.

Cottrell MT, Suttle CA (1991). Wide-spread occurrence and clonal variation in viruses which cause lysis of a cosmopolitan, eukaryotic marine phytoplankter, *Micromonas pusilla*. *Mar Ecol Prog Ser* **78:** 1-9.

Eilers H, Pernthaler J, Glockner FO, Amann R (2000). Culturability and in situ abundance of pelagic bacteria from the North Sea. *Applied and environmental microbiology* **66:** 3044.

Eilers H, Pernthaler J, Peplies J, Glöckner FO, Gerdts G, Amann R (2001). Isolation of novel pelagic bacteria from the German Bight and their seasonal contributions to surface picoplankton. *Applied and environmental microbiology* **67:** 5134-5142.

Fuchs BM, Zubkov MV, Sahm K, Burkill PH, Amann R (2000). Changes in community composition during dilution cultures of marine bacterioplankton as assessed by flow cytometric and molecular biological techniques. *Environmental microbiology* **2:** 191-201.

Fuhrman JA (1999). Marine viruses and their biogeochemical and ecological effects. *Nature* **399:** 541-548.

Gobler CJ, Hutchins DA, Fisher NS, Cosper EM, Sanudo-Wilhelmy S (1997). Release and bioavailability of C, N, P, Se, and Fe following viral lysis of a marine Chrysophyte. *Limnol Oceanogr* **42:** 1492-1504.

Gómez-Consarnau L, Lindh MV, Gasol JM, Pinhassi J (2012). Structuring of bacterioplankton communities by specific dissolved organic carbon compounds. *Environmental Microbiology***:** no-no.

Gomez-Pereira PR, Fuchs BM, Alonso C, Oliver MJ, van Beusekom JEE, Amann R (2010). Distinct flavobacterial communities in contrasting water masses of the North Atlantic Ocean. *ISME J* **4:** 472-487.

Guillard RRL (1975). Culture of phytoplankton for feeding marine invertebrates. *Smith, Walter L and Matoira H Chanley (Ed) Culture of Marine Invertebrate Animals Conference, Greenport, NY, Oct, 1972 Viii+338p Illus Plenum Press: New York, NY, USA; London, England Isbn 0-306-30804-5***:** 29-60.

Haaber J, Middelboe M (2009). Viral lysis of *Phaeocystis pouchetii*: Implications for algal population dynamics and heterotrophic C, N and P cycling. *Isme Journal* **3:** 430-441.

Huson DH, Mitra S, Ruscheweyh HJ, Weber N, Schuster SC (2011). Integrative analysis of environmental sequences using MEGAN4. *Genome Research* **21:** 1552-1560.

Ivanova EP, Bakunina IY, Sawabe T, Hayashi K, Alexeeva YV, Zhukova NV *et al* (2002). Two species of culturable bacteria associated with degradation of brown algae *Fucus evanescens*. *Microbial Ecology* **43:** 242-249.

Jacquet Sp, Miki T, Noble R, Peduzzi P, Wilhelm S (2010). Viruses in aquatic ecosystems: important advancements of the last 20 years and prospects for the future in the field of microbial oceanography and limnology. *Advances in Oceanography and Limnology* **1:** 97-141.

Lamy D, Obernosterer I, Laghdass M, Artigas F, Breton E, Grattepanche JD *et al* (2009). Temporal changes of major bacterial groups and bacterial heterotrophic

activity during a *Phaeocystis globosa* bloom in the eastern English Channel. *Aquatic Microbial Ecology* **58:** 95-107.

Lancelot C, Wassmann P, Barth H (1994). Ecology of *Phaeocystis*-dominated ecosystems. *Journal of Marine Systems* **5:** 1-4.

Lee S, Fuhrman JA (1987). Relationships between biovolume and biomass of naturally derived marine bacterioplankton. *Applied and Environmental Microbiology* **53:** 1298.

Liss PS, Malin G, Turner SM, Holligan PM (1994). Dimethyl sulphide and *Phaeocystis*: a review. *Journal of Marine Systems* **5:** 41-53.

Manz W, Amann R, Ludwig W, Wagner M, Schleifer KH (1992). Phylogenetic oligodeoxynucleotide probes for the major subclasses of proteobacteria: problems and solutions. *Systematic and Applied Microbiology* **15:** 593-600.

Manz W, Amann R, Ludwig W, Vancanneyt M, Schleifer K-H (1996). Application of a suite of 16S rRNA-specific oligonucleotide probes designed to investigate bacteria of the phylum cytophaga-flavobacter-bacteroides in the natural environment. *Microbiology* **142:** 1097-1106.

Mari X, Rassoulzadegan F, Brussaard CPDD, Wassmann P (2005). Dynamics of transparent exopolymeric particles (TEP) production by *Phaeocystis globosa* under N- or P-limitation: a controlling factor of the retention/export balance. *Harmful Algae* **4:** 895-914.

Moran MA, Belas R, Schell MA, Gonzalez JM, Sun F, Sun S *et al* (2007). Ecological genomics of marine roseobacters. *Applied and environmental microbiology* **73:** 4559-4569.

Musat N, Halm H, Winterholler B, Hoppe P, Peduzzi S, Hillion F *et al* (2008). A single-cell view on the ecophysiology of anaerobic phototrophic bacteria. *Proceedings of the National Academy of Sciences* **105:** 17861.

Parada V, oacute, nica, Herndl GJ, Weinbauer MG (2006). Viral burst size of heterotrophic prokaryotes in aquatic systems. *Journal of the Marine Biological Association of the UK* **86:** 613-621.

Peduzzi P, Weinbauer MG (1993). Effect of concentrating the virus-rich 2-200-nm size fraction of seawater on the formation of algal flocs (marine snow). *Limnology and Oceanography* **38:** 1562-1565.

Pernthaler A, Pernthaler J, Eilers H, Amann R (2001). Growth patterns of two marine isolates: Adaptations to substrate patchiness? *Applied and environmental microbiology* **67:** 4077.

Pernthaler A, Pernthaler J, Amann R (2004). Sensitive multi-color fluorescence in situ hybridization for the identification of environmental microorganisms. *Molecular Microbial Ecology Manual* **3:** 711–726.

Polerecky L, Adam B, Milucka J, Musat N, Vagner T, Kuypers MMM (2012). Look@NanoSIMS – a tool for the analysis of nanoSIMS data in environmental microbiology. *Environ Microbiol* **14:** 1009-1023.

Proctor LM, Fuhrman JA (1991). Roles of viral infection in organic particle flux. *Marine ecology progress series Oldendorf* **69:** 133-142.

Sandaa R-A, Gómez-Consarnau L, Pinhassi J, Riemann L, Malits A, Weinbauer MG *et al* (2009). Viral control of bacterial biodiversity – evidence from a nutrient-enriched marine mesocosm experiment. *Environmental Microbiology* **11:** 2585-2597.

Schäfer H (2007). Isolation of *Methylophaga* spp. from marine dimethylsulfide-degrading enrichment cultures and identification of polypeptides induced during growth on dimethylsulfide. *Applied and environmental microbiology* **73:** 2580-2591.

Schoemann V, Becquevort S, Stefels J, Rousseau V, Lancelot C (2005). *Phaeocystis* blooms in the global ocean and their controlling mechanisms: a review. *Journal of Sea Research* **53:** 43-66.

Shanks AL, Trent JD (1979). Marine snow: Microscale nutrient patches. *Limnology and Oceanography* **24:** 850-854.

Sheik AR, Brussaard CPD, Lavik G, Foster RA, Musat N, Adam B *et al* (2012). Viral infection of *Phaeocystis globosa* impedes release of chitinous star-like structures: quantification using single cell approaches. *Environmental Microbiology* **DOI: 10.1111/j.1462-2920.2012.02838.x**.

Shelford EJ, Middelboe M, Møller EF, Suttle CA (2012). Virus-driven nitrogen cycling enhances phytoplankton growth. *Aquatic Microbial Ecology* **66:** 41-46.

Shibata A, Kogure K, Koike I, Ohwada K (1997). Formation of submicron colloidal particles from marine bacteria by viral infection. *Marine Ecology Progress Series* **155:** 303-307.

Short SM (2012). The ecology of viruses that infect eukaryotic algae. *Environmental Microbiology* **DOI: 10.1111/j.1462-2920.2012.02706.x**.

Simon M, Grossart HP, Schweitzer B, Ploug H (2002). Microbial ecology of organic aggregates in aquatic ecosystems. *Aquatic Microbial Ecology* **28:** 175-211.

Sun Y, Wolcott RD, Dowd SE (2011). Tag-encoded FLX amplicon pyrosequencing for the elucidation of microbial and functional gene diversity in any environment. *Methods in molecular biology (Clifton, NJ)* **733:** 129-141.

Suttle CA (2005). Viruses in the sea. *Nature* **437:** 356-361.

Suttle CA (2007). Marine viruses - major players in the global ecosystem. *Nat Rev Microbiol* **5:** 801-812.

Tada Y, Taniguchi A, Nagao I, Miki T, Uematsu M, Tsuda A *et al* (2011). Differing Growth Responses of Major Phylogenetic Groups of Marine Bacteria to Natural Phytoplankton Blooms in the Western North Pacific Ocean. *Applied and Environmental Microbiology* **77:** 4055-4065.

Teeling H, Fuchs BM, Becher D, Klockow C, Gardebrecht A, Bennke CM *et al* (2012). Substrate-controlled succession of marine bacterioplankton populations induced by a phytoplankton bloom. *Science* **336:** 608-611.

Tittel J, Büttner O, Kamjunke N (2012). Non-cooperative behaviour of bacteria prevents efficient phosphorus utilization of planktonic communities. *Journal of Plankton Research* **34:** 102-112.

Veldhuis MJW, Kraay GW (2000). Application of flow cytometry in marine phytoplankton research: current applications and future perspectives. *Scientia Marina* **64:** 121-134.

Verity PG, Brussaard CPD, Nejstgaard JC, van Leeuwe MA, Lancelot C, Medlin LK (2007). Current understanding of Phaeocystis ecology and biogeochemistry, and perspectives for future research. *Biogeochemistry* **83:** 311-330.

Wilhelm SW, Suttle CA (1999). Viruses and nutrient cycles in the sea. *Bioscience* **49:** 781-788.

Zhou J, Bruns MA, Tiedje JM (1996). DNA recovery from soils of diverse composition. *Applied and environmental microbiology* **62:** 316-322.

Zubkov MV, Fuchs BM, Archer SD, Kiene RP, Amann R, Burkill PH (2001). Linking the composition of bacterioplankton to rapid turnover of dissolved dimethylsulphoniopropionate in an algal bloom in the North Sea. *Environmental Microbiology* **3:** 304-311.

Supplementary Figure 1: Comparison of the taxonomic analyses computed by MEGAN4 (Huson et al., 2011) for 16S rRNA amplicon sequences of *Gammaproteobacteria*, *Alphaproteobacteria* and *Bacteroidetes* performed at 6h, day 2 and 7 of the experiment from the infected and non-infected cultures. The Min Complexity item of the software was used to identify low complexity reads and is placed on special low complexity node, for example, *Bacteroidetes*.

6h Infected
Day2 Non-infected
Day 2 Infected
Day 7 Non-infected
Day 7 Infected

90
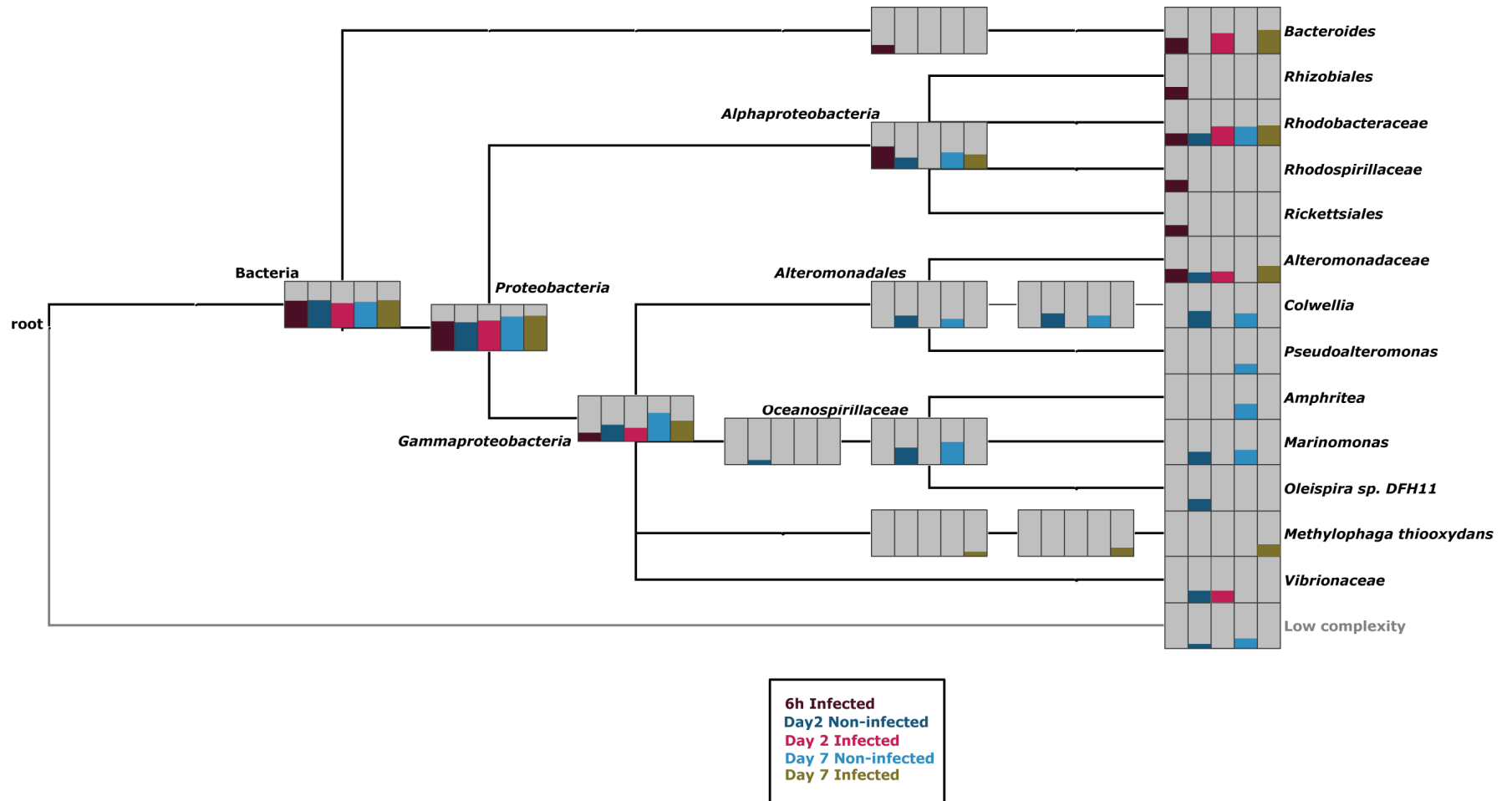
Supplementary Table 1: Species percentage composition of *Gammaproteobacteria*.

Species name	6h infected	Day 2 Non-infected	Day 2 Infected	Day 7 Non-infected	Day 7 Infected
Pseudomonas sp	0.02	1.96	0.00	0.44	1.13
Glaciecola sp	0.11	48.34	0.12	14.65	1.58
Haliea sp	0.00	0.37	0.00	0.12	0.15
Vibrio sp	0.00	4.66	6.72	0.31	0.08
Colwellia sp	0.00	9.19	0.00	6.23	0.00
Alteromonas sp	92.47	2.79	86.95	4.43	68.02
Alteromonas marina	7.01	0.00	3.34	0.06	0.60
Amphritea atlantica	0.00	0.12	0.00	36.78	0.00
Cellvibrio sp	0.09	0.79	0.00	0.00	2.56
Oceanospirillum sp	0.00	0.00	0.00	5.86	0.00
Marinobacterium rhizophilum	0.00	0.00	0.00	0.12	0.00
Methylophaga sp	0.02	0.00	0.40	0.00	14.20
Pseudoalteromonas sp	0.09	1.04	0.44	4.30	5.31
Marinobacter sp	0.00	0.12	0.08	0.62	0.23
Psychrobacter sp	0.00	0.67	0.00	1.81	0.00
Marinomonas sp	0.00	6.95	0.16	8.85	0.04
Amphritea japonica	0.00	1.62	0.00	8.73	0.00
Colwellia rossensis	0.00	0.00	0.00	0.12	0.00
Thalassomonas loyana	0.00	0.00	0.00	0.25	0.00
Pseudoalteromonas spongiae	0.00	0.00	0.00	0.12	0.00
Agarivorans sp	0.00	0.00	0.00	0.19	0.00
Haliea rubra	0.00	0.00	0.00	0.00	0.04
Salinimonas chungwhensis	0.00	0.00	0.00	0.00	3.28
Endozoicomonas elysicola	0.00	0.00	0.00	0.00	0.00
Pseudomonas putida	0.00	0.00	0.00	0.00	0.11
Shewanella sp	0.00	0.08	0.00	0.12	0.00
Pseudomonas marincola	0.00	0.00	0.00	0.00	0.00
Oleispira sp	0.00	8.24	0.00	0.69	0.00
Microbulbifer sp	0.00	0.00	0.00	0.19	0.00
Neptuniibacter sp	0.00	1.29	0.00	0.12	0.00
Shewanella fidelis	0.00	0.00	0.00	0.19	0.00
Colwellia piezophila	0.00	0.29	0.00	0.19	0.00
Thalassomonas sp	0.00	0.62	0.00	0.75	0.00
Amphritea balenae	0.00	0.50	0.00	0.94	0.00

Species percentage composition of *Gammaproteobacteria* (continued).

Species name	6h infected	Day 2 Non-infected	Day 2 Infected	Day 7 Non-infected	Day 7 Infected
Colwellia aestuarii	0.00	0.12	0.00	0.31	0.00
Thalassomonas haliotis	0.00	0.00	0.00	0.31	0.00
Neptuniibacter caesariensis	0.00	0.37	0.00	0.50	0.00
Colwellia psychrerythraea	0.00	1.91	0.00	0.31	0.00
Marinomonas dokdonensis	0.00	0.00	0.00	0.19	0.00
Pseudoalteromonas porphyrae	0.00	0.00	0.00	0.12	0.00
Aliivibrio salmonicida	0.00	0.00	0.00	0.06	0.00
Marinobacterium sp	0.00	1.83	0.00	0.25	0.19
Glaciecola siphonariae	0.00	0.00	0.16	0.12	0.00
Shewanella gaetbuli	0.00	0.00	0.00	0.12	0.00
Microbulbifer variabilis	0.00	0.00	0.00	0.12	0.00
Shewanella denitrificans	0.00	0.00	0.00	0.12	0.00
Thalassolituus sp	0.00	0.00	0.00	0.12	0.00
Reinekea sp	0.00	0.00	0.00	0.12	0.00
Vibrio splendidus	0.00	0.21	0.32	0.00	0.00
Alteromonas macleodii	0.20	0.00	0.76	0.00	0.38
Aestuariibacter halophilus	0.00	0.00	0.00	0.00	0.56
Vibrio crassostreae	0.00	0.08	0.20	0.00	0.00
Rheinheimera baltica	0.00	0.12	0.00	0.00	0.15
Teredinibacter turnerae	0.00	0.00	0.00	0.00	0.15
Vibrio fortis	0.00	0.00	0.04	0.00	0.00
Simiduia sp	0.00	0.00	0.00	0.00	0.11
Alkalimonas delamerensis	0.00	0.00	0.00	0.00	0.23
Marinobacterium stanieri	0.00	0.00	0.00	0.00	0.08
Saccharophagus sp	0.00	4.91	0.00	0.00	0.23
Bowmanella sp	0.00	0.00	0.00	0.00	0.53
Thiohalophilus thiocyanatoxydans	0.00	0.00	0.00	0.00	0.08
Vibrio aestuarianus	0.00	0.04	0.00	0.00	0.00
Psychromonas ingrahamii	0.00	0.00	0.08	0.00	0.00
Bowmanella denitrificans	0.00	0.00	0.08	0.00	0.00
Alteromonas hispanica	0.00	0.00	0.16	0.00	0.00
Photobacterium sp	0.00	0.04	0.00	0.00	0.00
Glaciecola mesophila	0.00	0.17	0.00	0.00	0.00
Marinobacter taiwanensis	0.00	0.17	0.00	0.00	0.00
Marinomonas aquimarina	0.00	0.21	0.00	0.00	0.00
Thalassomonas ganghwensis	0.00	0.08	0.00	0.00	0.00

Supplementary Table 2: Species percentage composition of *Alphaproteobacteria*.

Species name	6h infected	Day 2 Non-infected	Day 2 Infected	Day 7 Non-infected	Day 7 Infected
Leisingera sp	6.16	83.25	1.23	69.52	3.44
Pelagibacter sp	23.64	0.69	0.78	0.37	0.69
Thalassobius sp	1.84	5.53	0.78	2.79	0.28
Thalassobacter sp	0.22	0.34	0.24	2.49	0.80
Roseovarius nubinhibens	0.11	0.83	0.47	0.33	0.00
Sulfitobacter sp	1.34	1.33	3.99	6.89	2.92
Roseobacter sp	7.28	1.30	27.36	7.22	14.14
Sulfitobacter japonica	0.17	0.33	0.94	0.63	0.00
Phaeobacter daeponensis	0.45	0.12	1.15	0.35	1.86
Ruegeria sp	14.96	6.56	3.40	2.51	4.17
Sphingobacterium sp	0.84	0.28	0.00	0.00	0.00
Zhangella mobilis	0.17	0.00	0.00	0.23	0.00
Bradyrhizobium sp	0.54	0.00	0.00	0.00	0.00
Hellea balneolensis	0.34	0.83	0.00	0.93	0.00
Tateyamaria sp	0.17	0.55	0.00	0.47	0.00
Roseovarius aestuarii	0.17	0.28	0.00	0.47	0.00
Phaeobacter sp	6.22	0.14	27.37	1.75	23.52
Sulfitobacter dubius	0.00	0.00	0.00	0.70	0.00
Sphingomonas sp	0.56	0.55	0.00	0.93	0.00
Roseovarius sp	0.73	0.00	9.14	0.70	6.91
Devosia sp	0.28	0.00	0.00	0.00	0.00
Loktanella sp	2.63	0.00	5.12	0.49	9.83
Jannaschia sp	0.00	0.55	0.00	0.47	0.00
Loktanella koreensis	0.00	0.00	0.00	0.70	0.00
Caulobacter sp	7.68	0.28	0.47	0.00	0.00
Rasbo sp	0.11	0.00	0.00	0.00	0.00
Roseovarius pelophilus	0.00	0.00	0.00	0.47	0.00
Rhodobacter sp	0.62	0.00	0.00	0.47	0.00
Nereida sp	0.00	0.55	0.00	0.00	0.69
Ruegeria scottomollicae	13.73	0.28	19.54	0.93	28.38

Species percentage composition of *Alphaproteobacteria* (continued).

Species name	6h infected	Day 2 Non-infected	Day 2 Infected	Day 7 Non-infected	Day 7 Infected
Octadecabacter sp	0.00	0.00	0.00	0.35	0.00
Loktanella vestfoldensis	0.56	0.00	0.33	0.00	0.24
Glaciecola sp	0.00	0.28	0.00	0.23	0.00
Vibrio sp	0.39	0.00	0.14	0.00	0.45
Novosphingobium hassiacum	0.11	0.00	0.00	0.00	0.00
Parvibaculum sp	0.22	0.00	0.00	0.00	0.00
Phaeobacter gallaeciensis	1.34	0.00	1.13	0.00	1.77
Roseobacter litoralis	0.00	0.00	0.00	0.00	0.00
Blastobacter sp	0.11	0.00	0.00	0.00	0.00
Roseovarius mucosus	0.17	0.00	0.24	0.00	0.00
Nordella oligomobilis	0.00	0.00	0.00	0.00	0.00
Kordiimonas gwangyangensis	0.00	0.00	0.00	0.47	0.00
Sphingobium xenophagum	0.56	0.00	0.00	0.00	0.00
Phenylobacterium sp	0.22	0.00	0.00	0.00	0.00
Salipiger sp	0.11	0.00	0.00	0.00	0.00
Paracoccus sp	1.85	0.00	0.00	0.00	0.00
Rhodobacter veldkampii	0.11	0.00	0.00	0.00	0.00
Brevundimonas diminuta	0.17	0.00	0.00	0.00	0.00
Rhodomicrobium sp	0.22	0.00	0.00	0.00	0.00
Sulfitobacter mediterraneus	0.00	0.00	0.00	0.14	0.14
Marinovum sp	0.11	0.00	0.00	0.00	0.00
Hoeflea sp	0.00	0.00	0.00	0.00	0.69
Nisaea nitritireducens	0.11	0.00	0.00	0.00	0.00
Loktanella agnita	0.11	0.00	0.00	0.00	0.00
Azospirillum canadense	0.11	0.00	0.00	0.00	0.00
Roseobacter pelophilus	0.11	0.00	0.00	0.00	0.00
Agrobacterium sp	0.56	0.00	0.00	0.33	0.28
Phenylobacterium immobile	0.11	0.00	0.00	0.00	0.00
Sphingobium sp	0.34	0.00	0.00	0.00	0.00
Afipia felis	0.00	0.00	0.00	0.00	0.00
Stappia sp	0.17	0.00	0.00	0.00	0.00

Species percentage composition of *Alphaproteobacteria* (continued).

Species name	6h infected	Day 2 Non-infected	Day 2 Infected	Day 7 Non-infected	Day 7 Infected
Thiobaca sp	0.11	0.00	0.00	0.00	0.00
Hyphomonas sp	0.00	0.00	0.00	0.00	0.28
Pseudoruegeria aquimaris	0.11	0.00	0.00	0.00	0.00
Methylobacterium variabile	0.11	0.00	0.00	0.00	0.00
Mesorhizobium sp	0.56	0.00	0.00	0.00	0.56
Roseospirillum sp	0.11	0.00	0.00	0.00	0.00
Afifella marina	0.11	0.00	0.00	0.00	0.00
Paracoccus aminophilus	0.11	0.00	0.00	0.00	0.00
Rhodobium sp	0.17	0.00	0.00	0.00	0.00
Rhodovibrio sp	0.11	0.00	0.00	0.00	0.00
Sphingomonas oligophenolica	0.17	0.00	0.00	0.00	0.00
Filomicrobium sp	0.17	0.00	0.00	0.00	0.00
Seohicola saemankumensis	0.11	0.00	0.00	0.93	0.00
Psychromonas ingrahamii	0.00	0.00	0.00	0.00	0.00
Bartonella sp	0.39	0.00	0.00	0.00	0.00
Leisingera aquimarina	0.00	0.00	0.00	0.93	0.00
Pelagibaca sp	0.00	0.00	0.00	0.47	0.00
Oceanicola sp	0.00	0.00	0.00	0.70	0.00
Thalassobius aestuarii	0.00	0.00	0.00	0.84	0.00
Nautella italica	0.00	0.00	0.00	0.47	0.00
Shimia marina	0.00	0.00	0.00	0.47	0.00
Novosphingobium sp	0.00	0.00	0.00	0.00	0.00
Methylobacterium sp	0.22	0.00	0.00	0.00	0.00
Brevundimonas sp	0.11	0.00	0.00	0.00	0.00
Ahrensia sp	0.22	0.00	0.00	0.47	0.00
Leisingera methylohalidivorans	0.11	0.00	0.00	0.93	0.00
Ochrobactrum sp	0.56	0.00	0.00	0.23	0.00
Thalassobius mediterraneus	0.00	0.00	0.00	0.51	0.00
Maricaulis maris	0.00	0.00	0.00	0.47	0.00
Azospirillum melinis	0.00	0.00	0.00	0.47	0.00

Chapter 4: Viral infection of *Micromonas pusilla* hinders synthesis of new pyrenoid (starch and protein production) and structures specific bacterial community.

A.R. Sheik[1], C.P.D. Brussaard[2], P. Lam[1], G. Lavik[1], B. Adam[1], S. Littman[1], M.M.M. Kuypers[1]

[1] Dept. of Biogeochemistry, Max Planck Institute for Marine Microbiology, Bremen, Germany

[2] Virus Research Group, Dept. Biological Oceanography, NIOZ - Royal Netherlands Institute for Sea Research, Texel, The Netherlands.

Running title: Single-cell substrate quantification of bacterial communities due to *M. pusilla* viral lysis

Abstract:

Micromonas pusilla, a non bloom-forming unicellular algae, is a major component of the picophytoplankton community in various oceanic environments. A characteristic feature of *M. pusilla* cells is the presence of pyrenoid structure, a chloroplast sub-cellular particle hosting carbon fixation enzymes surrounded by a starch sheath. Viruses infecting *M. pusilla,* MpVs, play a significant regulatory role in population dynamics of the host species. However, the impact of *M. pusilla* viral infections on bacterial community structure and bacterial carbon and nitrogen assimilation is poorly understood. We investigated the *Bacteroidetes* substrate assimilation due to newly assimilated and previously incorporated organic matter released after *M. pusilla* viral lysis. The bulk carbon and nitrogen assimilation by infected *P. globosa* cultures did not differ to the non-infected cultures until viral lysis (30 h post-infection). Viral lysis of *M. pusilla* led to dominance of *Alteromonas* cells and *Bacteroidetes* (fluorescent *in situ* hybridisation, CARD-FISH), where as *Alteromonas* cells dominated the bacterial communities in non-infected cultures through out the experiment. Further, diverse gammaproteobacterial and alphaproteobacterial phylotypes emerged (amplicon pyrosequencing) within non-infected cultures suggested that *M. pusilla* derived exudates can be chemically diverse. The single cell substrate assimilation of *Bacteroidetes* members by day 4 using nano-scale secondary-ion mass spectrometry (nanoSIMS) indicated that newly assimilated substrates by *M. pusilla* cells may not be used for pyrenoid synthesis. We speculate that viral infection of *M. pusilla* might have diverted much of the newly assimilated carbon and nitrogen substrates towards viral production. We estimated that significant proportion of newly assimilated *M. pusilla* nitrogen ($\sim$0.63 μ mol N L^{-1}, 56%) and minimal amounts of carbon ($\sim$1.39 μ mol C L^{-1}, 9%) was utilized for the viral production. The ecological implication of pyrenoid impediment in *M. pusilla* cells may lead to the release of labile organic proteins and increased levels of polysaccharides, which directs the marine pelagic system to more regenerative processes.

Introduction:

Marine phytoplankton constituting of unicellular eukaryotic pico-algae, form the basis of most marine food webs. Picophytoplankton *Micromonas pusilla* is a wide-spread, non-bloom forming small flagellated unicellular algae. *M. pusilla* has been identified as a major component of the phytoplankton populations throughout the year (Not et al., 2004). The occurrence of *M. pusilla* has been documented in varied oceanic environments such as polar and temperate marine regions as well as in nutrient rich coastal environments (Kuylenstierna and Karlson, 1994; Not et al., 2005). A characteristic feature of *M. pusilla* cells is the presence of a sub-cellular strucutre called pyrenoid, which hosts carbon fixation enzymes and is surrounded by starch sheath (Salisbury and Floyd, 1978). Viruses infecting *M. pusilla* (MpVs), just like their host, have been found in many oceanic environments (Cottrell and Suttle, 1991, 1995). Previous studies conducted under natural systems have suggested that MpVs can have a profound impact on *M. pusilla* population dynamics (Zingone et al., 1999). However, the impact of *M. pusilla* viral infections structuring bacterial community is currently unknown.

Heterotrophic marine bacteria which are phylogenetically diverse (Giovannoni and Rappé, 2000; Fuhrman and Hagström, 2008) and metabolically versatile (Kirchman, 2000; Jørgensen, 2006), which drive biogeochemical cycles in the surface oceans. In the coastal environments, numerous studies revealed distinct patterns of marine bacteria occurring at the major bacterial groups of *Gammaproteobacteria, Alphaproteobacteria* and Bacteroidetes, which was related to the changes in the algal derived organic matter (Zubkov et al., 2001; Pinhassi et al., 2004; Tada et al., 2011). Furthermore, at the phylotypes level, few studies linked the changes in the algal organic matter to the succession of the gammaproteobacterial *Alteromonadaceae* (referred to as *Alteromonas* cells henceforth) and Alphaproteobacterial *Rhodobacteriaceae* (*Roseobacter* cells) (Tada et al., 2012; Teeling et al., 2012).

Viral lysis and exudation of algae both leads to the release of organic matter but differs in the quantity and quality of released elements. The composition of the virally released organic matter or exudates depends on the host cellular composition, which in general may constitute of readily labile organic substrates (e.g., amino acids, sugars) to high molecular weight compounds (polysaccharides such as starch). An important consideration is that after viral lysis there may be a broad range of host organic matter ranging from labile in availability to high molecular weight

compounds. The metabolic versatility of microbes and the availability of varied organic matter due to algal exudation and viral lysis, might determine the microbial community composition and further the flow of the biochemical elements with the marine pelagic environments. Therefore, understanding to what extent newly assimilated host labile matter (potentially labile in availability) and previously incorporated host organic matter (such as storage material) released due to virally lysed algae and facilitating bacterial substrate assimilation is of ecological importance.

In this current study, we quantified the substrate assimilation of *Bacteroidetes* members due to newly assimilated and previously incorporated *M. pusilla* organic matter released after viral lysis. Using a high resolution secondary-ion mass spectrometry approach (nanoSIMS), we deduced the single cell substrate assimilation of *Bacteroidetes*. Furthermore, the combined use of catalyzed reporter fluorescent *in situ* hybridization (CARD-FISH) and pyrosequencing allowed us to investigate the phylogenetic identity and specific phylotype succession within complex bacterial assemblage.

Materials and Methods:

Culturing: Axenic cultures of *M. pusilla* strain Lac38 obtained from the culture collection of Royal Netherlands Institute for Sea Research (NIOZ) was grown in a modified 1:1 mixture of f/2 medium (Guillard, 1975) and nutrient enriched artificial seawater (ESAW) (Cottrell and Suttle, 1991). Nutrients were added to the media to a final concentration of 1mM HCO_3^- and 80 μM of NO_3^-. The cultures were grown under 95 μmol quanta $m^{-2} s^{-1}$ irradiance with a light to dark regime of 16:8 hours and at a temperature of 15 ± 1°C. The lytic *M. pusilla* virus, MpV-08T from the virus culture collection at NIOZ, was produced using exponentially growing host cultures.

The bacterial populations used in this experiment were obtained from coastal North Sea, Marsdiep, Texel, The Netherlands on 06 April 2011. Prior to the bacterial inoculation (10% v/v), sea water was filtered through 0.8 μm pore size filters (45 mm in diameter; Microdisc) to minimise heterotrophic nanoflagellates and other phytoplankton. The filtered seawater was stored at 15°C until further processing (within 40 minutes before the experiment began).

Experimental Setup: This study consisted of two experimental setups which were performed in parallel. In experiment 1, isotopic labeled substrates (^{13}C-HCO_3^- and

^{15}N-NO$_3^-$, 20% final labelling percentage, sodium salts, 99 atom %, ISOTEC) were added to fresh ESAW media prior to inoculation of axenic algae and bacterial seawater. In experiment 2, instead of labeled substrates, the *M. pusilla* biomass itself was labeled with ^{13}C and ^{15}N. The ^{13}C and ^{15}N labelled algal biomass was obtained by incubating mid-exponentially growing axenic *M. pusilla* culture was grown in ESAW containing ~ 0.2mM of H^{13}CO$_3^-$ and 20µM of NO$_3^-$ (as sodium salts, 99 atom %, ISOTEC) for a period of 2 days. On day 3, labelled algal biomass were centrifuged at 1500 x *g* (with a swing rotor) for 10 minutes to remove unincorporated ^{13}C and ^{15}N labelled substrates from the media. Algal cell pellets formed after centrifugation were washed twice and re-suspended in an ESAW media with no nutrient loadings.

The respective *M. pusilla* cultures of each experimental setup were split into 4 inoculants and were transferred to a fresh 2L ESAW media (10% v/v). Two of these inoculants from both experimental setups were infected with MpV-08T virus (0.2 µm syringe filtered, cellulose acetate, Whatmann) at an initial virus to algae ratio of ~ 22:1. The remaining two cultures of each experimental setup served as non-infected controls and received medium instead of viral lysate in equal amount. The experiment was conducted during the mid light phase of the light to dark regime. Sampling for samples for algae and virus abundance, bulk ^{13}C and ^{15}N- particulate measurements, catalysed reporter fluorescent *in situ* hybridization (CARD-FISH) analyses and for nanoSIMS were taken and analyzed as described in the following.

Abundances: Algal abundance was monitored by flow cytometry using a Beckman Coulter EPICS XL-MCL benchtop flow cytometer (Veldhuis and Kraay, 2000), which was equipped with a laser with an excitation wavelength of 488 nm (15 mW) and emission bands for the chlorophyll autofluorescence (> 630 nm). The 1mL samples taken at each time point were diluted up to 10-fold in sterile sea water. The flow cytometer trigger was set on the red chlorophyll autofluorescence and algal cell abundance was estimated for 1 min at a flow rate of 2.3 µL min^{-1}.

The abundance of *P. globosa* virus MpV-08T and ambient bacteriophages were enumerated using a Becton-Dickson FACSCalibur flow cytometer (Brussaard, 2004). Samples of 1 mL at every time point were fixed with 25% glutaraldehyde (0.5% final concentration, EM grade, Sigma- Aldrich, St Louis, MO, USA) for 15 to 30 minutes at 4°C, flash frozen in liquid nitrogen and stored at -80°C until analysis. The thawed samples were diluted 50 to 1,000-fold in sterile TE-buffer (pH 8.0) and stained with the nucleic acid-specific dye SYBR Green I (Invitrogen-Molecular Probes, Eugene, OR,

USA) at a final concentration of 0.5×10^{-4} of the commercial stock for 10 min at 80°C. The flow cytometer trigger was set on the green fluorescence and the sample was delivered at a rate of 28 μL min^{-1} and analyzed for $\sim$ 1 min. The flow cytometry data files were analyzed as described by Brussaard *et al* (2010).

CARD-FISH and HISH-SIMS analyses:

CARD-FISH analyses were performed as described by Pernthaler et al (2004) to identify and quantify the bacterial populations. Subsamples taken at each time interval were fixed with paraformaldehyde (PFA, 1% final concentration) for 1 h at room temperature or overnight at 4°C. Subsamples were filtered onto white polycarbonate membrane filters (GTTP, 0.2 μm pore size, 25 mm in diameter, Millipore, Eschborn, Germany), washed with 5-10 ml of 1× Phosphate Buffer Saline (PBS), air-dried and stored at -20°C until analysis. Samples were hybridised with the following probes: CF319a for *Bacteroidetes* (Manz et al., 1996), Alt1413 for *Alteromonas* cells (Eilers et al., 2000b), Ros593 for *Roseobacter* cells (Eilers et al., 2001). Hybridised filters were counterstained with 1 μg ml^{-1} of 4,6-diamidino-2-phenylindole (DAPI). Subsequently, all hybridised and DAPI-stained cells were quantified by epifluorescence microscopy (Axioplan II Imaging epifluorescence microscope, Zeiss, Jena, Germany). Similarly, Halogen *In-Situ* Hybridization assay coupled to nanoSIMS (HISH-SIMS) (Musat et al., 2008) was performed to quantify the substrate assimilation of individual *Bacteroidetes members* (probe CF319a) with

^{19}F containing tyramides.

Bulk Carbon and Nitrogen Measurements:

For the determination of bulk ^{13}C and ^{15}N- particulate measurements, 80-100 mL of the experimental cultures were filtered onto pre-combusted GF/F filters (Whatmann, 25 mm diameter) freeze dried and stored at room temperature until analysis. The C- and N-isotopic component of particulate organic matter was determined as CO_2 and N_2 released by flash combustion in an automated elemental analyzer (Thermo Flash EA, 1112 Series) coupled to an isotope ratio mass spectrometer (Finnigan Delta^{plus} XP, Thermo Scientific). Over the course of the experiment, ^{13}C-bicarbonate in the medium escaped due to atmospheric CO_2 exchange. We corrected this exchange by measuring ^{13}C isotopic abundances in the medium by using gas chromatography-isotope ratio monitoring mass spectrometry (VG Optima, Micromass, Manchester, UK) as described previously (Sheik et al., 2012).

DNA extraction and amplicon pyrosequencing:

DNA was extracted from the samples which were collected for CARD-FISH analysis using protocol described by Zhou *et al* (Zhou et al., 1996). The extracted DNA was further purified using Wizard® DNA Clean-Up System (Promega Corporation, Madison, USA) as per manufacturer's instructions. The bacterial 16S rRNA genes were amplified and sequenced using amplicon pyrosequencing at the Research and Testing Laboratories (Lubbock, Texas). The pyrosequencing was performed at 6h, day 2 and 7 of the experiment from the infected and non-infected cultures targeting *Gammaproteobacteria* (forward primer 5'-CMATGCCGCGTGTGTGAA-3', reverse primer 5'- ACTCCCCAGGCGGTCDACTTA-3'), *Alphaproteobacteria* (forward primer 5'- ARCGAACGCTGGCGGCA-3', reverse primer 5'- TACGAATTTYACCTCTACA-3') and *Bacteroidetes* (forward primer 5'-AACGCTAGCTACAGGCTT-3', reverse primer 5'- CAATCGGAGTTCTTCGTG-3'). The generated sequences were processed and taxonomically identified as per company's standard procedure (Sun et al., 2011), to the species level according to the >97% sequence identity of 16S rRNA genes. Thereafter, the species percentage composition of each major bacterial group was based on the relative abundance information within and among the individual samples and relative numbers of reads (S.I. Table 1).

MEGAN 4, a metagenome analysing software was used to construct the heat plot of 16S rRNA amplicon sequence dataset (S.I. Figure 1, (Huson et al., 2011)). Amplicon sequences were clustered with >97% sequence identity and BLASTN was used to compare clustered sequences against the SILVA rRNA database (http://www.arb-silva.de). The output of this comparison was then parsed by MEGAN4 and mapped onto the NCBI taxonomy. The BLASTN comparison shown that *Bacteroidetes* 16S rRNA amplicon sequences targeted uncultured bacterial species and hence not described in the text.

NanoSIMS analyses:

To quantify the single-cell substrate assimilation of *Bacteroidetes* released from algal biomass, we applied a recently developed method as described by Musat *et al* (2008). Enrichment of the ^{13}C and ^{15}N in the bacterial cells were analyzed with NanoSIMS 50 L (CAMECA, Paris, France). The primary ion beam had a nominal size of approximately 150 nm and the sample was sputtered with a dwelling time of 6 ms per pixel. The primary current was 20-30 nA Cs$^+$ during acquisition for most images. For each analysis, we recorded simultaneously secondary-ion images of naturally

abundant ^{12}C (measured as $^{12}C^-$), ^{14}N atoms (measured as $^{12}C^{14}N^-$) and ^{19}F for the localization of biomass and similarly, of ^{13}C and ^{15}N for the uptake quantification. NanoSIMS data-sets were analyzed using the Look@NanoSIMS software (Polerecky et al., 2012). Regions of interest (ROI) around individual bacterial cells were defined manually using ^{19}F image. The isotope ratio ($r= {}^{13}C/{}^{12}C$ or $^{15}N/{}^{14}N$) was calculated for each ROI based on the total $^{13}C^-$ and $^{12}C^-$ counts for each pixel. Subsequently, the ^{13}C and ^{15}N ratios were calculated in terms of absolute abundance, defined as $A = {}^{13}C/({}^{13}C+{}^{12}C)$ and $^{15}N/({}^{15}N+{}^{14}N)$ respectively.

Biovolume calculations:

Epifluorescence microscopy images taken during CARD-FISH analyses and before nanoSIMS analyses were used to deduce the biovolume of *Bacteroidetes*. Assuming cells as rotational ellipsoids we deduced the biovolume of *Bacteroidetes* at day 4 of the experiment from both experimental set ups.

Statistical analyses: One-way analyses of variance (ANOVAs) was used to test for differences in the bacterial numbers and single cell ^{13}C and ^{15}N enrichments of *Bacteroidetes* members from non-infected and infected *M. pusilla* cultures at day 4. All analyses were carried out using the Sigmastat version 3.5 software package.

Results:

Dynamics of M. pusilla and MpV abundances:

This study consisted of two experimental setups: in experiment 1, isotopic labeled substrates were used and in experiment 2 ^{13}C and ^{15}N labeled *M. pusilla* biomass was utilised.

Cell abundances of *M. pusilla* in non-infected and infected cultures from both experimental setups remained stable at $\sim 1.4 \times 10^5$ ml^{-1} for the first 8 h. After a slight increase by 18 h, algal cell abundance in both infected cultures markedly declined ~ 30 h post-infection(Figure 1A-B). In contrast, an exponential increase in cell numbers was observed in the non-infected cultures (Figure 1A-B). The *M. pusilla* viral abundance increased between 8 h and 12 h post-infection (the latent period) in both experimental setups and reached a maximum of $\sim 8.4 \times 10^7$ ml^{-1} at day 3 (Figure 1C-D). From the net increase in viral abundance and the net decrease in algal abundance after day 3, we estimated a burst size (number of viruses released per cell lysed) of 364 and 325 MpV cell^{-1} in experimental setup 1 and 2, respectively.
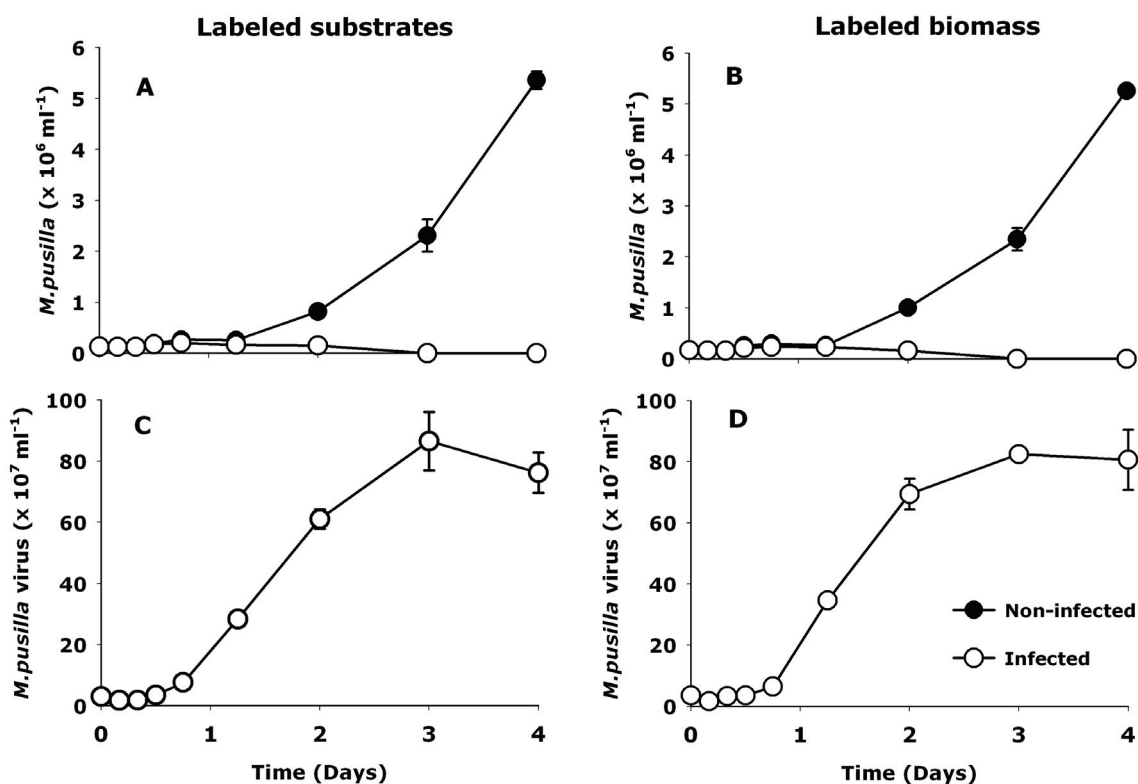
Figure 1: Viral infection dynamics of *M. pusilla.* Algal abundance and viral abundance from label substrates (A,C) and label biomass experiment (B, D). Error bars indicate standard deviation of mean (STDEV).

Temporal variation in bacterial community composition:

The bacterial abundance in the non-infected cultures from both the experimental setups increased steadily from $\sim 1.2 \times 10^5$ cells ml^{-1} to $\sim 3.9 \times 10^6$ cells ml^{-1} until day 2 (Figure 2). Viral lysis of *M. pusilla* has clearly stimulated bacterial abundance $\sim$ 4-fold relative to non-infected cultures by day 4 of the experiment ($\sim 1.3 \times 10^7$ cells ml^{-1}). CARD-FISH analyses revealed that *Alteromonas* cells dominated in all non-infected cultures by day 2, accounting for $\sim$ 86% and 78% of the total bacterial abundance, in labeled substrates and labeled biomass experiment, respectively (Figure 2A-B). Although viral mediated *M. pusilla* lysis resulted in substantially higher abundance of *Alteromonas cells* by day 2 in both the experimental setups, *Bacteroidetes* members increased linearly and co-dominated the bacterial populations especially towards the end of experiment (Figure. 2C-D). Interestingly, throughout the experiment, *Roseobacter* cells and *Bacteroidetes* maintained relatively low abundances in the non-infected and infected cultures from both

experimental setups (Figure 2).

Furthermore, tagged amplicon pyrosequencing of *Gamma-* and *Alphaproteobacteria* and *Bacteroidetes* illustrated significant changes in the bacterial diversity due to *M. pusilla* viral lysis at day 4 relative to *in situ* sea water (Figure. 3). Within non-infected cultures from both the experimental setups, there were contrasting differences of gamma- and alphaproteobacterial dominant phylotypes compared to *in situ* sea water. For infected cultures, however, similar gamma- and alphaproteobacterial phylotypes resulted in both experimental setups.
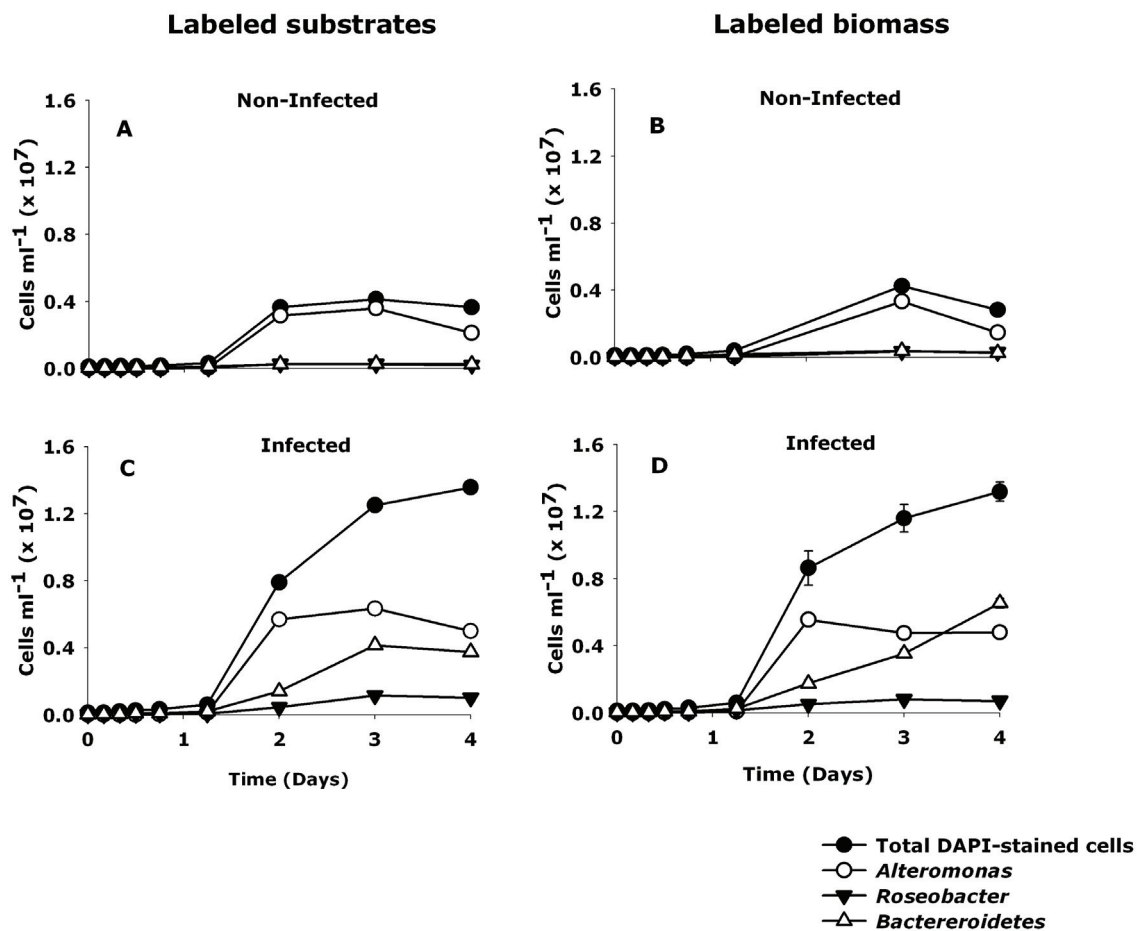

Figure 2: Temporal changes in the dynamics of *Alteromonas*, *Roseobacter* cells and *Bacteroidetes* members from labeled substrates experiment non-infected cultures (A) and infected cultures (C). Similarly from labeled biomass experiment non-infected cultures (B) and infected cultures (D). Error bars indicate STDEV.
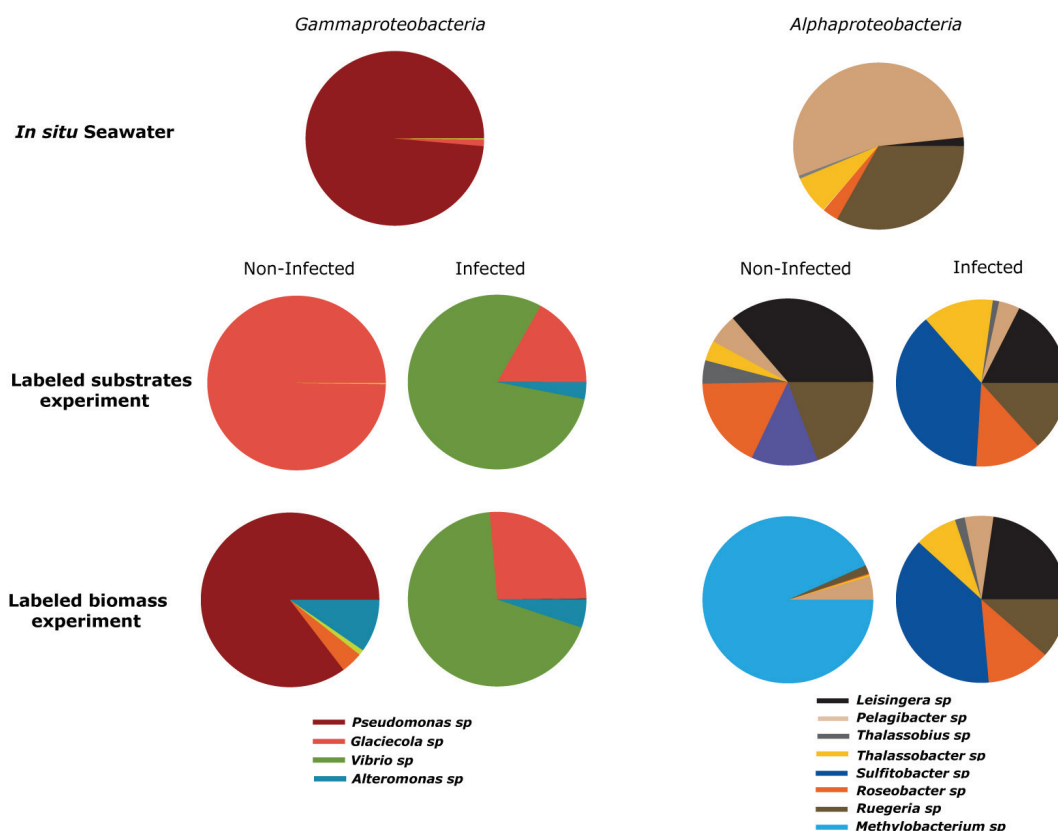
Figure 3: The percentage and changes of the diverse phylotypes belonging to gamma and alpha-proteobacterial as deduced from amplicon pyrosequencing analysis on the day 4 from the both experimental setups relative to the *in situ* North Sea water (0.8 μm filtered).

Bulk carbon and nitrogen assimilation:

In the experiment with labeled substrates, the rates of bulk carbon and nitrogen assimilation in non-infected and infected cultures increased linearly for the first 8 h (~3.8 μ C mol L^{-1} and ~0.04 μ N mol L^{-1}, Figure. 4). Thereafter, with the onset of the dark period until 18 h, carbon and nitrogen assimilation in non-infected and infected cultures remained stable. The carbon and nitrogen assimilation in non-infected cultures rose sharply after 18 h post-infection (~226 μ C mol L^{-1} and ~42 μ N mol L^{-1} at day 4) whereas infected cultures showed only a slight net increase in carbon assimilation until day 2 (~15 μmol C L^{-1}) and even less for nitrogen assimilation.
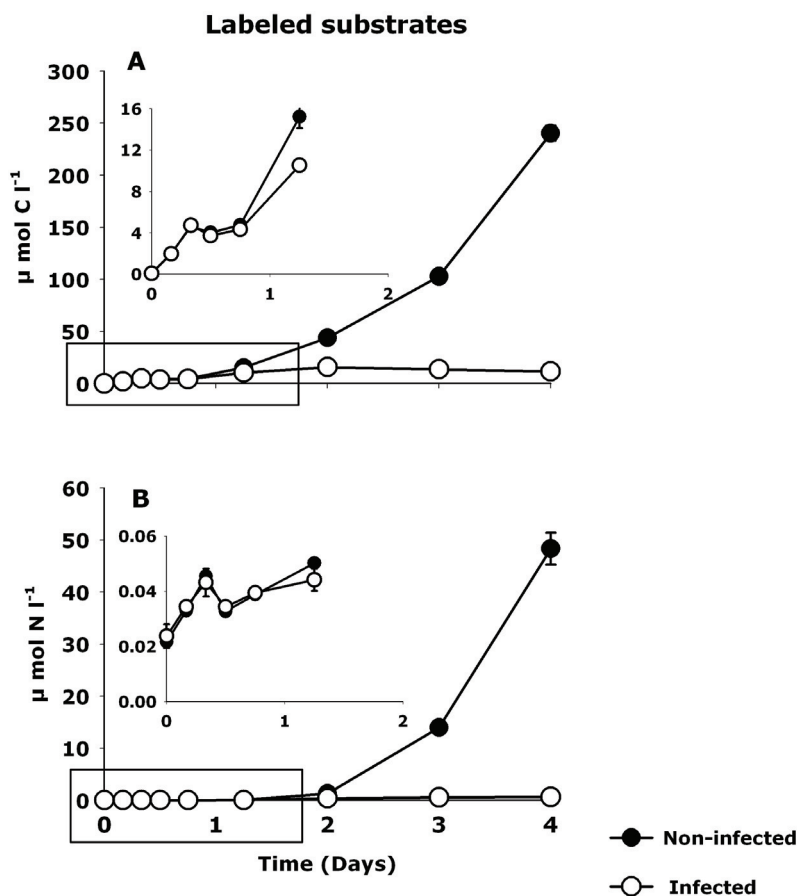
Figure 4: Bulk carbon (A) and nitrogen (B) assimilation of non-infected and infected *M. pusilla* cultures as determined by bulk measurements in label substrates experiment. Error bars indicate STDEV.

Single cell substrate assimilation of Bacteroidetes *members:*

We determined the single cell ^{13}C and ^{15}N enrichments belonging to *Bacteroidetes* using nanoSIMS imaging (^{19}F signal) combined with the CARD-FISH identification (Figure. 5, Table 1-2). The *Bacteroidetes* members were specifically chosen for nanoSIMS imaging as they posses the ability on the utilisation of complex algae-derived organic matter is well documented (Cottrell and Kirchman, 2000a). We quantified single-cell ^{13}C and ^{15}N substrate assimilation (f mol per cell^{-1}) of *Bacteroidetes* members at day 4 (non-infected and infected cultures, both experimental setups). All analyzed cells were substantially enriched in ^{13}C and ^{15}N relative to natural abundance. Based on the single cell ^{13}C and ^{15}N enrichments, calculated biovolume (0.08 µm^3 cell^{-1}) and a bacterial carbon conversion factor of

350 fg C μm^{-3} with C:N ratio of 4 (Lee and Fuhrman, 1987), we obtained cellular rates as illustrated in Table 1. The single cell substrate assimilation of *Bacteroidetes* from non-infected cultures was higher in the labeled substrates experiment relative to the experiment performed with labeled biomass (Table 2). In contrast, the *Bacteroidetes* ^{13}C and ^{15}N substrate assimilation in the infected cultures was similar for both the experiments with labeled substrates and labeled biomass
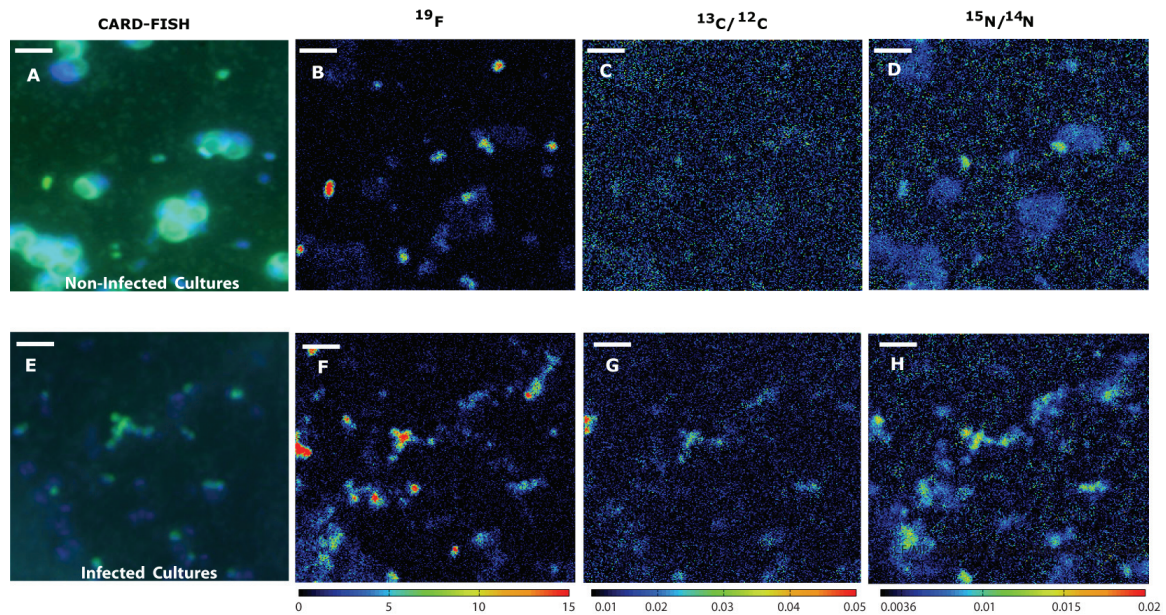
Figure 5: NanoSIMS imaging of *Bacteroidetes* members at day 4 of the label biomass experiment. Illustration represents the corresponding CARD-FISH image, ^{19}F signal which was used to draw regions of interest, ^{13}C and ^{15}N enrichment of *Bacteroidetes* members in non-infected cultures (A-D) and in infected cultures (E-H), respectively.

.

Table 1: Comparison of bulk^{13}C and ^{15}N excess atomic abundance and single cell nanoSIMS derived ^{13}C and ^{15}N excess atomic abundance of *Bacteroidetes* members at 0h and day 4 of the experiment.

	Labeled Substrates				Labeled Biomass			
	Non-Infected cultures		Infected cultures		Non-Infected cultures		Infected cultures	
Time	^{13}C At% Excess (mean ± SE)	^{15}N At% Excess (mean ± SE)	^{13}C At% Excess (mean ± SE)	^{15}N At% Excess (mean ± SE)	^{13}C At% Excess (mean ± SE)	^{15}N At% Excess (mean ± SE)	^{13}C At% Excess (mean ± SE)	^{15}N At% Excess (mean ± SE)
0 h								
Bulk	0.01 ± 0.02	0.02± 0.01	0.06 ± 0.02	0.01± 0.001	3.21 ± 0.06	2.9 ± 0.04	2.68 ± 0.9	3.18 ± 0.01
Single cell	N.A*	N.A	N.A	N.A	N.A	N.A	N.A	N.A
Day 4								
Bulk	8.49 ± 0.02	14.17 ± 0.01	2.75 ± 0	1.11 ± 0.09	0.35 ± 0.02	0.3 ± 0.01	0.95 ± 0.01	0.83 ± 0
Single cell	1.0 ± 0.24	5.31 ± 0.86	0.47 ± 0.11	0.45 ± 0.19	0.17 ± 0.06	0.19 ± 0.04	0.74 ± 0.9	0.48 ± 0.05

*N.A – Not analysed.
Bulk – Bulk measurements
Single cell – NanoSIMS deduced isotopic atomic abundance of *Bacteroidetes*.

Table 2: Single cell ^{13}C and ^{15}N substrate assimilation of *Bacteroidetes* members (f mol per cell) at day 4 of the experiment from both the experimental setups.

	Labeled Substrates						Labeled Biomass				
	Non-Infected cultures			**Infected cultures**			**Non-Infected cultures**			**Infected cultures**	
n	f mol ^{13}C cell $^{-1}$ (mean ± SE)	f mol ^{15}N cell $^{-1}$ (mean ± SE)	n	f mol ^{13}C cell $^{-1}$ (mean ± SE)	f mol ^{15}N cell $^{-1}$ (mean ± SE)	n	f mol ^{13}C cell $^{-1}$ (mean ± SE)	f mol ^{15}N cell $^{-1}$ (mean ± SE)	n	f mol ^{13}C cell $^{-1}$ (mean ± SE)	f mol ^{15}N cell $^{-1}$ (mean ± SE)
18	0.03 ± 0.007	0.03± 0.005	14	0.011± 0.002	0.002± 0.001	24	0.005 ± 0.0017	0.0012± 0.0003	5 3	0.017 ± 0.002	0.004 ± 0.0002

Discussion:

Bacterial community structure:

The gammaproteobacterial *Alteromonas* cells are typically rare in the marine environment (Acinas et al., 1999), but they have been found as a dominant component of the bacterial communities during the times of increased algal blooms (Schäfer et al., 2000; Tada et al., 2011). Despite their very low abundances at 0h, in both experimental setups, *Alteromonas* cells represented the majority of the bacterial abundance upon *M. pusilla* viral lysis after day 2. The predominance of *Alteromonas* cells is consistent with our previous study on the viral infection/lysis of the unicellular algae *Phaeocystis globosa*, where *Alteromonas* abundance increased significantly soon after algal viral lysis (Sheik *et al*, in preparation). Unlike the *Phaeocystis* study, however, *Alteromonas* cells were also abundant in the non-infected *M. pusilla* cultures after 2 days of the experiment. Although the total bacterial abundance in the non-infected and infected *M. pusilla* cultures differed significantly, the relative abundance of *Alteromonas* cells were similar (~75% of the total bacterial abundance by day 2). This might be attribute to the fact that *Alteromonas* cells are capable of utilising a high diversity of organic compounds for energy acquisition ranging from low molecular weight substrates such as hexoses (Gómez-Consarnau et al., 2012) to recalcitrant algal polysaccharides (Ivars-Martinez et al., 2008).

The *Roseobacter* cells (*Alphaproteobacteria*) were previously documented to be associated with high primary production, and might be involved in the breakdown of algal derived osmolytes such as dimethlysulfide (DMS) (Zubkov et al., 2001; Malmstrom et al., 2004). Viral lysis of *M. pusilla* may in fact lead to rapid release of DMS (Richard et al., 1998) and as such might stimulate can the growth of these bacterial populations. However, in our study, *Roseobacter* cells represented a lower proportion to the total bacterial abundance through out the experiment. This low abundance can be explained by selective phage mediated viral lysis, which prevented *Roseobacter* cells from blooming.

The *Bacteroidetes* members were the next dominant bacterial members due to viral lysis of *M. pusilla*. *Bacteroidetes* members are known to be able to degrade high molecular weight organic matter (Cottrell and Kirchman, 2000a) and are commonly associated with phytoplankton derived organic matter, for example, during the algal blooms (e.g., (Lamy et al., 2009)). Given the increasing abundance of *Bacteroidetes* members in the infected cultures, it could be speculated that these

bacteria were an important group in the degradation of high molecular weight organic matter released due to *M. pusilla* viral lysis. The abundance of *Alteromonas* cells and *Bacteroidetes* members due to viral lysis of *M. pusilla* might indicate that viral lysis products consisted of labile and high molecular weight compounds that allowed the niche of two ecologically diverse bacteria.

Apart from monitoring the bacterial succession using CARD-FISH, we used amplicon sequencing to investigate the diversity of specific bacterial phylotypes belonging to *Gammaproteobacteria*, *Alphaproteobacteria* and *Bacteroidetes* due to viral lysis and growing cells of *M. pusilla*. While *Gammaproteobacteria* and *Alphaproteobacteria* phylotypes differed distinctly, there was no distinct appearance of *Bacteroidetes* phylotypes in infected and non-infected cultures from both experimental setups. A plausible explanation on the absence of distinct *Bacteroidetes* phylotypes could be due to the underrepresentation of partial 16S rRNA gene generated sequences (Cottrell and Kirchman, 2000b; Alonso et al., 2007).

Based on amplicon sequencing, viral lysis of *M. pusilla* led to dominance of *Vibrio* sp. and *Glaciecola* sp. (both phylotypes belonging to *Alteromonas* cells) within *Gammaproteobacteria*. In the coastal North Sea, the presence of *Vibrio* and *Alteromonas* species is a common finding in seawater incubation experiments containing algal populations (Eilers et al., 2000a). Moreover, the diverse phylotypes of *Alphaproteobacteria* belonged to *Roseobacter* cells. The dominance of diverse roseobacterial phylotypes due to algal viral lysis is in line with our previous study of *P. globosa* viral lysis (Sheik *et al*, in preparation).

An interesting observation of this study was the phylotype diversity of gammaproteobacterial and alphaproteobacterial among non-infected cultures in experiments with labeled substrates and labeled biomass. Consistent with CARD-FISH analysis, *Alteromonas* populations from the non-infected *M. pusilla* cultures grown with label substrates mainly consisted of a single phylotype, *Glaciecola* sp. The *Alteromonas* populations also dominated in the non-infected *M. pusilla* cultures of labeled biomass experiment, however, *Pseudomonas* sp. constituted considerable proportions of the gammaproteobacterial phylotype. Similarly, diversity differences were observed for the *Alphaproteobacteria*, where varied *Roseobacter* phylotypes dominated in labeled substrates experiment, whereas in the labeled biomass experiment was dominated by a single phylotype *Methylobacterium* sp. The phylotype *Methylobacterium* is a methylotroph and is significant utiliser of one carbon containing (C_1) compounds such as DMS for energy generation (Hoeft et al.,

2000). Given that algal exudates are source of variety of low molecular weight substrates such as DMS, it could be conceived that algal exudates promoted the development of *Methylobacterium* phylotypes.

In contrast to the phylotype development in the non-infected cultures, gammaproteobacterial and alphaproteobacterial phylotype diversity among infected cultures from both experimental setups was similar. The development of specific phylotypes in infected cultures was in turn potentially related to the release of *M. pusilla* viral lysates. For instance, the emergence of diverse alphaproteobacterial phylotypes such as *Sulfitobacter* sp. (*Roseobacter* cells) in infected cultures potentially signifies the utilisation of virally induced release of DMS compounds.

Single cell substrate assimilation:

One of the key aspects of this study was to quantify the bacterial uptake of virally released algal material that was newly assimilated (labeled substrates) when compared to previously incorporated algal biomass (labeled biomass). A characteristic feature of *M. pusilla* cells is the presence of a pyrenoid structure, which is a chloroplast sub-cellular particle, composed of complex polypeptides and surrounded by a starch sheath. The starch sheath acts as a carbohydrate reserve and is mostly composed of amyloses and alpha-pectin (Salisbury and Floyd, 1978). Pyrenoids are the active centers for photosynthesis, containing newly assimilated carbon compounds (Salisbury and Floyd, 1978). We specifically chose *Bacteroidetes* members for single cell analyses as they have the capability to degrade high molecular weight substrates such as starch and other polypeptides (Bauer et al., 2006). Our results suggest that the release of starch sheath of pyrenoids together with high molecular weight proteins after *M. pusilla* lysis could have favoured the development of *Bacteroidetes* members as noticed by its dominance of the total bacterial abundance.

In infected cultures, the single cell ^{13}C and ^{15}N substrate assimilation by *Bacteroidetes* members in the *M. pusilla* cultures grown with the labeled substrates remained minimal by day 4. This is surprising since bulk carbon and nitrogen measurements indicated that virally infected cultures assimilated substantial amounts of new isotopic ^{13}C and ^{15}N substrates until the point of lysis. In contrast, in the labeled *M. pusilla* biomass experiment, *Bacteroidetes* members showed substantial ^{13}C and ^{15}N substrate assimilation when compared to its bulk measurements by day 4 (Table 1-2). Putting our observations together, given the plausible dependence of pyrenoid derived starch and complex peptides substrates of

Bacteroidetes members, it appears that during viral infection of *M. pusilla* much of the newly assimilated ^{13}C and ^{15}N substrates was not utilised in the pyrenoid accumulation.

Additionally, assuming a viral carbon content of 0.2 fg C virus^{-1} (Kepner et al., 1998) with C:N ratio of 10:4.5 (Hewson and Fuhrman, 2003) and net viral increase of 5.7 × 10^7 ml^{-1} by day 3 (labeled substrates experiment), we estimated that significant proportion of nitrogen (~ 0.63 µ mol N L^{-1}, 56%) and minimal amounts of newly assimilated *M. pusilla* carbon (~ 1.39 µ mol C L^{-1}, 9%) were utilized for viral production. In other words, viral infection of *M. pusilla* has likely impeded the accumulation of starch and proteins and diverted much of the newly assimilated material into viral production. Consequently, after viral lysis much of the newly algal assimilated carbon and nitrogen by the algae might be released as labile dissolved organic matter (MpVs being part of dissolved organic matter) that was not been taken up by *Bacteroidetes*. Indeed, in a culture study using axenic *M. pusilla* biomass, viral lysis was shown to stimulate production of substantial amounts of labile proteins as well as transparent exopolymer particles (TEP) (Lønborg *et al*, in preparation). Thus, it appears that the organic matter released due to *M. pusilla* viral lysis will most likely be regenerated in the euphotic zone.

In marine pelagic environments, the quality of the algal derived organic matter regulates the microbial community structure (Kirchman, 2000). The quality of the host organic matter released due to viral lysis is in turn dependent on virus-host interactions. Viruses lack defined cellular machinery and rely on host resources for viral synthesis. It is likely that they affect host carbon and nitrogen assimilation and alter host metabolism during the infection period. The current study for the first time provides an intriguing finding of how algal viral infections affect the host carbon and nitrogen assimilation by potentially hindering accumulation of new assimilated material and diverting it towards viral production, which in turn specifically structures the bacterial community and diversity. Given the ubiquitous distribution of *M. pusilla* and its co-occurrence with bloom forming micro-algae (Not et al., 2004), future studies are necessary to investigate if the remineralisation forms of pyrenoids by *Bacteroidetes* may act as a nutrient link to non-infected algal populations such as haptophytes and diatoms.

Acknowledgments:

References:

Acinas, S.G., Anton, J., and Rodriguez-Valera, F. (1999) Diversity of free-living and attached bacteria in offshore western Mediterranean waters as depicted by analysis of genes encoding 16S rRNA. *Applied and environmental microbiology* **65**: 514.

Alonso, C., Warnecke, F., Amann, R., and Pernthaler, J. (2007) High local and global diversity of *Flavobacteria* in marine plankton. *Environmental Microbiology* **9**: 1253-1266.

Bauer, M., Kube, M., Teeling, H., Richter, M., Lombardot, T., Allers, E. et al. (2006) Whole genome analysis of the marine *Bacteroidetes* 'Gramella forsetii' reveals adaptations to degradation of polymeric organic matter. *Environmental microbiology* **8**: 2201-2213.

Brussaard, C.P.D. (2004) Optimization of procedures for counting viruses by flow cytometry. *Appl. Environ. Microbiol.* **70**: 1506-1513.

Brussaard, C.P.D., J. P. Payet, C. Winter, and M. G. Weinbauer. (2010) Quantification of aquatic viruses by flow cytometry. *In S. W. Wilhelm, M. G. Weinbauer, and C. A. Suttle [eds.], Manual of Aquatic Viral Ecology. ASLO.* : p. 102–109.

Cottrell, M.T., and Suttle, C.A. (1991) Wide-spread occurrence and clonal variation in viruses which cause lysis of a cosmopolitan, eukaryotic marine phytoplankter, *Micromonas pusilla*. *Mar Ecol Prog Ser* **78**: 1-9.

Cottrell, M.T., and Suttle, C.A. (1995) Genetic diversity of algal viruses which lyse the photosynthetic picoflagellate *Micromonas pusilla* (Prasinophyceae). *Appl. Environ. Microbiol.* **61**: 3088-3091.

Cottrell, M.T., and Kirchman, D.L. (2000a) Natural assemblages of marine Proteobacteria and members of the *Cytophaga-Flavobacter* Cluster consuming low- and high-molecular-weight dissolved organic matter. *Appl. Environ. Microbiol.* **66**: 1692-1697.

Cottrell, M.T., and Kirchman, D.L. (2000b) Community composition of marine bacterioplankton determined by 16S rRNA gene clone libraries and fluorescence *in situ* hybridization. *Applied and environmental microbiology* **66**: 5116.

Eilers, H., Pernthaler, J., and Amann, R. (2000a) Succession of pelagic marine bacteria during enrichment: a close look at cultivation-induced shifts. *Applied and environmental microbiology* **66**: 4634.

Eilers, H., Pernthaler, J., Glockner, F.O., and Amann, R. (2000b) Culturability and in situ abundance of pelagic bacteria from the North Sea. *Applied and environmental microbiology* **66**: 3044.

Eilers, H., Pernthaler, J., Peplies, J., Glockner, F.O., Gerdts, G., and Amann, R. (2001) Isolation of novel pelagic bacteria from the German Bight and their seasonal contributions to surface picoplankton. *Applied and environmental microbiology* **67**: 5134.

Fuhrman, J.A., and Hagström, Å. (2008) Bacterial and archaeal community structure and its patterns. *Microbial ecology of the oceans*: 45-90.

Giovannoni, S., and Rappé, M. (2000) Evolution, diversity and molecular ecology of marine prokaryotes. . In *Microbial ecology of the oceans.* DL, K. (ed). New York: Wiley-Liss, pp. 47–84.

Gómez-Consarnau, L., Lindh, M.V., Gasol, J.M., and Pinhassi, J. (2012) Structuring of bacterioplankton communities by specific dissolved organic carbon compounds. *Environmental Microbiology*: no-no.

Guillard, R.R.L. (1975) Culture of phytoplankton for feeding marine invertebrates. *Smith, Walter L. and Matoira H. Chanley (Ed.). Culture of Marine Invertebrate Animals. Conference, Greenport, N.Y., Oct., 1972. Viii+338p. Illus. Plenum Press: New York, N.Y., U.S.A.; London, England. Isbn 0-306-30804-5*: 29-60.

Hewson, I., and Fuhrman, J.A. (2003) Viriobenthos production and virioplankton sorptive scavenging by suspended sediment particles in coastal and pelagic waters. *Microbial ecology* **46**: 337-347.

Hoeft, S.E., Rogers, D.R., and Visscher, P.T. (2000) Metabolism of methyl bromide and dimethyl sulfide by marine bacteria isolated from coastal and open waters. *Aquatic Microbial Ecology* **21**: 221-230.

Huson, D.H., Mitra, S., Ruscheweyh, H.J., Weber, N., and Schuster, S.C. (2011) Integrative analysis of environmental sequences using MEGAN4. *Genome Research* **21**: 1552-1560.

Ivars-Martinez, E., Martin-Cuadrado, A.-B., D'Auria, G., Mira, A., Ferriera, S., Johnson, J. et al. (2008) Comparative genomics of two ecotypes of the marine planktonic copiotroph *Alteromonas macleodii* suggests alternative lifestyles associated with different kinds of particulate organic matter. *ISME J* **2**: 1194-1212.

Jørgensen, B. (2006) Bacteria and marine biogeochemistry. In *Marine geochemistry*. Schulz HD, and M, Z. (eds). Berlin, Germany: Springer, pp. 169-206.

Kepner, R.L., Wharton, R.A., and Suttle, C.A. (1998) Viruses in Antarctic lakes. *Limnol Oceanogr* **43**: 1754-1761.

Kirchman, D.L. (2000) *Microbial ecology of the oceans*: Wiley-Liss, New York, N.Y.

Kuylenstierna, M., and Karlson, B. (1994) Seasonality and Composition of Pico- and Nanoplanktonic Cyanobacteria and Protists in the Skagerrak. In *Botanica Marina*, p. 17.

Lamy, D., Obernosterer, I., Laghdass, M., Artigas, F., Breton, E., Grattepanche, J.D. et al. (2009) Temporal changes of major bacterial groups and bacterial heterotrophic activity during a *Phaeocystis globosa* bloom in the eastern English Channel. *Aquatic Microbial Ecology* **58**: 95-107.

Lee, S., and Fuhrman, J.A. (1987) Relationships between biovolume and biomass of naturally derived marine bacterioplankton. *Applied and Environmental Microbiology* **53**: 1298.

Malmstrom, R.R., Kiene, R.P., Cottrell, M.T., and Kirchman, D.L. (2004) Contribution of SAR11 bacteria to dissolved dimethylsulfoniopropionate and amino acid uptake in the North Atlantic ocean. *Appl. Environ. Microbiol.* **70**: 4129-4135.

Manz, W., Amann, R., Ludwig, W., Vancanneyt, M., and Schleifer, K.-H. (1996) Application of a suite of 16S rRNA-specific oligonucleotide probes designed to investigate bacteria of the phylum cytophaga-flavobacter-bacteroides in the natural environment. *Microbiology* **142**: 1097-1106.

Musat, N., Halm, H., Winterholler, B., Hoppe, P., Peduzzi, S., Hillion, F. et al. (2008) A single-cell view on the ecophysiology of anaerobic phototrophic bacteria. *Proceedings of the National Academy of Sciences* **105**: 17861.

Not, F., Latasa, M., Marie, D., Cariou, T., Vaulot, D., and Simon, N. (2004) A single species, *Micromonas pusilla* (Prasinophyceae), dominates the eukaryotic picoplankton in the western English channel. *Applied and Environmental Microbiology* **70**: 4064-4072.

Not, F., Massana, R., Latasa, M., Marie, D., Colson, C., Eikrem, W. et al. (2005) Late summer community composition and abundance of photosynthetic picoeukaryotes in Norwegian and Barents Seas. *Limnology and oceanography*: 1677-1686.

Pernthaler, A., Pernthaler, J., and Amann, R. (2004) Sensitive multi-color fluorescence in situ hybridization for the identification of environmental microorganisms. *Molecular Microbial Ecology Manual* **3**: 711–726.

Pinhassi, J., Sala, M.M., Havskum, H., Peters, F., Guadayol, O., Malits, A., and Marrasé, C. (2004) Changes in bacterioplankton composition under different phytoplankton regimens. *Applied and environmental microbiology* **70**: 6753-6766.

Polerecky, L., Adam, B., Milucka, J., Musat, N., Vagner, T., and Kuypers, M.M.M. (2012) Look@NanoSIMS – a tool for the analysis of nanoSIMS data in environmental microbiology. *Environ Microbiol* **14**: 1009-1023.

Richard, W.H., Bradley, A.W., Matthew, T.C., and John, W.H.D. (1998) Virus-mediated total release of dimethylsulfoniopropionate from marine phytoplankton: a potential climate process. *Aquatic Microbial Ecology* **14**: 1-6.

Salisbury, J.L., and Floyd, G.L. (1978) Molecular, enzymatic and ultrastructure characterization of the pyrenoid of the scaly green monad *Micromonas squamata*. *Journal of Phycology* **14**: 362-368.

Schäfer, H., Servais, P., and Muyzer, G. (2000) Successional changes in the genetic diversity of a marine bacterial assemblage during confinement. *Archives of microbiology* **173**: 138-145.

Sheik, A.R., Brussaard, C.P.D., Lavik, G., Foster, R.A., Musat, N., Adam, B., and Kuypers, M.M.M. (2012) Viral infection of *Phaeocystis globosa* impedes release of chitinous star-like structures: quantification using single cell approaches. *Environmental Microbiology* **DOI: 10.1111/j.1462-2920.2012.02838.x**.

Sun, Y., Wolcott, R.D., and Dowd, S.E. (2011) Tag-encoded FLX amplicon pyrosequencing for the elucidation of microbial and functional gene diversity in any environment. *Methods in molecular biology (Clifton, NJ)* **733**: 129-141.

Tada, Y., Taniguchi, A., Sato-Takabe, Y., and Hamasaki, K. (2012) Growth and succession patterns of major phylogenetic groups of marine bacteria during a mesocosm diatom bloom. *Journal of Oceanography*: 1-11.

Tada, Y., Taniguchi, A., Nagao, I., Miki, T., Uematsu, M., Tsuda, A., and Hamasaki, K. (2011) Differing Growth Responses of Major Phylogenetic Groups of Marine Bacteria to Natural Phytoplankton Blooms in the Western North Pacific Ocean. *Applied and Environmental Microbiology* **77**: 4055-4065.

Teeling, H., Fuchs, B.M., Becher, D., Klockow, C., Gardebrecht, A., Bennke, C.M. et al. (2012) Substrate-controlled succession of marine bacterioplankton populations induced by a phytoplankton bloom. *Science* **336**: 608-611.

Veldhuis, M.J.W., and Kraay, G.W. (2000) Application of flow cytometry in marine phytoplankton research: current applications and future perspectives. *Scientia Marina* **64**: 121-134.

Zhou, J., Bruns, M.A., and Tiedje, J.M. (1996) DNA recovery from soils of diverse composition. *Applied and environmental microbiology* **62**: 316-322.

Zingone, A., Sarno, D., and Forlani, G. (1999) Seasonal dynamics in the abundance of *Micromonas pusilla* (Prasinophyceae) and its viruses in the Gulf of Naples (Mediterranean Sea). *Journal of Plankton Research* **21**: 2143-2159.

Zubkov, M.V., Fuchs, B.M., Archer, S.D., Kiene, R.P., Amann, R., and Burkill, P.H. (2001) Linking the composition of bacterioplankton to rapid turnover of dissolved dimethylsulphoniopropionate in an algal bloom in the North Sea. *Environmental Microbiology* **3**: 304-311.

Supplementary Figure 1: Comparison of the taxonomic analyses computed by MEGAN4 (Huson et al., 2011) for 16S rRNA amplicon sequences of *Gammaproteobacteria*, *Alphaproteobacteria* and *Bacteroidetes* performed on the *in situ* North Sea water sample and at day 4 of the experiment from the infected and non-infected cultures of both experimental setups. The Min Complexity item of the software was used to identify low complexity reads and is placed on special low complexity node, for example, *Bacteroidetes*.

Supplementary Table 1: Species percentage composition of *Gammaproteobacteria*.

Species name	*In situ* sea water (0.8µm filtered)	Labeled substrates Experiment - Non-infected cultures	Labeled substrates Experiment - Infected cultures	Labeled biomass Experiment - Non-infected cultures	Labeled biomass Experiment - Infected cultures
Pseudomonas sp	70.7	0.0	0.0	66.2	0.1
Glaciecola sp	0.9	99.1	15.9	3.1	24.6
Haliea sp	16.7	0.0	0.0	2.3	0.0
Afipia birgiae	0.0	0.0	0.0	0.0	0.0
Vibrio sp	0.1	0.0	75.4	0.8	64.2
Colwellia sp	0.1	0.4	0.0	1.1	0.3
Alteromonas sp	0.0	0.2	3.0	7.6	4.9
Alteromonas marina	0.0	0.0	0.0	0.1	0.0
Amphritea atlantica	0.1	0.0	0.0	0.0	0.0
Phaeospirillum sp	0.0	0.0	0.0	0.0	0.0
Novosphingobium hassiacum	0.0	0.0	0.0	0.0	0.0
Sphingobium yanoikuyae	0.0	0.0	0.0	0.0	0.0
Parvibaculum sp	0.0	0.0	0.0	0.0	0.0
Cellvibrio sp	1.2	0.0	0.0	3.9	0.0
Oceanospirillum sp	0.0	0.0	0.0	0.0	0.0
Marinobacterium rhizophilum	0.0	0.0	0.0	0.0	0.0
Pseudomonas argentinensis	0.0	0.0	0.0	0.4	0.0
Methylophaga sp	0.0	0.0	0.0	1.4	0.0
Pseudoalteromonas sp	0.0	0.0	0.0	0.6	0.0
Balneatrix alpica	0.2	0.0	0.0	0.4	0.0
Haliea rubra	6.5	0.0	0.0	1.2	0.0
Enhydrobacter sp	0.0	0.0	0.0	0.1	0.0
Acinetobacter sp	0.2	0.0	0.0	0.2	0.0
Alishewanella sp	0.0	0.0	0.0	0.1	0.0
Moraxella sp	0.0	0.0	0.0	1.9	0.0

Species percentage composition of *Gammaproteobacteria* (continued).

Species name	*In situ* sea water (0.8μm filtered)	Labeled substrates Experiment - Non-infected cultures	Labeled substrates Experiment - Infected cultures	Labeled biomass Experiment - Non-infected cultures	Labeled biomass Experiment - Infected cultures
Stenotrophomonas sp	0.0	0.0	0.0	0.1	0.0
Marinobacter sp	0.9	0.0	0.0	1.3	0.0
Psychrobacter sp	0.0	0.0	0.0	0.0	0.0
Marinomonas sp	0.1	0.0	0.0	0.0	0.1
Amphritea japonica	0.2	0.0	0.0	0.2	0.0
Colwellia rossensis	0.0	0.0	0.0	0.0	0.2
Salinimonas chungwhensis	0.0	0.0	0.0	0.3	0.0
Endozoicomonas elysicola	0.0	0.0	0.0	1.0	0.0
Pseudomonas putida	0.3	0.0	0.0	1.1	0.0
Pseudomonas marincola	0.0	0.0	0.0	0.4	0.0
Lysobacter sp	0.0	0.0	0.0	0.1	0.0
Hydrocarboniphaga effusa	0.0	0.0	0.0	1.5	0.0
Pseudomonas koreensis	0.0	0.0	0.0	0.1	0.0
Pseudomonas rhizosphaerae	0.0	0.0	0.0	0.2	0.0
Cycloclasticus sp	0.1	0.0	0.0	0.1	0.0
Microbulbifer sp	0.1	0.0	0.0	0.3	0.0
Neptuniibacter sp	0.0	0.0	0.0	0.1	0.0
Pseudomonas mendocina	0.0	0.0	0.0	0.1	0.0
Pseudomonas fluorescens	0.0	0.0	0.0	0.1	0.0
Marinimicrobium sp	0.0	0.0	0.0	0.2	0.0
Colwellia psychrerythraea	0.0	0.2	0.0	0.0	0.0
Aliivibrio salmonicida	0.0	0.0	0.4	0.0	0.0
Marinobacterium sp	0.1	0.0	0.0	0.0	0.0
Dasania marina	0.0	0.0	0.0	0.1	0.0
Pseudomonas cuatrocienegasensis	0.0	0.0	0.0	0.1	0.0
Nitrincola sp	0.0	0.0	0.0	0.1	0.0
Aestuariibacter halophilus	0.0	0.0	0.0	0.0	0.0

Species percentage composition of *Gammaproteobacteria* (continued).

Species name	*In situ* sea water (0.8μm filtered)	Labeled substrates Experiment - Non-infected cultures	Labeled substrates Experiment - Infected cultures	Labeled biomass Experiment - Non-infected cultures	Labeled biomass Experiment - Infected cultures
Vibrio splendidus	0.0	0.0	4.0	0.0	3.6
Photobacterium phosphoreum	0.0	0.0	0.0	0.0	0.1
Vibrio crassostreae	0.0	0.0	0.2	0.0	0.4
Rheinheimera baltica	0.1	0.0	0.0	0.0	0.0
Aliivibrio logei	0.0	0.0	0.5	0.0	0.6
Vibrio fortis	0.0	0.0	0.2	0.0	0.2
Vibrio cyclitrophicus	0.0	0.0	0.0	0.0	0.4
Aliivibrio wodanis	0.0	0.0	0.1	0.0	0.1
Vibrio aestuarianus	0.0	0.0	0.1	0.0	0.0
Psychromonas ingrahamii	0.0	0.0	0.0	0.0	0.0
Bartonella sp	0.0	0.0	0.0	0.0	0.0
Bowmanella denitrificans	0.0	0.0	0.0	0.0	0.0
Alteromonas hispanica	0.0	0.0	0.0	0.0	0.0
Vibrio cyclithrophicus	0.0	0.0	0.1	0.0	0.0
Vibrio gigantis	0.0	0.0	0.0	0.0	0.0
Photobacterium lipolyticum	0.0	0.0	0.1	0.0	0.0
Photobacterium sp	0.0	0.0	0.1	0.0	0.0
Rheinheimera aquimaris	0.1	0.0	0.0	0.0	0.0
Neptunomonas naphthovorans	0.1	0.0	0.0	0.0	0.0
Oceanospirillum maris	0.1	0.0	0.0	0.0	0.0
Oleiphilus sp	0.6	0.0	0.0	0.0	0.0
Pseudomonas vancouverensis	0.1	0.0	0.0	0.0	0.0
Congregibacter litoralis	0.1	0.0	0.0	0.0	0.0
Oleiphilus messinensis	0.2	0.0	0.0	0.0	0.0
Marinospirillum insulare	0.1	0.0	0.0	0.0	0.0
Endobugula glebosa	0.1	0.0	0.0	0.0	0.0
Marinobacter salicampi	0.1	0.0	0.0	0.0	0.0

Supplementary Table 2: Species percentage composition of *Alphaproteobacteria*.

Species name	*In situ* sea water (0.8μm filtered)	Labeled substrates Experiment - Non-infected cultures	Labeled substrates Experiment - Infected cultures	Labeled biomass Experiment - Non-infected cultures	Labeled biomass Experiment - Infected cultures
Leisingera sp	1.7	31.7	16.2	0.0	20.8
Pelagibacter sp	53.3	5.0	3.7	3.8	5.0
Thalassobius sp	0.6	3.4	1.1	0.0	1.7
Thalassobacter sp	7.3	3.9	12.3	0.3	7.4
Roseovarius nubinhibens	0.0	0.5	0.2	0.0	0.4
Sulfitobacter sp	0.1	15.6	34.6	0.0	35.1
Roseobacter sp	3.0	11.0	11.4	0.2	11.0
Sulfitobacter japonica	0.0	0.5	0.3	0.0	0.3
Phaeobacter daeponensis	0.0	0.8	0.1	0.0	0.2
Ruegeria sp	32.5	16.9	12.3	1.4	10.6
Sphingobacterium sp	0.0	0.0	0.0	0.0	0.0
Zhangella mobilis	0.1	0.0	0.0	0.0	0.0
Sulfitobacter brevis	0.0	0.1	0.0	0.0	0.0
Bradyrhizobium sp	0.1	0.1	0.2	0.7	0.0
Rhizobium sp	0.0	0.1	0.0	0.0	0.0
Azospirillum sp	0.2	0.0	0.0	0.0	0.0
Hellea balneolensis	0.1	0.1	0.0	0.0	0.0
Tateyamaria sp	0.2	0.1	0.0	0.0	0.0
Sulfitobacter delicatus	0.0	0.0	0.0	0.0	0.0
Rhodoplanes sp	0.0	0.1	0.1	0.1	0.0
Roseovarius aestuarii	0.1	0.0	0.0	0.0	0.0
Phaeobacter sp	0.0	1.6	0.4	0.0	0.6
Sphingomonas sp	0.1	0.3	0.7	8.2	0.4
Roseovarius sp	0.0	0.1	0.3	0.0	0.2
Devosia sp	0.1	0.1	0.0	0.0	0.1
Loktanella sp	0.2	5.9	4.1	0.0	3.5
Jannaschia sp	0.1	0.0	0.0	0.0	0.0

Species percentage composition of *Alphaproteobacteria* (continued).

Species name	*In situ* sea water (0.8µm filtered)	Labeled substrates Experiment - Non-infected cultures	Labeled substrates Experiment - Infected cultures	Labeled biomass Experiment - Non-infected cultures	Labeled biomass Experiment - Infected cultures
Loktanella koreensis	0.0	0.1	0.0	0.0	0.0
Caulobacter sp	0.0	0.4	0.6	3.6	0.8
Rasbo sp	0.0	0.2	0.1	0.1	0.0
Roseovarius pelophilus	0.0	0.0	0.1	0.0	0.0
Rhodobacter sp	0.1	0.0	0.1	0.2	0.1
Nereida sp	0.0	0.0	0.0	0.0	0.0
Leisingera methylohalidivorans	0.0	0.1	0.0	0.0	0.1
Maribius sp	0.0	0.2	0.0	0.0	0.0
Ochrobactrum sp	0.1	0.0	0.0	0.0	0.1
Thalassobius mediterraneus	0.0	0.3	0.1	0.0	0.0
Catellibacterium sp	0.0	0.1	0.0	0.0	0.0
Ruegeria scottomollicae	0.0	0.1	0.0	0.1	0.0
Octadecabacter sp	0.0	0.1	0.0	0.0	0.1
Thalassobius gelatinovorus	0.0	0.1	0.0	0.0	0.1
Loktanella vestfoldensis	0.0	0.1	0.0	0.0	0.0
Afipia birgiae	0.0	0.0	0.0	0.1	0.1
Novosphingobium hassiacum	0.0	0.0	0.1	0.2	0.0
Sphingobium yanoikuyae	0.0	0.0	0.1	0.0	0.0
Parvibaculum sp	0.0	0.1	0.0	0.0	0.0
Roseovarius crassostreae	0.0	0.0	0.1	0.0	0.2
Hyphomicrobium sp	0.0	0.0	0.0	0.0	0.0
Blastobacter sp	0.0	0.0	0.1	0.0	0.0

Species percentage composition of *Alphaproteobacteria* (continued).

Species name	*In situ* sea water (0.8µm filtered)	Labeled substrates Experiment - Non-infected cultures	Labeled substrates Experiment - Infected cultures	Labeled biomass Experiment - Non-infected cultures	Labeled biomass Experiment - Infected cultures
Nordella oligomobilis	0.0	0.0	0.1	0.0	0.0
Afipia sp	0.0	0.0	0.1	0.9	0.1
Sphingobium xenophagum	0.0	0.0	0.0	0.1	0.0
Phenylobacterium sp	0.0	0.0	0.0	0.1	0.0
Brevundimonas diminuta	0.0	0.0	0.0	0.1	0.0
Rhodomicrobium sp	0.0	0.0	0.0	0.4	0.0
Methylobacterium chloromethanicum	0.0	0.0	0.0	0.1	0.6
Sphingobium sp	0.0	0.0	0.0	0.2	0.0
Afipia felis	0.0	0.0	0.0	0.1	0.1
Methylobacterium sp	0.0	0.0	0.0	78.1	0.0
Brevundimonas sp	0.0	0.0	0.0	0.1	0.0
Methylobacterium organophilum	0.0	0.0	0.0	0.1	0.0
Chelatococcus sp	0.0	0.0	0.0	0.1	0.0
Rhodopseudomonas sp	0.0	0.0	0.0	0.1	0.0
Novosphingobium sp	0.0	0.0	0.0	0.1	0.0
Novosphingobium lentum	0.0	0.0	0.0	0.1	0.0

Chapter 5. Discussion and Outlook

As an emerging field in oceanography, relatively little is known about the ecological importance of algal viruses such as their ability to structure microbial communities and biogeochemical cycling. The goal of this thesis was hence to enhance our understanding of the roles of algal viruses in the microbial loop and biological carbon pump. An interdisciplinary approach was used that integrated recent advancements in molecular biology and biogeochemistry to gain novel insights into marine virus ecology from the view point of single cells as well as communities. This thesis investigated the interactions and carbon and nitrogen fluxes among viruses, algae and specific genera of marine bacteria. Using a stable isotope approach, incubation experiments were carried out with ecologically significant algae and their specific viruses along with the addition of natural bacterial assemblages. The application of the high resolution imaging techniques of atomic force microscopy (AFM) led to new insights into the impact of viral infections on algal host morphology and physiology. Furthermore, the combination of halogen fluorescent *in situ* hybridization and nanoSIMS (HISH-SIMS) was used to image and quantify the carbon and nitrogen release from bacterial cells due to algal viral infections. We could show the extent to which algal viral lysis structures the bacterial community composition (fluorescent *in situ* hybridization, CARD-FISH) and diversity (tagged amplicon pyrosequencing) and subsequently mediates flow of carbon and nitrogen.

5.1 The enigmatic virtue of algal viral infections

The form and fate of virally released host organic matter passing through the viral shunt depends on the interactions between viruses and hosts. Viruses are devoid of cellular machinery and rely on host resources for propagation. Findings of this thesis provided novel insights into the ability of viruses to alter host physiology and influence biogeochemical cycles, even before viral lysis occurred. Single cell analysis using AFM and nanoSIMS showed that viral infection of *Phaeocystis globosa* impedes the release of chitinous star-like structures, affecting host carbon assimilation **(chapter 2)**. We hypothesised that the impediment of the release of star-like structures in *P. globosa* causes the formation of flocs which are characterised by substantial attachment of newly produced viruses (~68%) prior to host cell lysis **(chapter 2)**. Other evidence of viral 'hijack' seems to appear during the viral infection period of the pico-algae, *Micromonas pusilla* **(chapter 4)**, during which

much of the newly host assimilated carbon and nitrogen was diverted towards viral synthesis.

In addition, it seems *P. globosa* viral infections can stimulate bacterial attachment to algal cell surroundings, known as the phycosphere (Bell and Mitchell, 1972), which is a habitat for diverse bacterial populations (Sapp et al., 2007) , the formation of which has been ascribed to various environmental factors (Gomez-Pereira et al., 2010; Teeling et al., 2012; Tittel et al., 2012). Viral infections of *P. globosa* stimulating leakage or excretion and triggering the growth of phycosphere-associated bacteria is a previously undocumented finding **(chapter 3)**. Subsequently, *P. globosa* viral lysis resulted in the formation of aggregates which were colonised densely with bacteria. The aggregate formation could partly be explained by the formation of flocs **(chapter 2)** and phage lysis products (Shibata et al., 1997).

Overall, the studies presented in this thesis suggest that viral infections of host cells can substantially affect the quality of the released organic matter prior to cell lysis. Also, algal viral infections can influence the occurrence of bacterial populations as aggregate-associated and/or free-living.

5.2 Structuring specific bacterial communities by algal viral lysis - The rise of 'rare' taxa

In the coastal North Sea, the succession of specific bacterial groups seems to be correlated to the availability of algal-derived organic matter together with different bacterial metabolic activities (Lamy et al., 2009; Teeling et al., 2012). The growth of particular bacterial lineages such as the gammaproteobacterial *Alteromonadaceae* and Alphaproteobacterial *Rhodobacteriaceae* (referred to as *Alteromonas* and *Roseobacter* cells thereafter) which are rare usually, can be stimulated by the input of certain substrates potentially released during algal blooms (Eilers et al., 2000; Allers et al., 2007). Since algal viral lysis leads to sudden and differential release of organic matter, combined with different energy requirements and physiological characteristics of bacterial populations, viruses can alter bacterial community structure to various degrees at different stages during the lytic cycle.

Prior to algal cell lysis, viral infections of *Phaeocystis globosa* triggered the initial doubling in the abundance of genus *Alteromonas* cells (**chapter 3**). Soon after *P. globosa* viral lysis, *Alteromonas* and followed by *Roseobacter* cells dominated bacterial communities (day 2). On the other hand, viral lysis of *Micromonas pusilla*

led to the dominance of *Alteromonas* cells, where *Roseobacter* cells maintained relatively low abundances (**chapter 4**). Furthermore, algal viral lysis triggered diverse gammaproteobacterial and alphaproteobacterial phylotypes relative to their respective non-infected cultures (**chapters 3 and 4**). In the experiments performed during this thesis, both the algal hosts *P. globosa* (Liss et al., 1994) and *M. pusilla* (Richard et al., 1998) are known to produce dimethylsulfide (DMS) compounds. The *Roseobacter* cells (*Alphaproteobacteria*) were previously documented to be assimilating algal derived osmolytes such as DMS (Zubkov et al., 2001; Malmstrom et al., 2004). While *P. globosa* viral lysis enhanced the development of *Roseobacter* cells, *M. pusilla* viral lysis was associated with a lower proportion of *Roseobacter* cellular abundance throughout the experiment. Nonetheless, the presence of *Roseobacter* phylotypes such as *Roseovarius* sp and *Sulfitobacter* sp. indicated that virally released DMS might have been assimilated or remineralised (**chapters 3 and 4**).

In addition, the extent of bacterial community structuring by viral lysis of a micro-algae (*P. globosa*) and pico-algae (*M. pusilla*) was verified. For example, as a result of *P. globosa* viral lysis, *Bacteroidetes* populations remained of relatively minor importance ($\sim 1.49 \times 10^5$ cells ml^{-1}), while *M. pusilla* viral lysis led to co-dominance of the bacterial populations ($\sim 3.6 \times 10^6$ cells ml^{-1}, day 4).

These observations confirm that viral lysis of algal host cells leads to drastic and very rapid changes in the bacterial composition and phylotype diversity. Particularly the rare bacterial genera such as *Alteromonas* cells appear to profit from cell lysis. Additional characteristics such as the varied bacterial metabolic activities suggest that the quality of virally released organic matter can be a strong selective force on bacterial community structure. Taken together, the studies documented in thesis provide an understanding of factors that govern the temporal variability and abundance of particular bacterial species, which is important for our understanding of how virally derived algal organic matter regulates bacterial structure in the water column.

5.3 The fate of virally released algal lysates

It is a general perception that viruses mediate microbial substrate assimilation through host cell lysis. The observations provided in this thesis hint at the existence of novel possibilities by which algal viruses could influence the organic matter availability.

In **chapter 2**, the impediment of release of *Phaeocystis globosa* star-like structures due to viral infection could enhance grazing. The scenario of enhanced grazing is in contrast to the current perspective that viral infections facilitate microbial mediated processes by diverting host material away from the higher trophic levels. Based on nanoSIMS imaging, **chapter 3** of this thesis showed that *P. globosa* cells leak substantial amounts of organic matter during early phases of viral infections and prior to cell lysis. With minimal amounts of *P. globosa* bulk biomass being utilized for viral production **(chapter 2)**, aggregate dissolution due to potential phage lysis appeared to be responsible for regeneration of copious amounts of dissolved inorganic carbon ($\sim$ 55% of the *P. globosa* particulate organic carbon biomass).

In contrast, in **chapter 4**, it is speculated that viral infection of *M. pusilla* diverted much of the newly assimilated *M. pusilla* carbon ($\sim$ 1.39 µ mol C L^{-1}, 9%) and a significant proportion of nitrogen ($\sim$ 0.63 µ mol N L^{-1}, 56%) in to the production of *M. pusilla* viruses. Consequently, after viral lysis much of the newly assimilated carbon and nitrogen might be released as labile dissolved organic forms together with high molecular weight compounds such as starch. Indeed, in a culture study using axenic *M. pusilla* biomass, viral lysis has been shown to the substantial amounts of labile proteins production (Lønborg *et al*, in preparation) and high concentrations of transparent exopolymer particles (TEP).

Observations presented in this thesis detailed and quantified changes in carbon availability due to the interplay between algae, bacteria and viruses. The significant organic carbon remineralisation of a bloom forming algae, *P. globosa,* can have large consequences for the rates of particulate carbon accumulation in the photic zone. Moreover, the formation of recalcitrant carbon at the same time can accelerate its vertical export to the oceanic interior. In contrast, the virally released organic matter of a non-bloom forming algae, *M. pusilla*, will most likely be regenerated within the euphotic zone.

5.4 Outlook

For the first time, this thesis has provided direct evidence of the impact of algal viruses in structuring bacterial community composition, diversity and the underlying mechanisms influencing biogeochemical cycles at a high resolution single cell level. Nevertheless, many questions remain, the answers to which will increase our understanding the significance of algal viruses.

Beginning with the infection period, the application of single cell techniques AFM and nanoSIMS, enabled us to visualize the impact of viral infections on host physiology and morphology **(Chapter 2)**. Further understanding of changes in the chemical composition of infected algal host cells, for example by Raman spectroscopy (Lambert et al., 2006) may reveal novel insights. Additionally, given that several virus-algae hosts are available in culture (Brussaard, 2008), molecular characterization of virally released dissolved organic material (DOM) either during infection or following lysis will be of significance. The recent advent of ultrahigh-resolution mass spectrometry by means of Fourier transform ion cyclotron resonance (FT-ICR-MS) could in part resolve the characterisation of distinct DOM released by various algal viral infection/lysis (Dittmar and Paeng, 2009). Furthermore, characterisation of viral released DOM in laboratory experiments could act as indicators of viral mediated process during algal blooms in the environment.

The application of isotopic incubation experiments using axenic algae-virus host systems and pre-filtered North Sea bacterial populations significantly influenced bacterial community structure and the flow of elements. Particularly, the finding that leakage of infected algal cells **(Chapter 3)** can have potential implications for oceanic DOM cycling if found to be a general feature. Therefore, similar isotopic incubations using varied bloom forming algal species and their viruses have to be performed. Furthermore, leakage from infected *P. globosa* cells may act as a chemical cue to induce colony formation by other *P. globosa* cells (as observed by ciliate grazing (Tang, 2003; Long et al., 2007)) and as such may explain the ecological and global success of this species.

It has yet to be confirmed whether the observed successional pattern of particular bacterial populations by viral lysis of two different algae was due to seasonal factors or due to operationally different organic composition of viral lysates or the combination of both. Thus, it may be of interest to sample bacterial populations during different seasons, for instance, before, during and after algal blooms and to investigate the bacterial community composition by CARD-FISH. This

may allow an initial overview of the impact of viral lysis due to varying environmental conditions. Furthermore, in the environment other predation factors such as grazing are also mortality agents (e.g., during *P. globosa* blooms (Baudoux et al., 2006)). The relatively easy accessibility of coastal environments where algal blooms occur and the use of experiments as described in the experimental procedures of **chapters 3 and 4** (with and without 0.8 µm filtration) will help to understand the implications of viral mediated processes when compared to grazing.

The composition of the virally released organic matter depends on the host cellular composition, which may consist of readily available labile organic substrates (e.g., amino acids, sugars) as well as high molecular weight compounds (e.g., polysaccharides such as starch and chitin). Based on the observations reported in this thesis, the temporal succession of bacterial communities in part appeared to depend on the chemical composition of the viral lysates **(Chapters 3 and 4)**. Additionally, given the diverse uptake preferences of marine bacteria, future studies involving the presence or expression of various functional genes such as expressions of carbohydrate metabolising enzymes and phosphate acquisition strategies will shed new insights into the nutritional demand of bacterial community structure due to algal viral lysis.

The blooming of algal viruses and their sudden disappearance is a commonly observed pattern in the coastal environments. As many bacteria are able to digest recalcitrant material it is necessary to elucidate if algal viruses can potentially be a source of organic matter.

5.6 References

Allers, E., Gómez-Consarnau, L., Pinhassi, J., Gasol, J.M., Šimek, K., and Pernthaler, J. (2007) Response of *Alteromonadaceae* and *Rhodobacteriaceae* to glucose and phosphorus manipulation in marine mesocosms. *Environmental Microbiology* **9**: 2417-2429.

Baudoux, A.C., Noordeloos, A.A.M., Veldhuis, M.J.W., and Brussaard, C.P.D. (2006) Virally induced mortality of *Phaeocystis globosa* during two spring blooms in temperate coastal waters. *Aquat. Microb. Ecol.* **44**: 207-217.

Bell, W., and Mitchell, R. (1972) Chemotactic and growth responses of marine bacteria to algal extracellular products. *Biological Bulletin* **143**: 265-277.

Brussaard, C.P.D.M., J. M. (2008) Algal Bloom Viruses. *Plant viruses, Global science books* **2 (1)**: 1-10.

Dittmar, T., and Paeng, J. (2009) A heat-induced molecular signature in marine dissolved organic matter. *Nature Geoscience* **2**: 175-179.

Eilers, H., Pernthaler, J., and Amann, R. (2000) Succession of pelagic marine bacteria during enrichment: a close look at cultivation-induced shifts. *Applied and environmental microbiology* **66**: 4634.

Gomez-Pereira, P.R., Fuchs, B.M., Alonso, C., Oliver, M.J., van Beusekom, J.E.E., and Amann, R. (2010) Distinct flavobacterial communities in contrasting water masses of the North Atlantic Ocean. *ISME J* **4**: 472-487.

Lambert, P.J., Whitman, A.G., Dyson, O.F., and Akula, S.M. (2006) Raman spectroscopy: the gateway into tomorrow's virology. *Virology journal* **3**: 51.

Lamy, D., Obernosterer, I., Laghdass, M., Artigas, F., Breton, E., Grattepanche, J.D. et al. (2009) Temporal changes of major bacterial groups and bacterial heterotrophic activity during a *Phaeocystis globosa* bloom in the eastern English Channel. *Aquatic Microbial Ecology* **58**: 95-107.

Liss, P.S., Malin, G., Turner, S.M., and Holligan, P.M. (1994) Dimethyl sulphide and *Phaeocystis*: a review. *Journal of Marine Systems* **5**: 41-53.

Long, J.D., Smalley, G.W., Barsby, T., Anderson, J.T., and Hay, M.E. (2007) Chemical cues induce consumer-specific defenses in a bloom-forming marine phytoplankton. *Proceedings of the National Academy of Sciences* **104**: 10512-10517.

Malmstrom, R.R., Kiene, R.P., Cottrell, M.T., and Kirchman, D.L. (2004) Contribution of SAR11 bacteria to dissolved dimethylsulfoniopropionate and amino acid uptake in the North Atlantic ocean. *Appl. Environ. Microbiol.* **70**: 4129-4135.

Richard, W.H., Bradley, A.W., Matthew, T.C., and John, W.H.D. (1998) Virus-mediated total release of dimethylsulfoniopropionate from marine phytoplankton: a potential climate process. *Aquatic Microbial Ecology* **14**: 1-6.

Sapp, M., Schwaderer, A.S., Wiltshire, K.H., Hoppe, H.G., Gerdts, G., and Wichels, A. (2007) Species-specific bacterial communities in the phycosphere of microalgae? *Microbial ecology* **53**: 683-699.

Shibata, A., Kogure, K., Koike, I., and Ohwada, K. (1997) Formation of submicron colloidal particles from marine bacteria by viral infection. *Marine Ecology Progress Series* **155**: 303-307.

Tang, K.W. (2003) Grazing and colony size development in *Phaeocystis globosa* (*Prymnesiophyceae*): the role of a chemical signal. *Journal of Plankton Research* **25**: 831-842.

Teeling, H., Fuchs, B.M., Becher, D., Klockow, C., Gardebrecht, A., Bennke, C.M. et al. (2012) Substrate-controlled succession of marine bacterioplankton populations induced by a phytoplankton bloom. *Science* **336**: 608-611.

Tittel, J., Büttner, O., and Kamjunke, N. (2012) Non-cooperative behaviour of bacteria prevents efficient phosphorus utilization of planktonic communities. *Journal of Plankton Research* **34**: 102-112.

Zubkov, M.V., Fuchs, B.M., Archer, S.D., Kiene, R.P., Amann, R., and Burkill, P.H. (2001) Linking the composition of bacterioplankton to rapid turnover of dissolved dimethylsulphoniopropionate in an algal bloom in the North Sea. *Environmental Microbiology* **3**: 304-311.

Acknowledgments

This thesis was a real journey and now it is my pleasure to thank many people who made this possible.

I am sincerely indebted to Marcel for believing in me and providing me the opportunity to perceive my dream research of 'viruses'. I still remember the evening when I bumped in your office and interrupted you. You agreed to provide me the opportunity in less than 10 minutes of our conversation, although you did not know me. Over these years, you taught me and helped me to be the person I am right now. Thanks for being there for me no matter what, especially during my down times.

Corina, yes viruses are absolutely amazing and gorgeous! I try not to think too much of the artwork viruses mediate in the oceans. I am so thankful to have the opportunity to work with you and learned so many things from you (professional and personal) that are imperishable. 'Multitasking, not to panic, one thing at a time' no one could teach me better than you. More than anything, I had great times working in your lab and your friendship although those were short periods of my stay in Texel.

Isotopes what? Gaute not sure if you recall when I looked at the GC-IRMS data for the first time, the numbers were in the range of 10^{-15} and you said look at it, the numbers are already self-explanatory. I giggled and thought these are less than zero what else they can tell. Of course you are right….they are very significant! I am grateful to have you as my supervisor, I sincerely appreciate your time and never ending guidance.

Lunch and science discussions followed by Soy latte….Rachel thanks for being such a great supervisor. You taught me how to write and construct a theme in scientific writing. Your never ending help even during the times when you are not here means a lot to me.

Its too wordy, shorten it…...Phyllis you are a fantastic teacher and supporter. Thanks for teaching me more about the ARB and sequencing analysis, updating me on current virus literature and improving my writing skills. I really enjoyed your supervision. I can not count on the instances where your words of advice made me calm and gave me the courage of a lion. Having lunch with you and Gabi were quite good times.

Niculina I can not thank enough for your support during my masters thesis and beginning of my PhD. Thanks for teaching how to perform CARD-FISH and HISH-SIMS.

Shalin, Birgit, Mari, Andi, Mimi, Oli and little M you guys are amazing and thanks for everything. You were always there for me when I needed you guys. I am so proud to be your friend.

Hannah and Jessika you girls are excellent scientists and lovely friends. I will miss all the gossip! I am so happy to share an office with you, having your support when I needed one. Gail, Sarah and Inigo thanks for being so nice to me ☺. Fabian thanks a lot for preparing samples for mass spec analyses during your lab rotation with me.

I am grateful to Gabi, Daniela, Thomas Max, Tomas Vagner, Sten Litmann and the staff of the Biogeochemistry department and Jörg Wulf, Nicole Rödiger of the Molecular Ecology department without whom working in the lab would have been impossible.

Kristina, Kate, Catia, Jezz, little Lizzy and Douwe thanks a lot for fun times during my stay in Texel. You guys provided me a home in the little 'island'.

I would like to express my gratitude to Anna Noordeloos, Evaline, Irene and Jan Von Ooijen from Royal Netherlands Institute for Sea Research (NIOZ) for their technical help.

I am thankful to Lubos Polerecky and Marc Strous for their scientific advice and help during my thesis.

I am grateful to our lovely secretary Ulrike Tietjen and the administration of MPI and NIOZ.

I would like to acknowledge my MarMic class 2011 and co-ordinators Christiane Glöckner and Karl-Heinz Blotevogel.

The Thiemes, my German family, Martina, Bernd and the cute kitty Francis I am glad that you are my in-laws. Thanks for your never ending support especially when I needed a family.

Here comes my husband, I can not sincerely express my words of gratitude to Max Thieme for cheering me up, understanding my working hours and being there for me no matter what. You are a great man and I am proud to be part of your life!

Finally, a long distance thank you to my family for never knowing quite what to expect, but being with me the entire way nonetheless; strange is only relative.

Appendix

Other experiments that were performed during this thesis:

1. Effect of varying light intensities on carbon and nitrogen assimilation of infected *Phaeocystis globosa* biomass.

2. Viral infection of *Emiliania huxleyi* affecting host assimilation response and structuring bacterial diversity.

3. Potential uptake of algal viruses as a nutrient source by of bacterial populations.

Conferences and workshops:

2012: The International Symposium on Microbial Ecology (ISME), Copenhagen, Denmark. Poster presentation: *'Effect of viruses on bacterial community structure and single-cell carbon and nitrogen assimilation'.*

2011: The 6th Aquatic Virus Workshop, Texel, The Netherlands. Oral presentation: '*Viruses and the microbial loop: A single cell approach*'.

2010: The 13th International Symposium on Microbial Ecology (ISME-13), Seattle, WA, USA.
Poster presentation: *'The effect of viruses on Prokaryotic and Eukaryotic nutrient assimilation: A single cell approach'.*

2008: Novel Insights into Redox and Nutrient Cycles in the Ocean, SFB 754 international workshop, Kiel, Germany.

2006: Sustained Indian Ocean Biogeochemical and Ecological Research (SIBER) workshop, Goa, India.

Sea Expeditions:

August – September 2011: Royal Research Vessel Discovery 369, North Atlantic gyre.

April – May 2008: Research Vessel MS Merian MSM 08/1, North-East Atlantic.

Erklärung

Name: Abdul Rahiman Sheik

Datum: 01.10.2012

Anschrift: Scharnhorststr. 73, 28211, Bremen

<u>**Erklärung**</u>

Hiermit versichere ich, dass ich

1. **die Arbeit ohne unerlaubte fremde Hilfe angefertigt habe,**

2. **keine anderen als die von mir angegebenen Quellen und Hilfsmittel benutzt habe und**

3. **die den benutzten Werken wörtlich oder inhaltlich entnommenen Stellen als solche kenntlich gemacht habe.**

Bremen, den 01.10.2012

_____

Unterschrift